

**Dissertation zur Erlangung des Doktorgrades
der Fakultät für Chemie und Pharmazie
der Ludwig-Maximilians-Universität München**



In situ-hardening hydrogels for the sustained release of
protein pharmaceuticals

Philipp Dominik Alexander Matthias

aus

München

2015

Erklärung

Diese Dissertation wurde im Sinne von § 7 der Promotionsordnung vom 28. November 2011 von Herrn Prof. Wolfgang Frieß betreut.

Eidesstattliche Versicherung

Diese Dissertation wurde eigenständig und ohne unerlaubte Hilfe erarbeitet.

München, 02.10.2015

.....
(Philipp Dominik Alexander Matthias)

Dissertation eingereicht am 13.10.2015

1. Gutachterin / 1. Gutachter: Prof Dr Wolfgang Frieß

2. Gutachterin / 2. Gutachter: Prof Dr Gerhard Winter

Mündliche Prüfung am 13.11.2015

Acknowledgment

This thesis was prepared at the Department of Pharmacy, chair of Pharmaceutical Technology and Biopharmaceutics at the Ludwig-Maximilians-Universität München, Germany, under supervision of Prof. Wolfgang Frieß.

First of all I would like to express my deepest gratitude to my supervisor Prof. Wolfgang Frieß for his scientific guidance, advice and for giving me the opportunity to becoming a member of his research group. I found a professional and pleasant working atmosphere and had the opportunity to attend international scientific conferences.

Also highly appreciated is the co-reference of Prof. Gerhard Winter. As leader of the chair he established excellent working conditions, an interesting scientific program and encourages students to also attend numerous social activities.

I would also like to thank Polymaterials, Kaufbeuren, for their collaboration. Special thanks to Dr. Hinrich Wiese and Dr. Gerhard Maier for providing us with the thermo-responsive polymers, advice and insights into their laboratory.

Thanks to Prof. Franz Bracher and his student Dr. Anne Wurzbauer for providing us with laboratory equipment and advice on chemical synthesis.

Furthermore, I want to thank the students who performed some of the experiments for their excellent work and friendly atmosphere: Alessandro Gamberin, Angelika Linder, Fabian Bischoff, Kristin Harnisch, Manuel Gregoritzka, Markus Grandl and Nico Erlewein.

Very special thanks and the kindest regards go to my colleagues at the LMU. Thank you all for the fantastic atmosphere, for cookies and cakes, movies and barbecue, chats and sport, open ears and many a joke. My “iLab” mate Tim Menzen is especially acknowledged for sharing my music and friendship.

Finally, I want to thank my parents for their encouragement and their life-long support, as well as my wife Anna and all our friends for their love and patience.

List of Abbreviations

APA	Alkyne-PEG-alkyne
API	Active pharmaceutical ingredient
Az3OA	11-Azido-3,6,9-trioxaundecane-1-amine
BDI	Butyldiisocyanate
BSA	Bovine serum albumine
BUL	Bifunctional urethane linker
cHA	crosslinked hyaluronic acid
CMT	Critical micellation temperature
cp	Cloud point
CuAAC	Copper-I catalyzed azide-alkyne cycloaddition
dHA	derivatized hyaluronic acid
DIC	Diisocyanate
DMSO	Dimethyl sulfoxide
DoS	Degree of substitution
FITC	Fluoresceine isocyanate
FNU	Formazine nephelometric unit
FTIR	Fourier-transformation infrared spectroscopy
G'	Storage modulus
G''	Loss modulus
GlcNAc	β -D-glucosamine
GluUA	β -D-glucuronic acid
GnRH	Gonadotropine releasing hormone
HA	Hyaluronic acid
HDI	Hexamethylene diisocyanate
hGH	Human growth hormone
i.m	intramuscular
i.v.	intravenous
IL-2	Interleukin-2
LCST	Lower critical solution temperature
MDI	H ₁₂ -4,4'-methylene diphenyl diisocyanate
MES	2(N-morpholino)ethanesulfonic acid
M _w	Molecular weight
mwco	Molecular weight cut-off
NHS	N-Hydroxysuccinimide
NMR	Nuclear magnetic resonance
PBS	Phosphate buffered saline
PEO	Polyethyleneoxide
PES	Polyethersulfon
PLGA	Poly(lactic-co-glycolic-acid)
PMT	PolyMaterials Thermopolymer
pNiPAAm	Poly(N-isopropylacrylamide)

PPO	Polypropyleneoxide
RT	Room temperature
s.c.	subcutaneous
SDS	Sodium dodecyl sulfate
SEC	(High pressure) Size exclusion chromatography
THF	Tetrahydrofuran
T _{max}	Temperature with maximal penetration resistance
VPTT	Volume phase transition temperature

Abstract

This thesis discusses two potential in situ-forming hydrogel systems for sustained protein release: (i) a chemically cross-linked Hyaluronic acid derivative and (ii) physically cross-linked thermo-responsive poloxamer derivatives (PMTs). The synthetic pathway to HA derivatives capable of in situ cross-linking by the Cu-I catalyzed azide-alkyne-cycloaddition is introduced. Using a commercially available bis-alkyne linker a significant increase in HA MW is achieved. However, MW and gel network density are too low to sustain gel dissolution and, hence, to serve as sustained release depot. Furthermore, protein stability issues for the generating of Cu-I by in situ reduction of Cu-II with ascorbic acid are seen. In contrast, upon heating to body temperature PMT gels offer fast hardening, prolonged dissolution time and sustained protein release up to several weeks with no indication for protein aggregation and degradation. They offer good storage stability and syringeability. Precipitation of the employed IGG is reversible and does not affect the protein stability.

Table of contents

Erklärung.....	I
Acknowledgment.....	II
List of Abbreviations.....	III
Abstract.....	V
Table of contents.....	VI
1. Introduction.....	1
1.1. Biopharmaceutics and sustained release.....	1
1.2. In situ-forming hydrogels by click-cross-linking in presence of protein.....	2
1.2.1. Hyaluronic acid.....	3
1.2.2. Click-cross-linking HA.....	4
1.3. In situ-forming thermo-responsive hydrogels.....	7
1.3.1. Thermo-responsive hydrogels for controlled protein delivery.....	9
1.3.2. PolyMaterials Thermopolymers (PMTs).....	10
1.4. Aims.....	11
2. Materials and Methods.....	12
2.1. Materials.....	12
2.1.1. Solvents.....	12
2.1.2. Salts, buffers and reagents.....	12
2.1.3. Proteins.....	13
2.1.4. Hyaluronic acid and derivatives.....	13
2.1.5. PMTs and poloxamers.....	14
2.1.6. Fluorescence labelled dHA.....	15
2.1.7. Cross-linked HA.....	16
2.2. Methods.....	16
2.2.1. Determination of protein and FITC-Dextran concentration.....	16
2.2.2. Determining the degree of substitution of dHA.....	17
2.2.3. HA quantification by modified carbazole method.....	17
2.2.4. Molecular weight analysis of HA species.....	18

2.2.5.	Molecular weight analysis of PMTs	18
2.2.6.	Viscosity of HA species	19
2.2.7.	Gel strength of PMT/poloxamer gels.....	19
2.2.8.	Disintegration time of PMT gels.....	19
2.2.9.	Cloud points of PMT gels.....	20
2.2.10.	Injection forces of PMT gels.....	20
2.2.11.	Protein precipitation in PMT gels.....	20
2.2.12.	Release of protein and FITC-Dextran from PMT gels.....	20
2.2.13.	Intrinsic fluorescence	21
2.2.14.	Turbidity, visible and sub-visible particles	21
3.	Click-cross-linked hyaluronic acid gels	22
3.1.	Preparation and characterization of derivatized HA	22
3.2.	Preparation and characterization of cross-linked HA	24
3.3.	Protein stability during cross-linking reactions.....	27
4.	Physico-chemical characterization of PMT gels	28
4.1.	Physico-chemical properties of H6P gels.....	28
4.2.	Gel strength of PMT gels.....	33
4.2.1.	Effect of PMT molecular weight on gel strength	33
4.2.2.	Effect of PMT concentration on gel strength.....	34
4.2.3.	Effect of diisocyanate linker on gel strength	35
4.2.4.	Impact of the poloxamer type on gel strength.....	37
4.2.5.	Effect of the addition of PEO and PPO on gel strength	39
4.2.6.	Influence of protein load on gel strength	40
4.3.	Dissolution of PMT depots.....	42
4.3.1.	Effect of PMT molecular weight on dissolution of PMT depots.....	42
4.3.2.	Effect of gel concentration on dissolution of PMT depots	43
4.3.3.	Effect of the diisocyanates on dissolution of PMT depots	44
4.3.4.	Effect of the poloxamer type on dissolution of PMT depots.....	44
4.3.5.	Effect of PEO addition on dissolution of PMT depots.....	45
4.3.6.	Effect of protein load on dissolution of PMT depots.....	46

4.3.7.	Effect of temperature on dissolution of PMT depots.....	46
4.3.8.	Dissolution of pre-formed and in situ-formed PMT depots	47
4.4.	Cloud point of PMT solutions and gels	47
4.4.1.	PMT molecular weight effect on cp	48
4.4.2.	PMT concentration effect on cp	49
4.4.3.	Effect of diisocyanate structure on cp	49
4.5.	Injectability of PMT gels.....	50
5.	PMT depots for controlled protein delivery.....	55
5.1.	Protein precipitation in PMT systems.....	55
5.2.	Release of IgG from PMT gels	57
5.2.1.	Impact of PMT molecular weight on IgG release.....	58
5.2.2.	Impact of PMT concentration on IgG release	60
5.2.3.	Impact of IgG concentration on release from PMT gels.....	61
5.2.4.	Impact of diisocyanate structure on IgG release	63
5.2.5.	In situ-formed PMT depots for controlled IgG delivery.....	64
5.2.6.	IgG release from PMT depots at different temperatures.....	65
5.2.7.	Impact of PMT gel shelf-life on IgG release	66
5.3.	Integrity of released IgG	67
5.3.1.	Visible particles	67
5.3.2.	Turbidity	68
5.3.3.	SEC analysis	68
5.3.4.	Subvisible particles.....	68
5.3.5.	Intrinsic fluorescence	70
5.4.	Chemical stability of H7P	70
6.	Summary and outlook	72
6.1.	In situ cross-linked HA gels	72
6.2.	Thermo-responsive PMT gels	73
7.	References	75

1. Introduction

1.1. Biopharmaceutics and sustained release

Biopharmaceutics such as peptides, proteins and gene vehicles have become more and more important within the last decades [1]. Every year several new biopharmaceutics enter the market. Search for new targets for biopharmaceutics, as well as for new manufacturing and analytical technologies of biopharmaceutics, are ongoing worldwide. Nonetheless, there are some drawbacks for biopharmaceutics: (i) high costs for development and production, (ii) physical and chemical stability issues like unfolding, oxidation, aggregation and particle formation, (iii) mostly parenteral application via injection, resulting in immunogenicity concerns and in many cases the need for well-trained medical personnel and/or hospitalization [2-6].

To minimize the injection frequency, which may increase patient compliance and decrease hospitalization costs, sustained release could be an option [5, 7-9]. Numerous different sustained release systems for biopharmaceutics have already been studied. Among them microparticles, implants and hydrogels are the most frequently tested [9-12]. Each system offers a unique set of advantages and disadvantages. Microparticles may contain residual organic solvent and degradation products with negative impact on protein stability and biocompatibility [11, 13-16], and lead to high production costs [9, 14]. On the other hand, a large variety of available microparticle forming polymers allows a wide range of drug characteristics, drug loading, and release profile [9]. Implants have to be administered through needles with large diameter or by surgery, causing pain and reduced patient compliance [17], but their less restricted size and the possibility to use non-biodegradable materials offers further increased flexibility in drug loading and very long release periods of up to several years [9]. In hydrogels drug load and homogeneity as well as the available release period are limited (hours to days), and increased viscosity might restrict the ease of application [5, 18]. However, hydrogels are especially interesting for the controlled delivery of protein pharmaceuticals as they offer an aqueous environment and usually mild fabrication conditions (aqueous media, room or lower temperature), both being beneficial in terms of protein stability and biocompatibility [5, 16, 18].

Hydrogels consist of an insoluble, three-dimensional, porous, hydrophilic polymer network, enabling high water content and a semi-solid character [5, 18, 19]. The semi-solid mechanical properties originate from physical or chemical polymer-polymer interactions [20-22]. Hydrogel-forming materials are a heterogeneous group of hydrophilic molecules and can be classified by their chemical structure, origin, size, and many other parameters [18, 23]. Drugs can be physically embedded in the gel matrix and subsequently released by diffusion or matrix erosion/disintegration, rendering slowly dissolving, high-density gel networks especially interesting [5, 18]. However, gels with high network density might be too stiff for injection, necessitating surgical application [18]. To overcome administration issues, so called in situ-forming hydrogels are interesting and emerging systems for controlled drug delivery by s.c. or i.m. application [18, 24]. They offer low viscosity prior to application, and form mechanically stable gels in situ by a specific physical or chemical trigger such as temperature or pH [25]. To achieve in situ-forming hydrogels specific limitations have to be overcome: (i) the correct viscosity to enable both syringeability in the low viscosity state and sufficient mechanical stability of the formed gel depots at the application site of interest; (ii) a fast network-formation speed, limiting diffusion of the gel-forming polymer and drug upon injection; (iii) maintaining biodegradation and biocompatibility [18, 25]. The main focus of this thesis is to establish an in situ-hardening hydrogel for sustained protein delivery.

1.2. In situ-forming hydrogels by click-cross-linking in presence of protein

Chemical in situ cross-linking of polymers is characterized by covalent bond formation between individual polymer molecules [5, 20]. This leads to a strong increase in molecular weight and, ideally, to a well-defined three-dimensional network structure. Furthermore, chemically cross-linked molecules offer a reduced solubility compared to linear molecules of the same molecular weight [26]. As they have an increased capacity of swelling (i.e., uptake of water) compared to unmodified polymers [27-29], chemically cross-linked polymers show increased hydrogel forming capacity compared to linear polymers [18].

The number of macromolecules which can be utilized for gel formation via chemical cross-linking is limited as the chemical cross-linking requires accessible reactive moieties on the initial molecule. In addition, the position of the reactive moiety within the

macromolecule is important: terminal functionalities can be used for chain elongation, leading to an increased M_w but not to actual cross-linking and network formation; instead, cross-linking between reactive functional groups on non-terminal monomers within the macromolecule chain is required. Many well-known polymers, like PEG or PLGA, lack moieties that fulfil these criteria. Many approaches to introduce suitable chemical properties for cross-linking by chemical derivatization of polyacrylates, PEG, polysaccharides such as Hyaluronic acid, and peptides or structural proteins have been published [5, 20, 21].

1.2.1. Hyaluronic acid

In this study hyaluronic acid (HA) is chosen, being an intensively studied polymer for pharmaceutical and medical applications [30-36]. HA is a highly water soluble linear polymer of a β -D-glucuronic acid (GlcUA) and β -N-acetyl-D-glucosamine (GlcNAc) disaccharide called Hyaluronan (Fig. 1.1). HA is biocompatible and biodegradable, and is commercially available in molecular weights ranging from a few kDa to several MDa [37-39]. Low molecular weight species < 10 kDa can interact with specific Hyaluronan receptors, inducing angiogenesis [39]. Also a pro-inflammatory effect of low molecular weight HA species, but excellent safety profile for the medium and high molecular weight species, are reported [40, 41]. There is no evidence for negative effects on protein stability by HA. In contrary, Meyer et al. showed that the stability and activity of a recombinant granulocyte colony stimulating factor is maintained upon sustained release from viscous HA solutions within four to five days in vivo [42]. HA was also shown to sustain peptide release for hours to days [43, 44]. This makes medium to high M_w Hyaluronic acid a preferred hydrogel platform for protein pharmaceuticals [32]. In this study a 100 kDa HA quality is chosen.

However, HA gels readily disintegrate in aqueous body fluid, and HA has a short half-life [32]. In order to enhance sustained protein release properties HA has been modified, e.g. by esterification, to yield an increased half-life and reduced water solubility [45-48]. This makes HA an interesting model for chemical cross-linking in presence of protein, developing an injectable, protein loaded hydrogel.

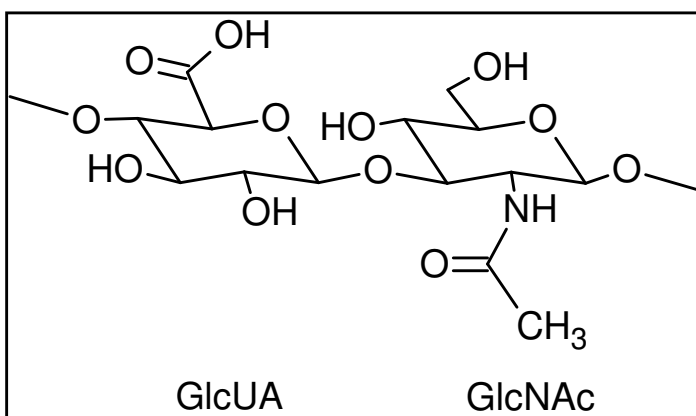


Fig. 1.1: The Hyaluronan monomer

HA contains two types of accessible reactive moieties: hydroxyl groups and free carboxylic acid groups. Reactions available to link these functionalities, e.g. via active-ester intermediates like NHS-esters, will lead to significant intramolecular cross-linking as well as cross-reactions in presence of proteins, as most proteins also contain hydroxyl and carboxylic acid groups. Consequently, HA has to be derivatized to introduce a new functionality that allows selective cross-linking reactions in presence of protein. Several methods to introduce a large diversity of functional groups into HA are reported in literature [45, 49-56]. For the cross-linking of HA in presence of protein introducing alkyne and azide groups is especially attractive. Those two functional groups can undergo a [3+2] cycloaddition (or 1,3 dipolar cycloaddition) to form triazole rings [57-60]. This reaction is frequently utilized in polymer and material sciences [58, 61-63].

1.2.2. Click-cross-linking HA

To start the azide-alkyne cycloaddition an activation of the alkyne is required – which can be achieved by elevated temperature, metal catalysis (mostly Cu(I) is used), or by usage of permanently activated electron-deficient or strained cyclic alkynes [57, 59, 61, 64-72]. The use of elevated temperatures may result in protein damage. Furthermore, this reaction is not regioselective [59]. The Cu(I) catalyzed azide-alkyne cycloaddition (CuAAC, also referred to as Huisgen-Reaction), is one of the most frequently used click-reactions [59, 70]. It is irreversible, offers high reaction rates and yields in aqueous systems, and is highly selective (Fig. 1.2). As neither native peptides, proteins or nucleic acids contain azide or alkyne moieties, no side reaction with biopharmaceutics occurs [73]. Successful usage of CuAAC in

living environments is reported in literature, despite the potential toxic effects of copper ions [60, 65, 73, 74]. The metal-free alternatives might further enhance biocompatibility due to the lack of metal ions, but require more complex alkyne-structures, e.g. strained cyclic alkynes [75-79], which are less accessible than terminal alkynes. Triazoles, the final product of the azide-alkyne cycloaddition, are inert and biocompatible [80]. Thus, the CuAAC is an appropriate reaction to cross-link azide or alkyne derivatives of HA in presence of protein. For later studies, a transition to metal-free alternatives, further enhancing the safety profile, could be possible.

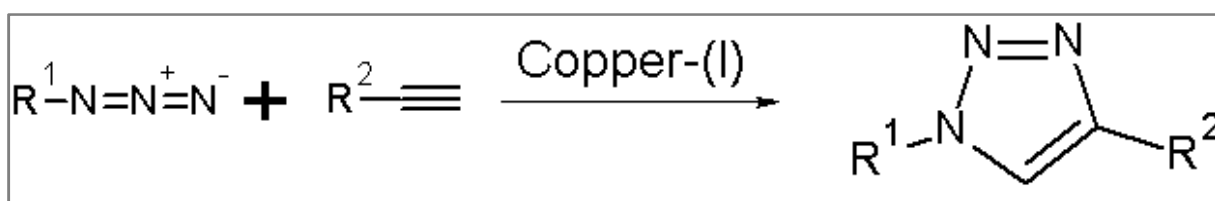


Fig. 1.2: The Cu-I catalyzed azide-alkyne cycloaddition

To cross-link HA by CuAAC three options are possible: (I) prepare and cross-link two HA qualities, one bearing azide groups, the other one terminal alkyne groups [81]; (II) synthesise and cross-link HA derivatives with a mixture of both azide and alkyne functionalities on each molecule, which, however, would most likely result in substantial intramolecular ring-formation; (III) attach either azide or alkyne to HA and add a corresponding bis-azide or bis-alkyne linker molecule [82]. Major benefit of the latter method is the flexibility of the linker molecule (in both chemical structure and concentration), which provides control over the mesh density formed by cross-linking. This mesh density is crucial to embed and release protein from the gel matrix and needs to be adjusted properly [5, 26, 83, 84].

To generate controlled release formulations based on cross-linked HA, the cross-linking has to induce a significant increase in molecular weight and, maybe, viscosity. The cross-linked HA has to show a reduced solubility in comparison to unmodified HA to become a potential controlled release hydrogel material with adequate sustainability in the body. In this study 100 kDa HA was modified with 11-Azido-3,6,9-trioxaundecane-1-amine (Az3OA) to yield azido derivatized HA (dHA, Fig. 1.3) with a known degree of substitution (DoS) and, thus, number of azide residues per HA chain. The dHA concentration was set to 2.5 mg/ml – at this concentration, the viscosity is still low enough to ensure easy handling, and an increase in viscosity due to cross-linking should be easily notable.

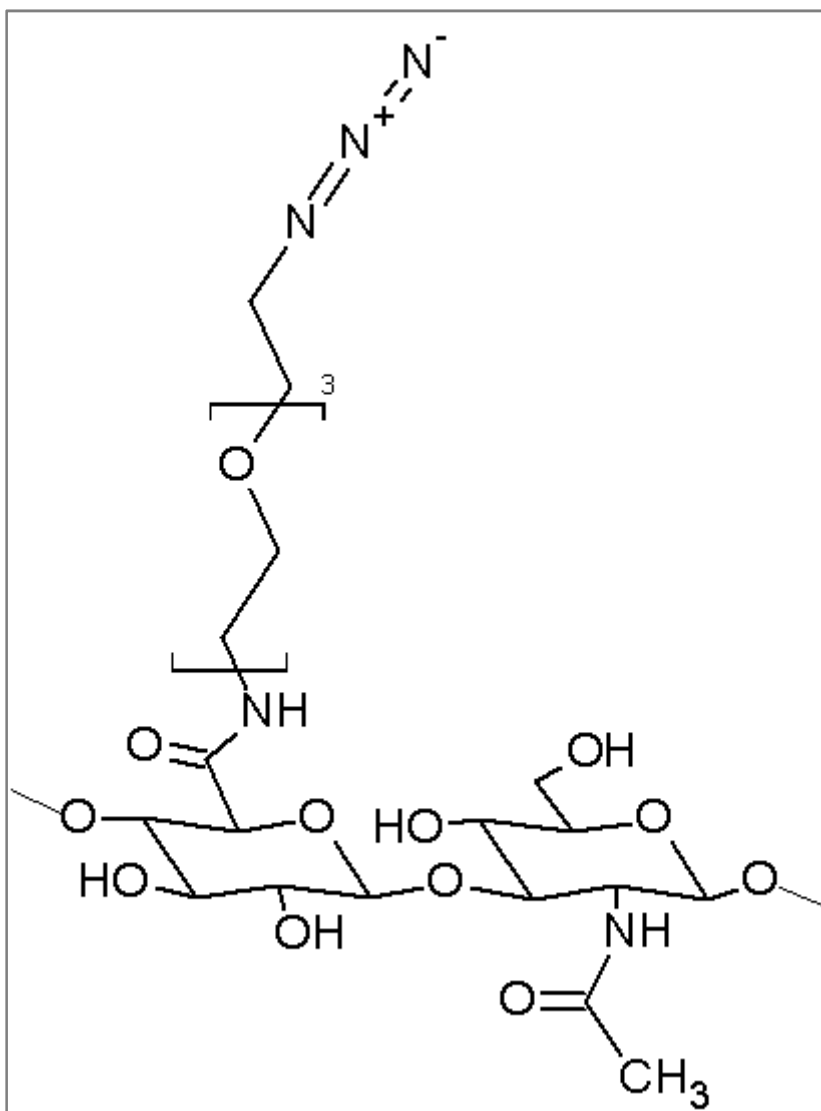


Fig. 1.3: Chemical structure of an Hyaluronan monomer derivatized with Az3OA.

The linker based approaches published in literature use low molecular weight lipophilic dialkyne linkers, leading to harsh reaction conditions and the use of organic solvent [49, 82]. Also the shortness of the linker molecules appears less suitable for the entrapment of large molecular weight components like proteins [5, 26, 83, 84]. Therefore, the more hydrophilic Alkyne-PEG-Alkyne (APA) linker with 1 kDa M_w was chosen (Fig. 1.4). Its solubility in water is still limited to approx. 0.5 mg/ml, corresponding to approx. 1.0 mM alkyne. Increasing the M_w of APA might increase the mass solubility [mg/ml] due to an increased number of hydrophilic ethyleneoxide blocks. Also the molar solubility [mM] may be increased. However, for the intended cross-linking process the alkyne concentration is more relevant and the chosen APA represents an acceptable compromise.

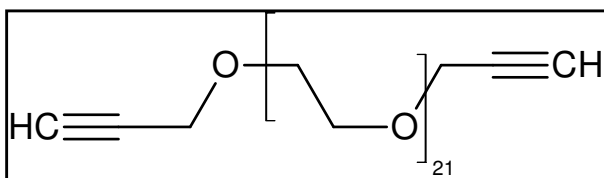


Fig. 1.4: The APA linker

Usually, CuAAC reactions and their copper-free derivatives use large excess of alkyne over azide [63, 70, 85]. For cross-linking dHA this large excess of alkyne would be disadvantageous, rendering a high degree of only single-sided linker attachment to HA. A high azide:alkyne ratio, however, slows down the reaction rate [63, 70, 85]. As a compromise an azide:alkyne ratio of 1.2 was chosen.

As common for CuAAC systems, ascorbic acid was used to generate Cu^+ from CuSO_4 in situ and both copper and ascorbic acid were used in large molar excess compared to the alkyne [63, 70, 86]. Cross-linking was carried out at 20 °C in PBS, as this is reported to yield sufficient reaction rate and efficacy of the cycloaddition without negative impact on protein stability [61, 64, 70, 72].

1.3. In situ-forming thermo-responsive hydrogels

Physical in situ cross-linking of hydrogel forming polymers is based on varying the strength of inter- and intramolecular hydrophilic and lipophilic interactions of the polymer chains in solution, inducing swelling or de-swelling of the polymer matrix [18, 22, 25, 87]. One of the most intensely studied class of physically cross-linked hydrogels are thermo-responsive, or thermo-reversible, systems [5, 25, 87]. Most thermo-responsive hydrogels are based on amphiphilic block-co-polymers [88]. Important examples are poloxamers, Poly(N-isopropylacrylamid) (pNiPAAm), Poly(butylene terephthalate-polyethyleneoxide) (PolyActive®), and Poly(lactic-co-glycolic)-polyethyleneoxide block-co-polymers [5, 25, 89].

Thermo-reversible hydrogels are characterized by the lower critical solution temperature (LCST). For systems with polymer concentration higher than approx. 10 % (w/v) instead LCST the term volume phase transition temperature (VPTT) is often used [90]. At this temperature polymers change from a solubilised, swollen sol state into a more condensed, precipitated gel state [25, 90]. The condensed state is characterized by organized molecular patterns such as micelles or lyotropic crystalline structures [88, 91-93]. Water is present in hydrophilic

domains or between hydrophilic domains of the condensed state [25, 90]. The rearrangement is caused as hydrogen bonding between the polymer and water becomes unfavourable compared to polymer–polymer and water–water interactions [87]. Micelles might already be present in the sol state but their concentration increases roughly linearly with temperature, until either saturation is reached, where all polymers are part of a micelle, or the volume density of micelles is so high that they lock into a crystalline structure [92]. The process of micelle formation and subsequent micelle packaging is also described in [94-96] and illustrated in Fig. 1.5.

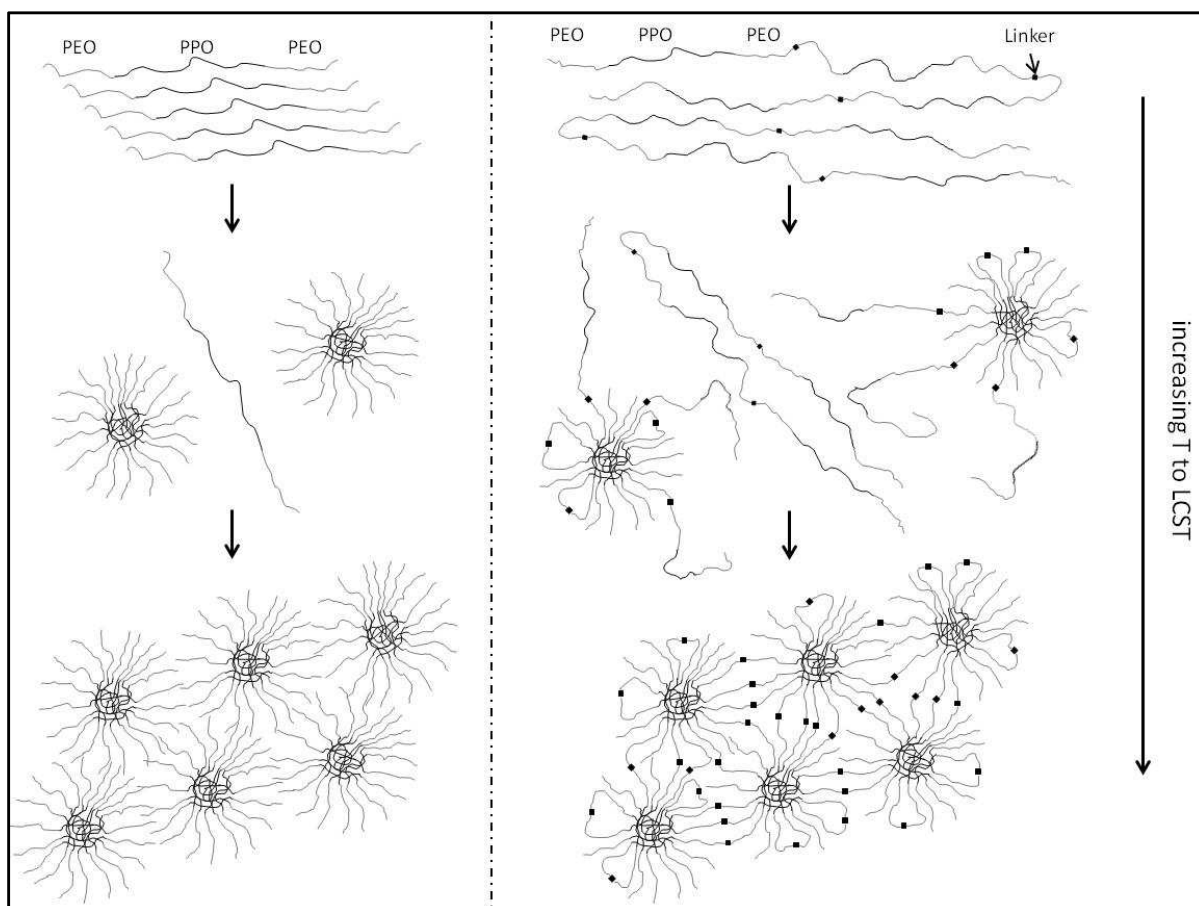


Fig. 1.5: Schematic image of block-co-polymer (e.g. poloxamer, left) and chain-elongated block-co-polymer (e.g. PMT, right) forming micelles and packed micelle structures upon warming above the LCST.

Increasing the temperature even further leads to decreasing intermicelle interaction [92] and, therefore, gel weakening. Obviously, besides temperature also the polymer concentration plays an important role [92, 96-99]. In literature several examples of gel formation by thermo-responsive polymers can be found. E.g. poloxamer 403 (5.8 kDa total

M_w , consisting of 30 % w/w PEO attached to a 4 kDa PPO block) forms gels at approx. 20 % (m/m) concentration and 40 °C by formation of cubic phases [100]. At lower and higher temperatures gels can still be formed using higher poloxamer 403 concentrations of up to 40 %. To form gels poloxamer 407 (12.6 kDa with 70 % PEO and a 4 kDa PPO block) requires slightly lower gel concentration than poloxamer 403, approx. 15 % at 37 °C [99, 100]. For PLGA-PEG polymers a concentration of 23 % is reported to yield mechanically stable gels between 30 and 40 °C [101]. Garripelli et al. showed that 25 % chain-elongated poloxamer 304 (5.9 kDa, 40 % PEO, 3 kDa PPO block) and 205 (4 kDa, 50 % PEO, 2 kDa PPO block) polymers show a strong increase in viscosity at approx. 20 °C [102].

1.3.1. Thermo-responsive hydrogels for controlled protein delivery

Many studies have been performed to analyse the suitability of thermo-responsive hydrogels for controlled drug release purposes, specifically proteins [93, 103-105]. Johnstan et al. achieved a release of Interleukin-2 (IL-2) from a poloxamer 407 gel for several hours both in vitro and in vivo [106]. BSA delivery with pNiPAAm-PEG gels continued for approx. 5 days in vitro [107]. Sustained growth hormone release can be achieved by PLGA-PEG-PLGA gels [108]. Thus, the hydrogels exhibit a rather fast release compared to other parenteral depot systems like PLGA microparticles or implants [5].

As poloxamer is approved by the FDA for parenteral use and products including this excipient (e.g. RheotRX® or Orenicia®) are marketed, it is a highly interesting system for further optimization [93, 109]. Although poloxamer 407 gels dissolve in PBS in less than two days even at concentrations above 30 % [17] they are described as potential in situ gelling controlled release vehicle for hGH, Insulin, GnRH or IL-2 [87, 106]. However, poloxamer 407 gels render only release times of less than 24 h [99]. To enhance the mechanical stability and slow down erosion and, thus, drug release, poloxamer molecules can be grafted to less water soluble materials like polyacrylates or PLGA [99, 110, 111]. Thereby biodegradability may get lost and copolymers that are not approved by the authorities are formed.

Other studies increased the M_w of poloxamer 407, 205 or 304 by chain-elongation to trimers and tetramers [102, 112, 113] to yield prolonged release times of days to weeks. This is a very promising approach, as long as the final M_w of polymers or their biodegradation products remain low enough to ensure renal extraction of the non-biodegradable PEO/PPO

(approx. < 40 kDa) [114, 115]. The thermo-responsive hydrogels studied in this thesis follow the same idea, employing oligomers of the less water soluble poloxamer 403. The oligomers are designed to increase gel half life and protein release to more than one week while maintaining syringeability through 20 G (or smaller) needles.

Fig. 1.5 demonstrates the changes induced by poloxamer chain-elongation. The micellar network becomes additionally covalently linked. This micelle bridging causes an increase in mechanical strength of the formed gel and less flexible pores with limited macromolecular diffusion [116-119].

An additional requirement for thermo-responsive hydrogels is protein stability within the system. Due to the aqueous environment adequate stability is to be expected and literature typically states good protein stability [99, 108, 120, 121]. However, the integrity of protein pharmaceuticals within the hydrogel sample (preparation), as well as the activity and safety of released API have to be evaluated critically [4, 24, 122].

1.3.2. PolyMaterials Thermopolymers (PMTs)

The Thermopolymers by Polymaterials AG (PMTs) are derived from poloxamer by chain-elongation using diisocyanates (Fig. 1.6). The urethane groups linking separate poloxamer molecules undergo hydrolysis under physiological conditions [123]. Poloxamers themselves are regarded as fast eroding and non-toxic in s.c. and i.m. parenteral formulations [87, 99]. Furthermore, poloxamer can be extracted by the kidneys [87]. Thus, PMTs can be considered biodegradable and biocompatible.

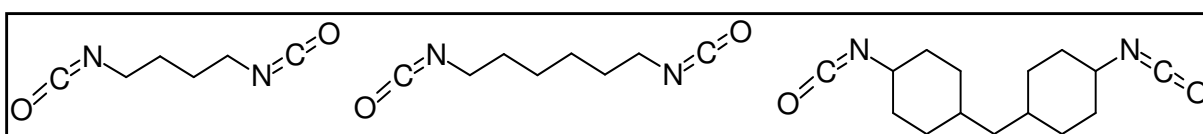


Fig. 1.6: Chemical structures of diisocyanates (DIC) and corresponding bifunctional urethane linker (BUL). From left to right: Butyldiisocyanate (BDI), Hexamethylene diisocyanate (HDI) and H₁₂-4,4'-methylene diphenyl diisocyanate (MDI).

1.4.Aims

The aim of this thesis is to establish in situ-forming, injectable depot formulations for protein pharmaceuticals on the basis of either click-cross-linked HA or thermo-responsive PMT gels. Release periods of days to weeks, biocompatibility, biodegradation and maintained protein stability are aimed for. As the required HA derivative is not commercially available, the derivatization process of HA is discussed. To characterize both potential hydrogel systems the ease of preparation and application, gel hardness and stability, as well as protein release and integrity are studied. The results of both hydrogel systems are critically discussed and compared with data for established materials.

2. Materials and Methods

2.1. Materials

2.1.1. Solvents

Throughout the thesis water from an Elga (Celle, D) PureLab Plus or a Sartorius (Göttingen, D) Arium system was used. Sulfuric acid (Aldrich, Taufkirchen, D) is 98 %, Ethanol (Th. Geyer, Renningen, D) is 96 %. DMSO and THF (both Fluka, Buchs, CH) are analytical grade and dried over molecular sieve 4 Å (Sigma, Taufkirchen, D). 0.1 and 1.0 M HCl and NaOH (all VWR, Ismaning, D) are analytical grade standard solutions.

2.1.2. Salts, buffers and reagents

Table 2.1 shows a list of salts and reagents, their corresponding provider and grade. APA and EDC were stored under nitrogen atmosphere at -20 °C. Az3OA was stored under nitrogen atmosphere at 2-8 °C. All other substances were stored at RT.

Name	Provider	Grade
NaCl	Fluka (D) and Aldrich (D)	analytical
NaH ₂ PO ₄ waterfree	Sigma (D)	analytical
Na ₂ HPO ₄ waterfree	Fluka	analytical
CuSO ₄ pentahydrate	Sigma	analytical
Ascorbic acid	Sigma	reagent
2-(N-morpholino)ethanesulfonic acid (MES)	Sigma	analytical
N-Hydroxysuccinimide (NHS)	Aldrich	≥ 98 %
1-Ethyl-3-(3-dimethylaminopropyl)carbodiimide hydrochloride (EDC)	Sigma	≥ 99 %
11-Azido-3,6,9-trioxaundecane-1-amine (Az3OA)	Aldrich	≥ 90 %
Alkyne-PEG-Alkyne 1.0 kDa (APA)	Creative PEGworks (US)	≥ 98 %
Carbazole	Sigma	≥ 95 %
Sodium Dodecyle Sulfate (SDS)	Sigma	≥ 99 %

Table 2.1: List of salts and reagents, their corresponding provider and grade.

Two different buffers were used: 10 mM isotonic PBS pH 7.2 and 50 mM MES buffer pH 4.0. If not noted otherwise, they will be referred to as “PBS” and “MES buffer” in the remaining text. PBS contained 335.9 mg NaH₂PO₄, 1007.9 mg Na₂HPO₄ and 7,595 mg NaCl per litre. MES buffer contained 9.76 g MES per litre. pH was adjusted at RT by drop wise addition of either HCl or NaOH under continuous stirring. Buffers were filtered (0.2 µm PES 50 mm Ø by Sartorius) prior to usage.

Further solutions used were saturated NaCl, 1 % SDS, 5 mM CuSO₄ (in PBS), 50 mM ascorbic acid (in PBS), 1 mg/ml Carbazole (in Ethanol) and 1 mg/ml APA (in DMSO). Saturated NaCl und 1 % SDS were stored at RT. All other solutions were stored at 2-8 °C and allowed to reach RT prior to usage.

2.1.3. Proteins

Spray dried lysozyme from hen egg white (22,300 units per gram, M_w 14.3 kDa) was purchased by Dalian Greensnow (Dalian, CN) and stored at 2-8 °C. 100 mg/ml lysozyme stock solutions in PBS were freshly prepared and filtered (0.2 µm 25 mm Ø PES syringe filters by VWR).

A 2 mg/ml solution in PBS of a recombinant human IgG1 with approx. 150 kDa M_w was used as bulk. This solution was concentrated in PBS to approx. 20 mg/ml using VivaFlow 50 PES (Sartorius), filtered (0.2 µm 25 mm Ø PES syringe filters), and further concentrated to approx. 100 mg/ml using 20 ml VivaSpin PES with mwco 30 kDa (Sartorius).

2.1.4. Hyaluronic acid and derivatives

100 kDa and 1.0 MDa sodium hyaluronan API grade (HA) were purchased from Shiseido (Tokyo, JP). Three different HA derivatization processes were carried out, each using approx. 500 mg HA and a final lyophilisation step as described in [81] (primary drying at -22 °C and 160 mTorr for 20 h, secondary drying at 20 °C and 75 mTorr for 22 h using an Epsilon 2 by Martin Christ, Osterode, D). Corresponding HA derivatives are depicted as dHA-1 to 3 in the following text. Yields (w/w) were calculated as total mass after freeze-drying divided by the sum of total HA mass and Az3OA mass employed.

dHA-1 was obtained as described in [81] by dissolving 100 kDa HA in approx. 20 ml MES buffer. This solution was transferred to a solution of 232 mg EDC and 139 mg NHS in 5 ml MES buffer under stirring. 480 µl Az3OA were added and the reaction mixture was incubated at RT for 24 h under continuous stirring and subsequently dialyzed for 24 h against 4 l saturated NaCl and finally three times for 24 h against 4 l water using a 14 kDa mwco cellulose membrane by Roth (Karlsruhe, D).

For dHA-2 dialysis was replaced by centrifugation of the reaction mixture using VivaSpin 20 with 10 kDa mwco (Sartorius). The material was concentrated and washed with 5 ml saturated NaCl and finally water.

For dHA-3 70 ml MES buffer, 489 mg EDC, 293 mg NHS and 1010 μ l Az3OA were used. Purification was analogue to dHA-2.

2.1.5. PMTs and poloxamers

PolyMaterials Thermopolymers (PMTs) were provided by PolyMaterials® AG (Kaufbeuren, D). They were derived from poloxamers purchased from Sigma. Molecules of one type of poloxamer, or defined mixtures of several poloxamers, respectively, were covalently linked to undergo chain-elongation in an organic solvent using a special catalyst as well as three different diisocyanates (DIC) as linkers: Hexamethylene diisocyanate (HDI), H₁₂-4,4'-methylene diphenyl diisocyanate (MDI) and Butyldiisocyanate (BDI). Thus, complex multiblock copolymers of "ABAC" building block structure with A being PEO, B PPO and C a small bifunctional urethane linker were formed. Each polymer was subsequently purified and dried. Polymaterials certified PMTs to be free of catalyst, unreacted DIC, organic solvent and other relevant impurities. Biodegradation to poloxamer remnants by urethane hydrolysis allows renal extraction of the material.

Table 2.2 lists the PMTs used throughout this study. The short name given therein is of a XyZ type, with X indicating the DIC (H for HDI, M for MDI and B for BDI), y representing the average number of poloxamer unimers per PMT (based on M_w information provided by PolyMaterials), and Z depicting the poloxamer type(s) used (P referring to poloxamer 403, F to poloxamer 407, f to poloxamer 308, respectively). E.g. H6P stands for 6 poloxamer 403 (6P) unimers linked by HDI (H). H1.5P1.5F1.5f also used HDI as linking DIC; but molecules of this PMT contained on average 1.5 poloxamer 403 (1.5P) units, 1.5 poloxamer 407 (1.5F) units and, at the same time, 1.5 poloxamer 308 (1.5f) units. As reference materials unmodified poloxamer 403 (Sigma) and poloxamer 407 (BASF, Ludwigshafen, D) were used. Their corresponding M_w was 5.8 kDa (403) and 12.6 kDa (407), respectively. PMTs were stored at -80 °C and allowed to reach RT prior to processing. Unmodified poloxamers were stored at RT.

Short name	Batch number	M _w [kDa]
H4P	GAM19	26
H6P	AP1384 / AP1976	36
H7P	AP2102	43
H8P	AP1977	45
H11P	GAM23	64
M6P	AP1975	37
B7P	AP1476 / AP1966	42
H5P2F	GAM36	51
H2.5P2.5F	AP2047	48
H1.5P1.5F1.5f	AP2087	49
H4F	AP2035	55

Table 2.2: list of PMT batches.

To generate PMT or poloxamer gels, an adequate amount of dry polymer was weighted into a 2 or 5 ml male luer lock syringe (Braun, Melsungen, D) with removed plunger. If required, proper amounts of 1, 4 or 20 kDa polyethyleneglycole (PEG, all by Aldrich), or 2 or 4 kDa polypropyleneglycole (PPO, both by Aldrich) were added to the dry PMT/poloxamer. Using female-female luer adapters (Braun), a second, empty male luer lock syringe of identical size was connected. The necessary volume of cooled (2-8 °C) PBS was added on top of the polymer in the open part of this two-syringe-system. If required, also adequate amounts of cooled (2-8 °C) lysozyme, IgG or FITC-Dextran 150 kDa (Aldrich) stock solutions were added. The plunger was reinstalled, the air removed and the two-syringe-system was cooled to 2-8 °C for 15 min. Subsequently, polymers were dissolved and solutions homogenised by repeated transfer from one syringe to the other and back for approx. 2 min. After this cycle of cooling and homogenisation was repeated for 3-4 times samples were incubated at 2-8 °C for 12 h. This process was repeated until the polymers were completely dissolved and samples were homogenous. Subsequently, all samples were stored at 2-8 °C.

2.1.6. Fluorescence labelled dHA

Atto 655 labelled 100 kDa dHA was prepared by incubating 4 nmol of the corresponding dHA with 200 nmol Atto 655 alkyne (Atto Tec, Siegen, D) in 100 µl PBS with 0.2 mM CuSO₄ and 2.0 mM ascorbic acid in the dark at RT for 3 d and subsequent dialysis against water by centrifugation using VivaSpin 500 with mwco 5 kDa. The excess of dye, copper and ascorbic acid as well the long reaction times were necessary to secure complete labelling of all azide

moieties present in dHA. As reference 100 kDa HA was processed analogously. Filtrates were collected and supernatant volume was restored to 100 μ l with water. Dye concentration of the reference sample filtrate was monitored by fluorescence (ex. 663 nm, em. 684 nm) using a Cary Eclipse Fluorescence Spectrophotometer (Varian, Palo Alto, US) and the centrifugation procedure was repeated until no more dye was detected in the reference filtrate (approx. 10 to 15 times).

2.1.7. Cross-linked HA

dHA with known DoS (refer to chapter 2.2.3.), APA, CuSO_4 and ascorbic acid were mixed in PBS to yield final concentrations of 2.5 mg/ml dHA, 0.2 mM Cu^{2+} and 2.0 mM ascorbic acid as well as an azide to alkyne ratio of 1.2 : 1.0. This mixture was incubated at RT for 3 days to achieve cross-linked HA (cHA). Excess of azide as well as copper and ascorbic acid were necessary to suppress single-sided linker binding.

2.2. Methods

2.2.1. Determination of protein and FITC-Dextran concentration

To determine protein concentrations an Agilent (Waldbronn, D) 8453 UV-Vis spectrometer was used. Samples were analysed in quartz cuvettes at 280 nm and 20 °C at absorbance values between 0.1 and 1.0. ϵ_{280} was 2.64 ml mg^{-1} cm^{-1} for Lysozyme and 1.5875 ml mg^{-1} cm^{-1} for IgG.

Alternatively, concentration of protein monomers, oligomers and fragments was analysed by HPSEC using either a Tosoh (Stuttgart, D) TSK Gel G5000 PWXL 7.8 x 300 mm (for lysozyme, FITC-Dextran and IgG) or a Tosoh TSK Gel SuperAW 6000 6.0 x 150 mm column (only IgG) and one of two different Agilent HPSEC systems with each Tosoh SWXL guard column, 0.333 ml/min PBS, injection of 50 to 100 μ l cooled (5 °C) samples using a 100 μ l dosing loop at 100 μ l/min followed by needle wash with PBS, column temperature 20 °C, UV absorbance detection at 280 nm, manual peak integration with Agilent ChemStation for LC systems B.02 and quantification against a freshly prepared concentration series of the corresponding material. The first system was used for protein samples with known or estimated concentration > 0.1 mg/ml and employed 1100 series quaternary pump G1311A, sample

thermostat G1330A, autosampler G1329A, column compartment G1316A and DAD G1315A. The second system employed was composed of a 1200 binary pump G1312A, a sample thermostat G1330B, an autosampler G1329A, a column compartment G1316A, a VWD G1314B and an HP (Palo Alto, US) FAD 1046A (ex. 280 nm, em. 315 nm for protein, ex 492 nm, em. 518 nm for FITC-Dextran). FAD signals were used for protein concentrations < 0.1 mg/ml as well as for FITC-Dextran quantification, otherwise VWD signals were used.

2.2.2. Determining the degree of substitution of dHA

To determine the degree of substitution (DoS) of derivatized HA (dHA) the corresponding dHA was labelled with Atto 655 nm fluorescent dye (refer to chapter 2.1.6.). After restoring to 100 µl volume both sample and reference supernatant were analysed with an Agilent 8453 UV-Vis spectrophotometer with Agilent 89090 temperature control unit at 663 nm and 20 °C. ϵ_{663} was $1.25 \cdot 10^5 \text{ mol l}^{-1} \text{ cm}^{-1}$. Dye found in the reference supernatant was considered as unspecific binding.

The number of specifically bound dye molecules represents the number of azide moieties per dHA molecule. To determine the DoS this number of azide moieties was correlated with the average number of Hyaluronan monomer per 100 kDa HA molecule (274).

2.2.3. HA quantification by modified carbazole method

Based on the method using carbazole to quantify uronic acid species by Dische et al. as well as modifications of this method published in later years [124-126] 30 µl HA samples in PBS were mixed with 160 µl sulfuric acid in 2 ml secure closure caps (Eppendorf, Wesseling-Berzdorf, D) and incubated in an aluminium heating block at 90 °C for 30 min. After cooling to RT 12 µl 1 mg/ml Carbazole in ethanol were added and the sample was incubated in the dark at RT for 2 h. Colour intensity was detected at 530 nm in a 96 well quartz well plate using a FLUOstar Omega (BMG Labtech, Ortenberg, D). Employing a concentration series of 100 kDa HA as well as comparing 100 kDa with 1 MDa HA this method was found to be applicable from approx. 30 µg/ml to 1 mg/ml HA, but only semi-quantitative information is gained.

2.2.4. Molecular weight analysis of HA species

To gain M_w information of HA, dHA and cHA, 100 μ l 2.5 mg/ml samples of HA, dHA or cHA were injected to an HPSEC system employing Tosoh SWXL guard column followed by a Tosoh TSK Gel G5000 PWXL 7.8 x 300 nm and a Tosoh TSK Gel SuperAW 6000 6.0 x 150 mm using an Agilent 1200 binary pump G1312A at 0.6 ml/min PBS, sample cooling to 5 °C with 1200 sample thermostat G1330B, a 100 μ l dosing loop at 100 μ l/min and subsequent needle wash with PBS by a 1200 autosampler G1329A and 1200 column compartment G1316A at 20 °C. After discarding the first 7 ml elution volume 0.3 ml samples were collected manually until an elution volume of 10 ml followed by 0.6 ml samples until 14.2 ml elution volume were reached. HA concentration in each sample was subsequently determined by the modified carbazole method (refer to chapter 2.2.3).

Alternatively, 200 μ l 2.5 mg/ml samples of HA, dHA or cHA were centrifuged for 1 h using VivaSpin 500 with either 10 or 300 kDa mwco, respectively. HA concentration in both supernatant and filtrate were subsequently analysed by the modified carbazol method (refer to chapter 2.2.3).

2.2.5. Molecular weight analysis of PMTs

Using an Agilent HPSEC system with 1100 quaternary pump G1311A at 1 ml/min THF, SDV guard column, SDV 100 Å and SDV 10,000 Å (all by PSS, Mainz, D), 1100 sample thermostat G1330A at 5 °C, 1100 autosampler G1329A with 100 μ l dosing loop at 100 μ l/min and needle wash in THF, 1100 column compartment G1316A at 20 °C, 1200 RID 1362A and stainless steel capillaries (VWR), 75 μ l samples of approx. 5 mg/ml PMT with 1 % Acetone in THF were analysed. Relative retention times against acetone as internal standard were calibrated with a Polystyrene ReadyCal Kit by PSS.

2.2.6. Viscosity of HA species

An mVROC viscosimeter (RheoSense, San Ramon, US) equipped with an A05 chip (50 μ l flow channel) at 25 $^{\circ}$ C was used. Samples were transferred to 250 μ l Hamilton syringes (Fisher Scientific, Hampton, US) and equilibrated for 2 min to flush the instrument with 50 μ l samples at 50 μ l/min. Subsequently, measurements were performed in triplicates of 50 μ l at 50 μ l/min for each sample.

2.2.7. Gel strength of PMT/poloxamer gels

To analyse the hardening profile of PMT/poloxamer gels 0.5 g gel were placed on the Peltier element (10 $^{\circ}$ C) of an Anton Paar Physica (Ostfildern, D) MCR 100 rheometer equipped with a 50 mm 1 $^{\circ}$ stainless steel cone. The cone tip was then placed 42 μ m above the Peltier surface and excess gel was removed with soft tissue (VWR). After a hold time of 5 min a temperature ramp from 10 to 45 $^{\circ}$ C at 1 $^{\circ}$ C/min was employed and storage and loss modulus (G' and G'') were determined in oscillating mode at $f = 1$ Hz and $\gamma = 0.5$ % every 30 sec.

Alternatively, a TA.XT plus texture analyser (Texture Technologies, Hamilton, US) equipped with a 4.2 mm stainless steel punch was used. 0.5 g of each sample were transferred to a 1.5 ml secure closure cap (Eppendorf), cooled to 2-8 $^{\circ}$ C to secure a smooth and homogenous surface, subsequently placed in an aluminum heating block at a defined temperature (21-45 $^{\circ}$ C) with a hold time of 10 min before measurement. The punch penetrated into the gel for 40 s with a constant test speed of 0.05 mm/s and the maximal indentation force is considered the penetration resistance of this sample at the specific temperature.

2.2.8. Disintegration time of PMT gels

Approx. 0.5 g of cool (2-8 $^{\circ}$ C) gel were transferred to the wall of a lying 37 $^{\circ}$ C warm 50 ml tube (VWR) and hardened by incubation at 37 $^{\circ}$ C for 15 min to yield pre-formed depots. The tube was erected and placed in a shaking water bath ($f = 1$ Hz) at 32, 35, 37, 39 or 42 $^{\circ}$ C, and 20 ml of 32, 35, 37, 39 or 42 $^{\circ}$ C warm PBS, respectively, were added. Alternatively, depots were formed in situ by injection (1ml syringe and 4 cm 20G needle, both Braun) of 0.5 g cool (2-8 $^{\circ}$ C) gel into 20 ml PBS at 37 $^{\circ}$ C. Depot erosion was monitored visually on a daily basis for four days and then weekly for another twelve weeks.

2.2.9. Cloud points of PMT gels

Approx. 1 g of 2-8 °C gel was transferred to a 1.5 ml quartz glass cuvette, equilibrated at 2-8 °C for 15 min and analysed in an Agilent 8453 UV-Vis spectrometer equipped with an Agilent 89090 temperature control unit. After a hold time of 5 min at 10 °C a temperature ramp from 10 to 45 °C at 1 °C/min was employed and absorbance at 350 nm was measured every 30 sec. As most samples reached the instrument's detection limit, no mathematical fit of data curves could be applied. Instead, cloud points were defined as the lowest temperature with absorbance > 2.

2.2.10. Injection forces of PMT gels

1 ml luer lock syringes (Terumo, Eschborn, D) were filled with approx. 0.7 ml cool (2-8 °C) gel, equipped with 4 cm 20 G stainless steel needles (Braun), and allowed to reach RT. Subsequently, they were placed in a stand under a TA.XT plus texture analyser (Texture Technologies, Surrey, GB) equipped with a plastic punch (square area 1.13 cm²) and gels were injected into air at 100 µl/sec and RT.

2.2.11. Protein precipitation in PMT gels

To study protein precipitation in PMT gels protein loaded PMT gels were prepared (refer to chapter 2.1.5) and at defined time points images were taken. Alternatively, 0.5 g freshly homogenized gel were transferred to 1.5 ml secure closure caps (Eppendorf) and centrifuged at 5 °C and 10 kG for 60 min. Protein concentration in both supernatant and filtrate was determined by UV (chapter 2.2.2) at 5 °C.

2.2.12. Release of protein and FITC-Dextran from PMT gels

In a standard set-up approx. 0.5 g of cool (2-8 °C) gel, containing either defined amounts of lysozyme, IgG or FITC-Dextran, were transferred to the wall of a lying 37 °C warm 50 ml tube (VWR) and hardened by incubation at 37 °C for 15 min to yield pre-formed depots. The tube was erected and placed in a shaking water bath (f = 1 Hz) at 37 °C. To initialize release 20 ml of 37 °C warm PBS were added. Alternatively, pre-formed depots were processed at 35 or 39 °C, or depots were formed in situ by injection of 0.5 g cool (2-8 °C) gel through 4 cm 20 G

stainless steel needles into 20 ml PBS at 37 °C. In each case samples of 200 µl incubation liquid were sampled without replacement at defined time points and analysed by HPSEC. After the last sampling point depots were liquefied and dissolved in the remaining acceptor medium by cooling to 2-8 °C for 12 h and a final sample of 200 µl was taken and analysed. For further protein stability testing, some release experiments were performed under laminar air flow (LAF) conditions with pre-formed depots at 37 °C using pre-rinsed tubes. At defined time points samples of 2.0 ml were taken and replaced by 2 ml fresh 37 °C warm PBS.

2.2.13. Intrinsic fluorescence

200 µl samples taken from protein stability release experiments as well as 200 µl samples of freshly prepared IgG solution were transferred to 96 deepwell fluorescence plates (NUNC, Roskilde, DK). A Cary Eclipse Fluorescence Spectrophotometer (Varian) was used to detect intrinsic fluorescence emission spectra from 310 to 450 nm at constant excitation wavelength of 280 nm (5 nm threshold). Fluorescence spectra of freshly prepared IgG solutions (representing native IgG) and release samples were compared to determine alterations of secondary protein structure.

2.2.14. Turbidity, visible and sub-visible particles

Visible particles in the release sample were detected at RT following Ph.Eur. 2.9.20. A NEPHLA laboratory turbidimeter with 1.8 ml test tubes (all Hach Lange, Düsseldorf, D) operating at 860 nm and 90 ° scattering angle was used to determine sample turbidity. Results were depicted as formazine nephelometric units (FNU). Subvisible particles > 1, > 10 and > 25 µm were analysed via light obscuration with a PAMAS SVSS-C (PAMAS, Rutesheim, D). The instrument was flushed with 1 ml 1 % SDS and subsequently 3 ml water prior to usage. For each measurement 0.5 ml sample were used to flush the system, followed by particle measurement of three 0.3 ml sample fractions and another cleaning step with 1 ml water. After three measurements initial cleaning with SDS and water was repeated. Particle counts for three sample fractions of each measurement were averaged.

3. Click-cross-linked hyaluronic acid gels

3.1. Preparation and characterization of derivatized HA

By introducing azide groups to the carboxylic acid moieties of 100 kDa HA via active-ester synthesis three batches of derivatized HA (dHA-1 to 3) were prepared. A degree of substitution (DoS) of approx. 12 % is aimed for, corresponding to approx. 33 azide moieties per HA chain. This high number of azide groups would offer sufficient binding sites for linker molecules to foster a coherent network formation. This significant introduction of azide moieties and the corresponding reduction of free carboxylic groups are not considered to change the overall properties of HA [127]. However, a high DoS may trigger the undesired side reaction of intramolecular ring formation. Thus, there is no linear correlation between DoS and effective degree of cross-linking. Furthermore, if the DoS is too high, the resulting network could become too dense for protein release [83, 84].

As the overall yield for dHA-1 synthesis was only 25 %, the synthesis protocol was optimized without further analysis of dHA-1. The obtained dHA-2 material showed an overall yield of 79 %, but a low DoS of 1.25 %, corresponding to on average 3.4 azide groups per dHA molecule. Hence, further optimization of the synthetic protocol was performed and dHA-3 was formed with an overall yield of 75 % and DoS of 2.53 %, corresponding to 6.94 azide groups per molecule (see sections 2.1.4 and 2.2.2).

For similar materials derived from 200 kDa HA the degree of cross-linking after the cross-linking reaction can be determined by $^1\text{H-NMR}$ analysis as described by Crescenzi et al. [81], calculating integrals for the aromatic triazole protons as well as acetylene protons of the N-acetylglucosamine present in the HA chain. The number of triazole protons directly represents the number of cross-links, as long as cross-linking is performed with azide- and alkyne-modified HA without bi-functional linker. Using bi-functional linker approaches single-sided linker reaction can introduce triazole protons without cross-links. Acetylene protons indicate the number of N-acetylglucosamine units, representing the number of Hyaluronan monomers and therefore the HA chain length. The resulting degree of cross-linking was reported to be 8 to 21 % [49, 81, 82, 86]. However, using $^1\text{H-NMR}$ to determine the degree of cross-linking is limited by the low intensity of triazole peaks compared to acetylene signals and partial overlap of acetylene signals with other proton

signals. Furthermore, as HA is reported to have de-acetylated monomers [128-130], the HA chain length is underestimated by the $^1\text{H-NMR}$ method. Finally, the $^1\text{H-NMR}$ method cannot distinguish between inter- and intramolecular cross-linking. Therefore the degree of cross-linking as determined by $^1\text{H-NMR}$ has to be considered higher than the actual DoS.

The method used to determine the DoS in this study is based on complete labelling of all accessible azide groups and removal of unbound dye. Unspecific binding of the dye to 100 kDa HA was found to be as low as 0.04 dye molecules per HA chain. Potentially, the centrifugation step employed to remove free dye could lead to a loss in HA mass despite the fact that the mwco is tenfold lower than the HA M_w , leading to an underestimation of the true DoS. A possible explanation for the lower DoS of the obtained dHA materials compared to literature values is the different HA quality used in literature. Nevertheless, a 2.5 mg/ml dHA-3 gel in PBS was chosen for further analysis and cross-linking.

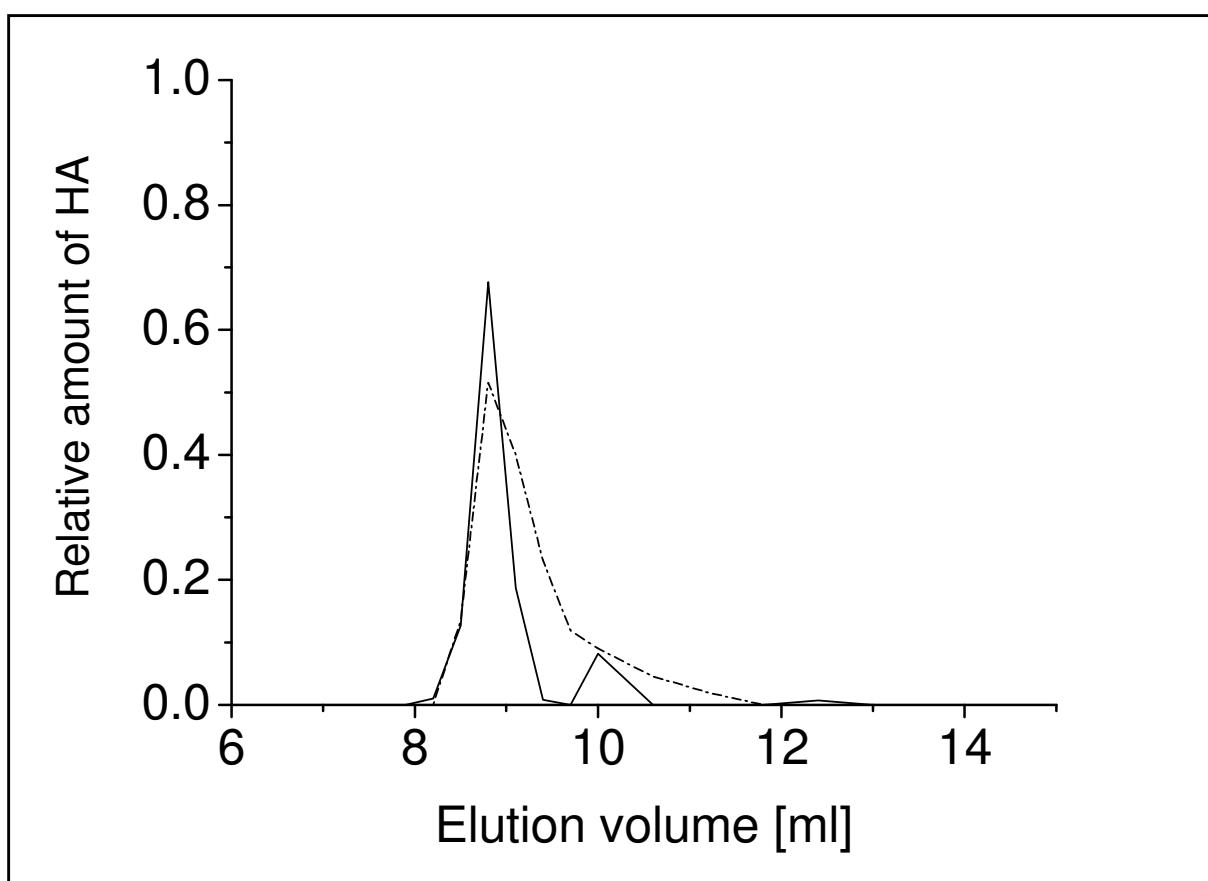


Fig. 3.1: SEC profile of dHA-3 (—) and 100 kDa HA (---).

The viscosity of 2.5 mg/ml dHA-3 as measured by mVROC analysis was 29.3 ± 2.4 mPas. 2.5 mg/ml unmodified 100 kDa HA showed 27.6 ± 3.4 mPas. Hence, derivatization shows no effect on viscosity. At a concentration of 2.5 mg/ml dHA-3 solutions show easy handling and manual syringability through 20 G needles.

To analyse M_w and M_w distribution of dHA-3 HPSEC analysis as well as centrifugation experiments were performed. Quantification of HA was performed using the modified carbazole method, although this method does not show good linearity and effects of HA derivatization, M_w , and M_w distribution are unclear.

In HPSEC dHA-3 showed a broad peak from 8.2 to 9.4 ml as well as a small peak at 10 ml elution volume (Fig. 3.1). Unmodified 100 kDa HA showed a very broad peak from 8.5 to 11.2 ml elution volume, reflecting a broad M_w distribution. After centrifugation through a 10 kDa mwco PES membrane 80.3 % of dHA-3 remained in the supernatant. For unmodified 100 kDa HA 74.3 % were found. Using a 300 kDa mwco membrane 1.44 % of d-HA3 and 1.56 % 100 kDa HA remained in the supernatant. Thus, esp. low M_w HA molecules were lost during the derivatization and purification process of dHA-3 (overall yield: 74 %), but still a detectable low M_w fraction remained. There is no indication for significant chain cleavage or unspecific cross-linking. The fact that a substantial fraction of 100 kDa HA passes the 10 kDa mwco membrane is due to the broad M_w distribution of HA and the stretched shape of HA in PBS [33, 131, 132].

3.2. Preparation and characterization of cross-linked HA

Cross-linking dHA should lead to a strong increase in M_w . Therefore, HPSEC and centrifugation experiments were performed with 2.5 mg/ml cross-linked HA (cHA). As reference material 2.5 mg/ml 1.0 MDa HA was used.

cHA showed a sharper SEC peak at approx. 9 ml elution volume (Fig. 3.2) compared to dHA-3. Furthermore, a second peak at elution volumes of 7.0 to 7.9 ml and diffuse signals at high elution volumes were found. 1 MDa HA showed a broad peak from 7.9 to 9.7 ml elution volume, indicating a broad M_w distribution. Centrifugation through 10 kDa mwco membrane left 88.4 % cHA and 100 % of 1 MDa HA in the supernatant. Using a 300 kDa mwco membrane 32.3 % of cHA and 46.9 % of 1 MDa HA were found in the supernatant.

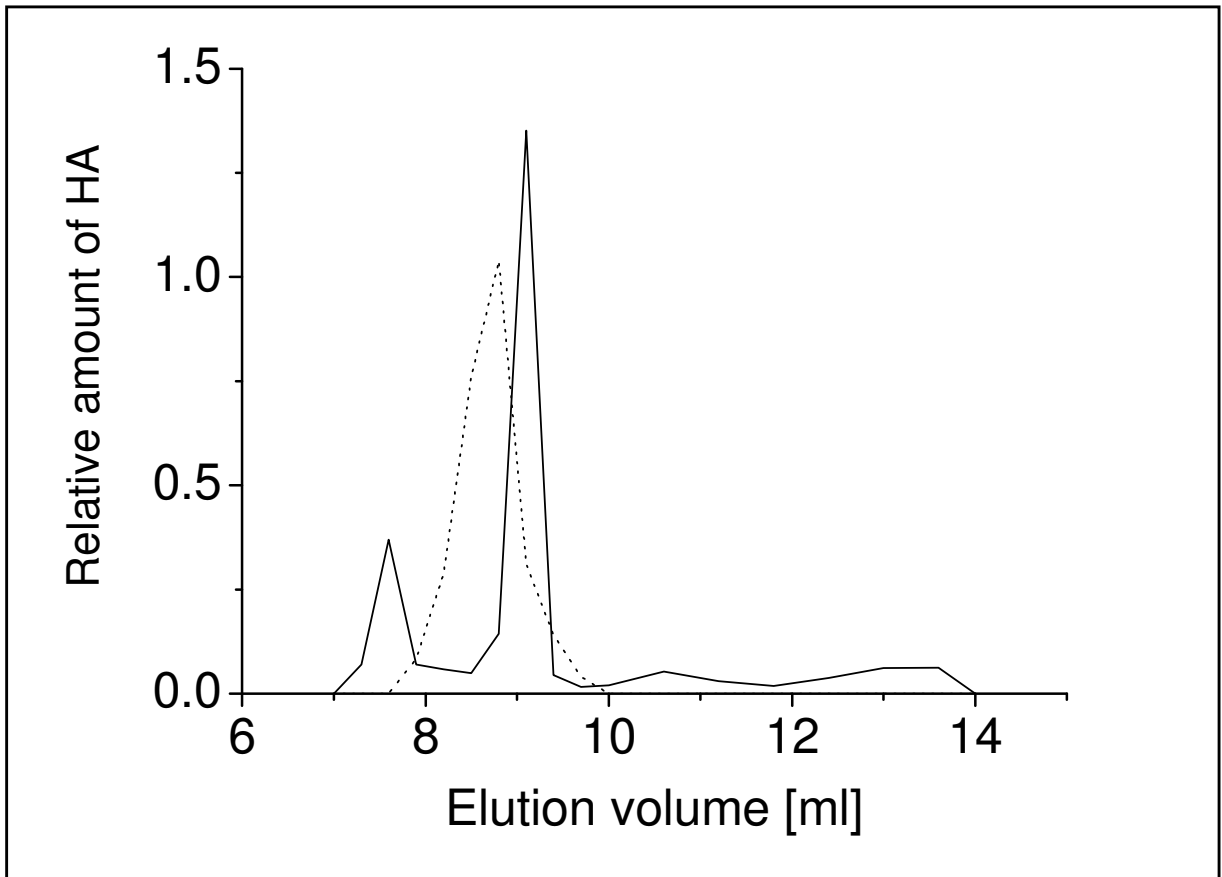


Fig. 3.2: SEC profiles of cHA (—) and 1 MDa HA (…)

This indicates the formation of cross-linked material with a higher M_w in cHA compared to dHA-3. However, a large amount of unreacted dHA is still present. The reduced elution volume for the high M_w fraction of cHA compared to 1 MDa HA is likely due to the changed three-dimensional structure of cross-linked material, limiting interaction with the SEC column. The increase in retention of cHA in centrifugation experiments compared to dHA-3 is less pronounced than the difference between 1 MDa and 100 kDa unroll-linked HA. Signals at high elution volume in cHA samples might be due to potential cleavage of dHA during the cross-linking reaction, as Cu-(II) and ascorbic acid, among other cross-linking reagents/catalysts, are reported to induce partial HA cleavage [133-135]. A simultaneous degradation would compete with cross-linking. Valachova et al. [134] report that 1 μ M Cu-(II) and 100 μ M ascorbic acid lead to a significant reduction of viscosity for approx. 1 MDa HA within an hour – which is at lower concentrations and within shorter timeframe than applied for the cross-linking protocol employed in this study. Also Soltes et al. observe a decrease in viscosity for HA species > 800 kDa [135]. At the same time Crescenzi et al. and Testa et al. do not report any effects indicating HA cleavage [49, 54, 81, 82]. However, the reaction times

employed in these studies are far below one hour and the reaction was terminated by dialysis. Also the absolute amount of potential HA fragments found in SEC is apparently low. Hence, there is no prove for HA cleavage in CuAAC systems for 100 kDa or similar HA species. We conclude that HA chain cleavage is, if occurring at all during or after the cross-linking reaction, a minor effect under the given circumstances. However, a cleavage of M_w fractions above 800 kDa would be a significant limitation to the entire concept of cross-linking HA by CuAAC. Further studies would be required. The methods of choice to determine the M_w distribution more precisely are mass spectrometry (for the low molecular weight fractions) or light scattering detectors (esp. for the high molecular weight fractions) on-line to SEC or AF₄ systems [37, 136-138].

Crescenzi and Testa described an increased viscosity for cross-linked HA materials [49, 81, 82]. Compared to dHA-3 as well as unmodified 100 kDa HA, showing 29.3 ± 2.4 and 27.6 ± 3.4 mPas, respectively, the viscosity of 2.5 mg/ml cHA remained unchanged: 26.3 ± 2.8 mPas. The HA solutions remain free-flowing.

The viscosity of HA samples increases strongly once a certain M_w threshold is reached; likely approx. 360 kDa [41]. At the same time a strong concentration dependency is introduced. For smaller HA species viscosity values are less affected by M_w and concentration changes. As SEC and centrifugation experiments show the increase in overall M_w is only minor and obviously insufficient to increase viscosity. The increased viscosity observed by Crescenzi and Testa is likely due to the increased initial M_w (200 kDa), being closer to the 360 kDa threshold, combined with a higher DoS leading to more effective cross-linking.

The goal of this study is to develop in situ hardening hydrogel systems that can entrap and subsequently release protein pharmaceuticals. However, there is no increase in viscosity by the cross-linking protocol employed. Furthermore, the formed material readily dissolved in water (visual inspection only). Thus, the cross-linked HA obtained during this study is inadequate for controlled release purposes and requires further optimization.

3.3. Protein stability during cross-linking reactions

Some proteins, like e.g. hGH, HSA and Heme, are reported to be stabilized in presence of Cu^{2+} [139-141]. At the same time the Cu^{2+} /ascorbic acid system is also reported to cleave several proteins [142]. This holds also true for the model IgG protein used in this study. Within 120 min incubation in 0.2 mM CuSO_4 and 2.0 mM ascorbic acid, concentrations representing the cross-linking conditions described earlier, visible particles were formed. HPSEC showed a loss of monomer content of approx. 30 % and formation of both aggregates and fragments after 120 min. Turbidity was increased from 0 to 1.2 FNU. Obviously, the Cu^{2+} /ascorbic acid system leads to both aggregation and degradation of the antibody. Both are driven by metal induced oxidation [4, 143].

However, successful click reactions (also including the Cu^{2+} /ascorbic acid system) are reported for living systems [73, 144, 145] and in presence of protein [146-149]. For the IgG used in this study, even rather short time frames of ten minutes led to significant loss in protein integrity by Cu^{2+} /ascorbic acid. We conclude that the stability of each protein has to be carefully evaluated. Cu(I) based or, even more so, copper-free systems, are the most likely candidates to secure protein integrity.

4. Physico-chemical characterization of PMT gels

4.1. Physico-chemical properties of H6P gels

The first preliminary testing of PMT was performed with H6P which is derived from poloxamer 403 and hexamethyldiisocyanate (HDI) to form a 36 kDa polymer. The dry polymer formed white blocks with a semi-solid consistency and was readily soluble in water and PBS up to 25 %. At low temperatures (2-8 °C) clear solutions were formed. Upon heating to ambient temperature (\approx 20-22 °C) spontaneous clouding occurred. Furthermore, viscosity increased and flowability was notably decreased. Heating to 37 °C, the white color remained and hardening continued. However, reaching 37 °C, the flowability increased again, indicating a loss in viscosity once a certain optimal temperature, which appears to be below 37 °C for H6P gels, was exceeded. Further increase in temperature led to continuous loss in viscosity and upon storage > 40 °C for one hour separation of an aqueous, transparent, low viscosity phase from the gel phase occurred. There was no visually detectable change in total sample volume within 2-45 °C. Manual injection via 20 G needle of a cooled (2-8 °C) 20 % gel into air as well as 37 °C warm PBS could easily be performed. Even at ambient temperatures, despite increased viscosity, manual injection through 20 G needle was possible.

This overall profile is typical for poloxamer based thermo-responsive hydrogels [96, 114, 115, 153]. From the mechanistic point of view this temperature profile represents the formation, interconnection and deformation of micelles as described by Mortensen et al. [92] and Walz et al. [96]. At low temperatures, the polymer is dissolved or assembled in a low number of micelles. With increasing temperature, more and more micelles form. When a certain micelle concentration and/or density is reached, clouding occurs. At even higher temperature and higher micelle concentration and density the hydrophilic PEO segments interconnect more strongly and rearrangement of micelles into lyotropic crystalline structures can occur. This interconnection and/or rearrangement leads to hardening [92, 96]. Increasing the temperature even further induces loss of interconnectivity by micelle-deformation or matrix melting [92] and causes the gel strength to decrease. For H6P maximal gel strength appears to be reached below body temperature. The phase separation

observed for temperatures $> 40\text{ }^{\circ}\text{C}$ were also described by Ruel-Gariépy et al. and are caused by water exclusion upon further energetic optimization of the polymer matrix [87].

Gel hardness and pore size depend on the density of polymer molecules and micelles. As summarized in [18], it can therefore be stated that usually drug release is sustained by increasing gel hardness [154, 155] as diffusion is slowed down by increasing gel density and hardness [116]. To analyse the hardening of thermo-responsive gels most studies use viscosimetric measurements [26, 28, 156]. In Fig 4.1 the rheological profile of 20 % H6P gel is shown. At approx. $10\text{--}25\text{ }^{\circ}\text{C}$ both storage (G') and loss modulus (G'') were below 1 Pa, reflecting very low viscosity. These low viscosity values were maintained until approx. $25\text{ }^{\circ}\text{C}$, although visual and manual inspection indicated an earlier hardening onset at approx. $20\text{ }^{\circ}\text{C}$. At $25\text{ }^{\circ}\text{C}$ a strong increase in both G' and G'' , with G' crossing G'' , was seen. Both G' and G'' showed maxima at approx. $40\text{ }^{\circ}\text{C}$, being 2100 Pa for G' and 750 Pa for G'' . Again, visual and manual observations pointed to a lower temperatures of maximal viscosity below $37\text{ }^{\circ}\text{C}$. Above $40\text{ }^{\circ}\text{C}$ both G' and G'' decreased, indicating gel melting as described in [92]. This loss in viscosity was not nearly as pronounced as noted visually and manually in that temperature range. Obviously, network formation/deformation was shifted to higher T ($\approx 5\text{ }^{\circ}\text{C}$) in rheometry. Furthermore, the variability as indicated by the standard deviation is rather high. Likely both T shift and high variability are due to the shear forces employed, altering network structure.

Therefore, penetration resistance analysis was established for further investigations. Similar tests to study mechanical properties of hydrogels were also reported in literature [157]. The penetration resistance profile of the H6P gel is in accordance to the manual and visual changes observed upon temperature increase (Fig. 4.2), showing $< 1\text{ mN}$ at $21\text{ }^{\circ}\text{C}$, followed by a strong increase between 21 and $35\text{ }^{\circ}\text{C}$ and subsequent decrease from 37 to $42\text{ }^{\circ}\text{C}$. At $35\text{ }^{\circ}\text{C}$, the temperature of maximal penetration resistance (T_{max}) with approx. 120 mN was reached. Variability as indicated by standard deviation is much lower compared to the rheological measurements. 10 cycles of gel hardening and liquefying showed no significant ($p = 0.05$) impact on penetration resistance at $35\text{ }^{\circ}\text{C}$.

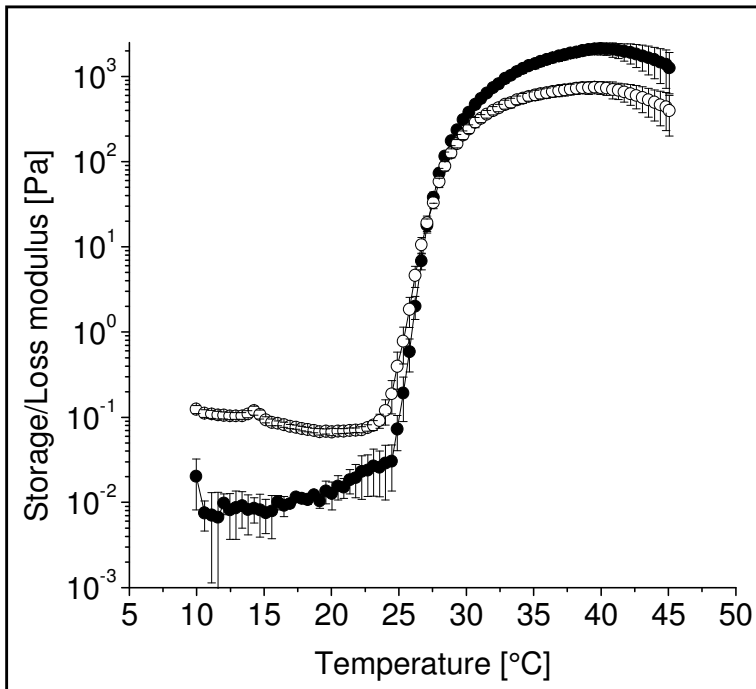


Fig 4.1: Storage \blacklozenge (G') and loss \diamond modulus (G'') of 20 % H6P gels; n=3

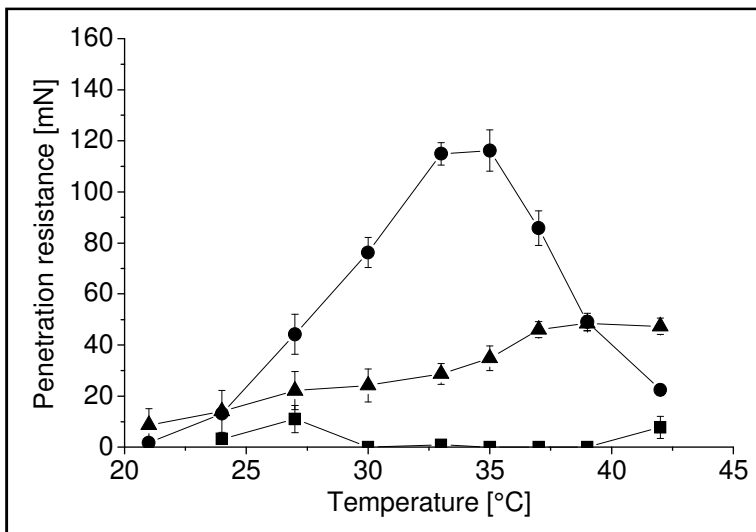


Fig. 4.2: Penetration resistance of 20 % gels of poloxamer 403 (\blacksquare), poloxamer 407 (\blacktriangle) and 20 % H6P (\bullet); n=3

Drury et al. state that for tissue engineering adequate mechanical performance of a scaffold depends on specifying, characterizing, and controlling the material mechanical properties including elasticity, compressibility, viscoelastic behavior, tensile strength, and failure strain [158]. In muscle tissue approx. 20 N/cm^2 , corresponding to 2.0 MPa, are generated [159]. Okay et al. report loss and storage moduli $< 100 \text{ kPa}$ for hydrogels [156]. Bromberg et al. report values $< 1 \text{ kPa}$ for a thermo-responsive gel [29]. These values correspond to moduli obtained for the 20 % H6P gel (see Fig. 4.4). Penetration resistance is determined with a

punch of 13.9 mm² square area. Thus, a penetration resistance of approx. 14 mN corresponds to a gel strength of 1.0 kPa and could be considered as the threshold for minimal gel strength. This threshold is reached by 20 % H6P gels between 27 and 42 °C.

In contrast, a 20 % poloxamer 403 gel did not exhibit a relevant increase in penetration resistance up to 42 °C, while a 20 % poloxamer 407 gel showed continuous increase in penetration resistance from 21 to 39 °C, reaching a maximum of approx. 50 mN (Fig. 4.2). Thus, at body temperature penetration resistance of 20 % H6P gels more than doubles that of the 20 % poloxamer 407 gels. While 20 % poloxamer 403 und 407 gels dissolved quickly in PBS at 37 °C, inherently stable depots of 20 % H6P could be formed, although T_{max} was exceeded. Fig. 4.3 shows such 20 % H6P depots, pre-formed as well as formed in situ via injection (20 G needle) at 37 °C. There was no visible degradation or swelling within four weeks in PBS at 37 °C followed by slow disintegration over several months (chapter 4.3). The described mechanical properties of 20 % H6P systems were not altered upon storage at 2-8 °C for six months. Fulfilling these requirements, H6P is a promising candidate for more detailed studies, showing the desired thermo-reversible gelling profile and increased gel strength and reduced solubility at 37 °C compared to poloxamer 403 und 407 gels.

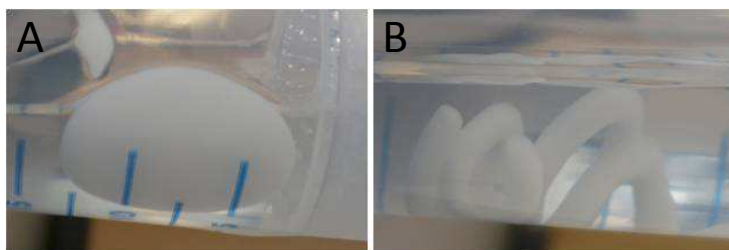


Fig. 4.3: Depots derived from 20 % H6P gels in PBS at 37 °C; A: pre-formed, B: in situ-formed via injection (20 G needle)

Like most thermo-responsive gels, the 20 % H6P gel exhibits a cloud point. The cloud point can be correlated with the lower critical solution temperature (LCST) of the gel [90, 160] as clouding is caused by a reduced transparency of the higher ordered structures formed at the LCST [87, 92, 96]. Thus, clouding and hardening depend on the LCST of the gel. This makes the cloud point as detected by UV spectroscopy [160] an interesting parameter for gel optimization. For 20 % H6P gels a cloud point of 25.2 °C was found (chapter 4.4). The first notable increase in turbidity was detected at approx. 20 °C, being in accordance with visual observations.

For initial release studies 20 mg/ml lysozyme or 150 kDa FITC-Dextran were dissolved in 20 % H6P gels. Depots were pre-formed and overlaid with 37 °C warm PBS and the released amount of model substance was monitored. For 150 kDa FITC-Dextran less than 20 % were released within the first 24 h, followed by complete release within 5 weeks (Fig. 4.4). Lysozyme was released faster with approx. 80 % within 24 h and 100 % after 48 h. Thus, for 150 kDa FITC-Dextran the release is strongly delayed compared to literature data for unmodified poloxamer systems [17, 99]. In contrast to many hydrogel systems showing incomplete release [5, 24], 20 % H6P gels showed complete release of both lysozyme and 150 kDa FITC-Dextran.

As 20 % H6P gels exhibited both promising mechanical properties and sustained release of 150 kDa FITC-Dextran, a series of PMT gels is investigated. The following chapters discuss temperature-sensitive gel strength, gel dissolution, cloud point and injectability of PMT systems. The aim was to identify candidates that offer adequate gel strength and erosion at body temperature. A sharp transition between sol and gel is preferred. Furthermore, the addition of protein should not negatively impact the gel forming process. Choosing candidates with the most promising physico-chemical properties, release and stability of an IgG antibody from/in PMT gels as well as PMT stability are investigated.

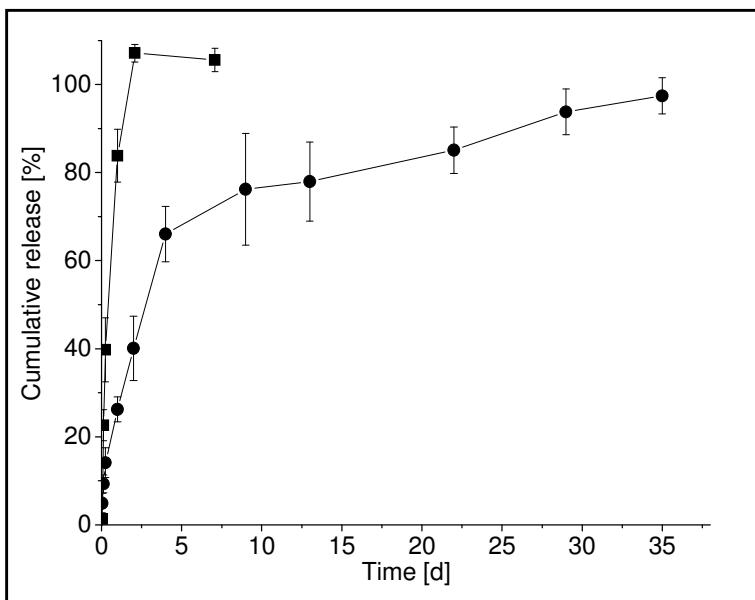


Fig. 4.4: Cumulative release of 20 mg/ml 150 kDa FITC-Dextran (●) and 20 mg/ml lysozyme (■) from pre-formed 20 % H6P depots; n=3

4.2. Gel strength of PMT gels

4.2.1. Effect of PMT molecular weight on gel strength

For a series of HDI linked poloxamer 403 the impact of molecular weight on gel hardness was investigated. The range of 26 to 64 kDa, corresponding to four to eleven unimers, was analysed at 20 % gel concentration. A continuous increase in penetration resistance with increasing M_w was observed (Fig. 4.5), reaching approx. 80 mN, 100 mN and 160 mN for the 26 kDa, 43 kDa and 64 kDa polymer, respectively. At the same time the corresponding T_{max} slightly decreased from 35 °C (26 and 36 kDa) to 33 °C (43 kDa) and 30 °C (48 and 64 kDa). Interestingly, the penetration resistance at 37 °C was nearly identical for the five polymers investigated. As all gels reveal satisfying penetration resistance of more than 14 mN they are candidates for further analysis.

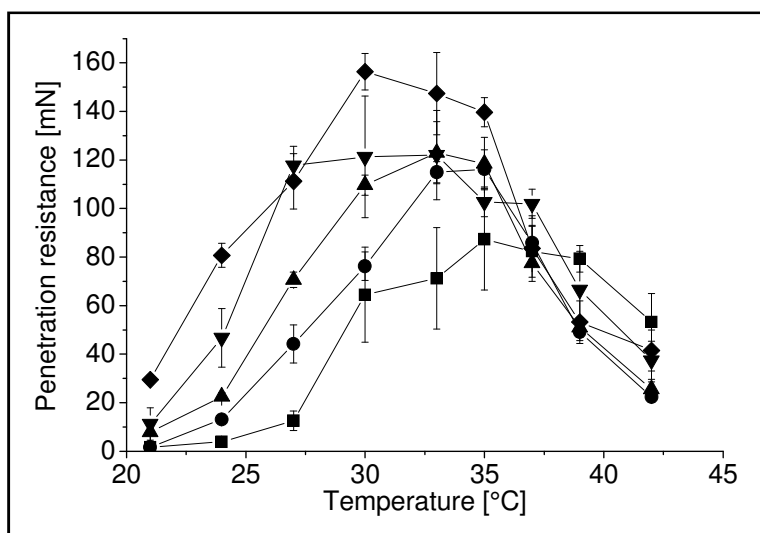


Figure 4.5: Penetration resistance of 20 % gels of HDI linked poloxamer 403 polymers with 26 kDa (H4P, ■), 36 kDa (H6P, ●), 43 kDa (H7P, ▲), 48 kDa (H8P, ▼) and 64 kDa (H11P, ◆); n=3

An increase in gel hardness with increased M_w is known for various gel systems [27, 29, 154]. As gel formation in poloxamer systems is caused by micelle formation and packing [92, 94], gel strength is mainly driven by interactions between PEO chains of adjacent micelles [161]. With increasing M_w and, correspondingly, the number of poloxamer and PEO unimers, the range of this interaction is either expanded over two or more micelles, or intensified between directly adjacent micelles. This leads to increased gel hardness. This is in

accordance with results by Cohn et al. who found that the viscosity of poloxamer 407 oligomer gels increases with the oligomer chain length [112].

Alexandridis et al. found that for a given PPO to PEO ratio, poloxamers of higher molecular weight form micelles more readily, i.e. at lower concentrations and temperatures [162] as the free energy change for the transfer of one mole of poloxamer from solution to the micellar phase increases [163]. Considering PMTs as high molecular weight poloxamers, and knowing that micelle concentration is an important trigger to gel hardening [92], this effect can be seen for the M_w series investigated: the higher the M_w the lower T_{max} . Also for poloxamer 407 gels T_{max} decreased with higher number of poloxamer unimers in a chain-elongated system [112].

As the hardness at the in vivo release temperature of 37 °C is similar for the polymers of different M_w investigated, differences in release profiles at 37 °C should be minor [116, 118, 154, 155]. However, the lower T_{max} at high M_w may counteract easy handling and syringeability and lower M_w PMTs with high T_{max} may be favourable.

4.2.2. Effect of PMT concentration on gel strength

Subsequently, a concentration series of H6P gels was analysed. A strong impact of polymer concentration on penetration resistance is seen (Fig. 4.6). At 10, 15, 20 and 25 % the maximal penetration resistance was approx. 20, 60, 120 and 140 mN, respectively. At 25 % H6P the T_{max} was 31 °C, for the other concentrations approx. 35 °C. At 37 °C 20 % and 25 % H6P result in the same penetration resistance of approx. 100 mN. For 15 % and 10 % the mechanical strength at 37 °C was reduced to approx. 60 and 20 mN, respectively. All values were above the 14 mN threshold and all concentrations could be considered as possible candidates for further analysis.

An increase in gel hardness due to an increase in gel concentration is known for most gel systems [27, 29, 154]. At high concentrations the effect diminishes and the 20 % and 25 % H6P gels show very similar penetration resistance at 37 °C. The increased gel strength is caused by an overall increase in micelle concentration and, thus, density, or by an increased micelle size as found by Cohn et al. for similar chain-elongated poloxamer systems [112]. Also the shift in T_{max} corresponds to the micelle-packing mechanism [92, 94], as for

increasing poloxamer 403 concentration the transition temperatures from micelle solutions to mechanically more stable liquid crystalline states decreases [100].

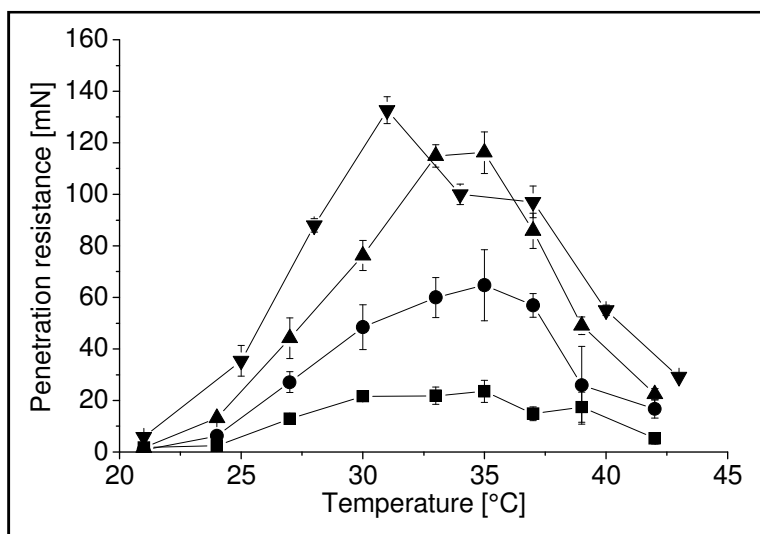


Figure 4.6: Penetration resistance of 10 (■), 15 (●), 20 (▲) and 25 (▼) % gels of 36 kDa H6P; n=3

A concentration of 20 % PMT appears to be optimal. Lower concentrations could lead to faster drug release as the hardness, i.e. mesh density, is decreased [154]. A higher concentration may hinder injectability. This ideal concentration is 10 % lower than found by Cohn et al. for similar poloxamer derivatives [112]. Other environmentally-sensitive hydrogel systems require similar to higher concentrations as well, e.g. > 20 % for PEO-PLA [164], > 30 % for poloxamer-cellulose derivatives [165] or > 25 % for pNiPAAm systems [166].

4.2.3. Effect of diisocyanate linker on gel strength

Three different diisocyanates were used to obtain polymers of similar M_w : BDI, MDI and HDI. The impact of the diisocyanate linker on the penetration resistance was investigated at 20 % gel concentration (Fig. 4.7). It was found that M6P gels, cross-linked with MDI, had a lower overall penetration resistance than H6P gels, cross-linked with HDI, showing approx. 90 mN compared to 120 mN at the corresponding T_{max} of approx. 33 °C and 35 °C, respectively. 20 % B7P gels, cross-linked with BDI, showed the same maximal penetration resistance as 20 % H7P gels of approx. 125 mN. However, for 20 % B7P gels T_{max} was shifted to approx. 38 °C and, thus, the hardness at 37 °C was markedly increased.

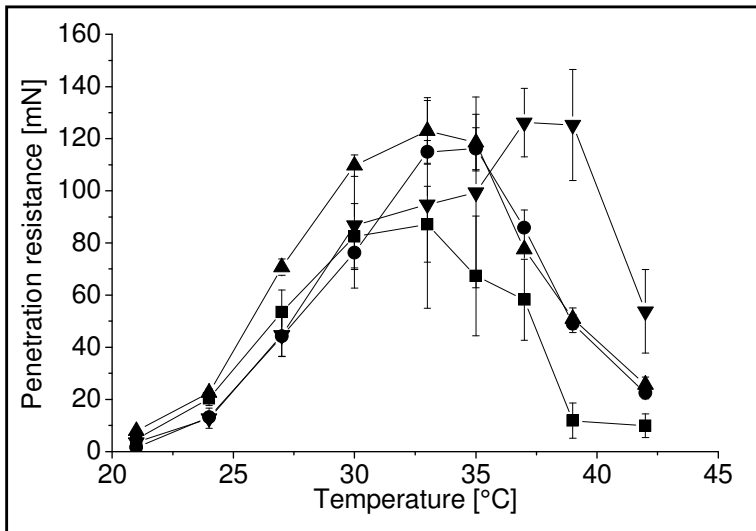


Figure 4.7: Penetration resistance of 20 % H6P (●), M6P (■), H7P (▲) and B7P (▼) gels; n=3

All three diisocyanates act as lipophilic linkers, and lipophilic linker lengths increases from BDI to HDI and MDI. However, the linker size is small compared to the poloxamer building blocks with approx. 5800 Da for each poloxamer 403 unimer. As gel formation is caused by interpenetration of micelles by the PEO segments [94], introducing a lipophilic moiety next to this anchor might reduce gel strength. This could explain why polymers linked with the most lipophilic linker, MDI, render softer gels than HDI linked polymers, while gels from BDI linked polymers show highest penetration resistance. The difference between HDI and BDI is only minor, as the difference in lipophilicity is small.

Less lipophilic poloxamers require higher temperatures to form ordered structures, as their critical micellation temperature (CMT) is increased [162, 163, 167]. This probably causes the increased T_{max} for BDI linked polymer gels compared to HDI and MDI linked polymer gels. Due to the higher gel strength at 37 °C, B7P might lead to an enhanced sustained release effect in vivo compared to polymers linked with HDI or MDI. However, penetration resistance remained > 14 mN for all three differently linked polymer gels, making any of these PMTs potential candidates for further analysis.

4.2.4. Impact of the poloxamer type on gel strength

The PMTs consist of either poloxamer 403, 407, 308 or defined mixtures of them. Poloxamer 403 has a lower PEO content (30 %) than 308 (80 %) or 407 (70 %) and is thus more lipophilic. At the same time poloxamer 308 and 407 have markedly higher molecular weights compared to 403 (14.6 and 12.6, respectively, vs. 5.8 kDa). Thus, at the similar final M_w of the PMT the number of poloxamer unimers differs strongly. To analyse the effect of the poloxamer type on gel hardness the penetration resistance profiles of five different PMTs with increasing PEO to PPO ratio at 20 % were measured (Fig. 4.8). The PMTs chosen were H8P (48 kDa, PEO:PPO 3:7), H5P2F (51 kDa, PEO:PPO 3:4), H2.5P2.5F (48 kDa, PEO:PPO 1:1), H1.5P1.5F1.5f (49 kDa, PEO:PPO 3:2) and H4F (55 kDa, PEO:PPO 7:3). They have a similar M_w of approx. 50 kDa and increasing hydrophilicity in the above mentioned order due to PEO:PPO ratios of 3:7, 3:4, 1:1, 3:2 and 7:3, respectively. The PEO chain length of the underlying poloxamer qualities are 20 units for poloxamer 403, 100 units for poloxamer 407 und 133 units for poloxamer 308. Interestingly, at the entire temperature range investigated H4F gels were almost transparent, in contrast to all other gels which exhibited slight turbidity.

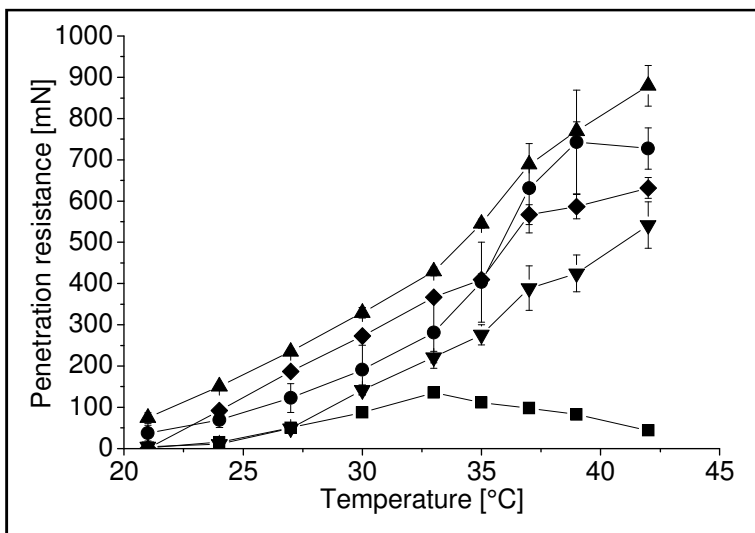


Figure 4.8: Penetration resistance of 20 % H8P (■), H5P2F (●), H2.5P2.5F (▲), H1.5P1.5F1.5f (▼) and H4F (◆) gels; n=3

It was found that an increased PEO:PPO ratio led to a strong increase in penetration resistance compared to H8P with approx. 100 mN at a T_{max} of 33 °C. H5P2F gels showed approx. 700 mN gel strength at T_{max} of 39 °C. For gels with even higher PEO:PPO ratio T_{max} could not be detected as it was shifted to temperatures > 42 °C and a continuous increase in

penetration resistance was found between 21 and 42 °C. At 42 °C 20 % gels of H2.5P2.5F, H1.5P1.5F1.5f and H4F presented a gel strength of approx. 850 mN, 500 mN and 600 mN, respectively. Also at 21 and 24 °C H5P2F, H2.5P2.5F and H4F gels showed increased gel strength compared to H8P gels. For H1.5P1.5F1.5f gels the increased gel strength was detected from 30 to 42 °C compared to H8P gels. Also at low temperatures (2-8 °C) PMT gels with increased PEO:PPO ratio showed markedly increased viscosity (manual inspection only). This increased gel strength at low temperatures could compete with syringeability.

Increased gel strength of PMTs with increased PEO content and/or longer PEO chains is caused by their increased physical polymer cross-linking capacity [92, 94] and was also found by Cohn et al. for similar chain-elongated poloxamers [112]. The increase in T_{max} with increasing PEO:PPO ratio is caused by the increased CMT of more hydrophilic polymers [162, 163, 167], increasing the temperature required to form (interconnected) PMT micelles.

As the penetration resistance values at 37 °C vary strongly, differences in release profiles at this temperature are expected [116, 154, 155]. However, Moore et al. reported that release from poloxamer 407 systems is mainly caused by fast erosion/solution of the gel, not diffusion [168]. Therefore, the dissolution of gels based the more hydrophilic PMTs has to be evaluated critically (chapter 4.3.4) In general more hydrophobic gels show more pronounced sustained release than more hydrophilic matrices [154]. Overall, despite their high mechanical strength, poloxamer 407 and 308 based PMTs are expected to show faster protein release than poloxamer 403 based systems. In addition, the impact of the increased gel strength at low temperatures on syringeability has to be evaluated.

4.2.5. Effect of the addition of PEO and PPO on gel strength

As seen for PMTs based on different poloxamer qualities and elongated with different diisocyanates, hydrophilicity plays an important role in gel hardening affecting both maximal gel strength and T_{\max} . Hence, addition of hydrophilic or lipophilic molecules like PEO or PPO could be an option to influence gel formation. Consequently, 5 % PEO and PPO of different M_w were added to 20 % H8P and the penetration resistance was characterized.

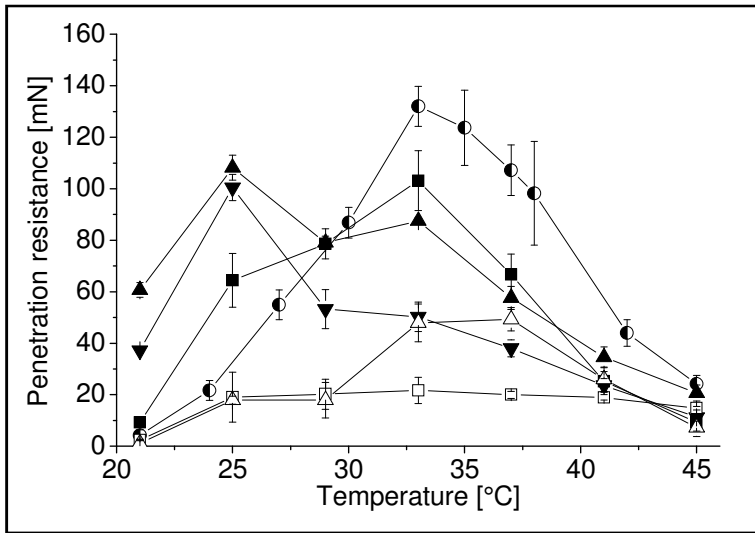


Figure 4.9: Penetration resistance of 20 % H8P (●) gels with additional 5 % PEO 1kDa (■), PEO 4 kDa (▲), PEO 20 kDa (▼), PPO 2 kDa (□) or PPO 4 kDa (△); n=3

Addition of PEO leads to a shift in T_{\max} to lower temperatures and reduced overall penetration resistance compared to 20 % H8P gels without additive (Fig. 4.9). With increasing PEO M_w from 1 to 4 and 20 kDa this effects becomes more pronounced. The non-covalently bound PEO appears to reduce the binding strength of the poloxamer PEO units within the micelle-network, as it can compete for binding sites. The decrease in T_{\max} can be explained by interactions between the PEO blocks of poloxamer unimers and the free PEO. This additional interaction leads to a more favorable micelles formation at lower temperature and, hence, a reduction of CMT [87]. The reduced gel strength at 37 °C will likely lead to increased release rates of PEG loaded gels compared to 20 % H8P gels without additive, and an increase in gel strength at low (2-8 °C) and ambient temperature is likely to compete with syringeability. Adding 5 % PPO strongly reduces the overall penetration resistance strongly. As seen before, more lipophilic PMT gels lead to softer gels as lipophilicity competes with PEO interactions, the main driving force of gel formation.

Thus, both PEO and PPO addition leads to a decrease in gel hardness at 37 °C and may lead to a faster drug release. For a PMT which would show a T_{max} significantly above 37 °C, addition of free PEO could be used to adapt T_{max} . PEO might also show positive effects on protein stability, while the lipophilic PPO might destabilize proteins [4]. Therefore, PMTs with PPO additives are excluded from further experiments.

4.2.6. Influence of protein load on gel strength

Incorporation of any drug can influence the mechanical properties of gels, as it introduces polymer-drug and drug-solvent interactions [18, 169]. Therefore, the penetration resistance of a set of protein loaded gels was analysed. These were 20 % H6P gels with 80 mg/ml IgG, 20 % H8P gels with 50 mg/ml Lysozyme and 20 % H6F gels with 20 mg/ml IgG (Fig. 4.10).

For 20 % H6P and 20 % H8P gels 80 mg/ml IgG (Fig. 4.10A) and 50 mg/ml Lysozyme (Fig. 4.10B), respectively, had no effect on the penetration resistance at 37 °C. Overall gel hardness was reduced, but simultaneously T_{max} increased to approx. 37 °C. The hydrophilic proteins may compete for binding sites in the shell of PMT micelles leading to decreased interconnectivity and, thus, reduced mechanical strength. Furthermore, the reduced penetration resistance could be caused by steric hindrance of micelle interaction by the large protein molecules. Both effects may also explain the increased T_{max} . As gel strength is expected to strongly influence drug release protein loaded 20 % H6P and H8P gels with T_{max} values close to 37 °C may be especially promising matrices for sustained protein release.

For 20 % H6F gels with 20 mg/ml IgG (Fig. 4.10C) the onset of hardening was shifted to approx. 33 °C compared to approx. 28 °C for the protein free gel, followed by the strong increase in gel hardness for the PEO rich PMT gel. Thus, for the protein loaded gel the penetration resistance at 37 °C was reduced to 650 mN compared to 800 mN found for the protein free gel. The reduced gel strength and increased temperature required to induce gel hardening may be explained by protein molecules competing for PEO binding sites and sterically hindering micelle formation and interconnection. Despite the high gel strength at 37 °C of 20 % H6F gels with 20 mg/ml IgG a fast gel dissolution as seen for all PEO rich PMT gels is expected, which should lead to a fast protein release.

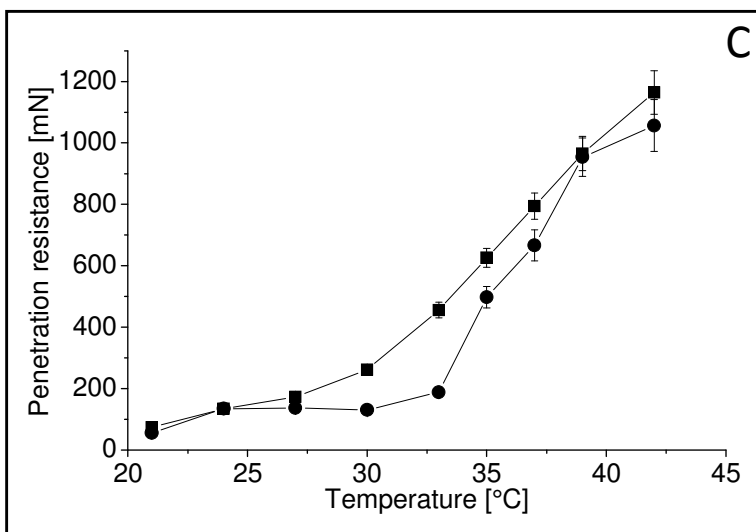
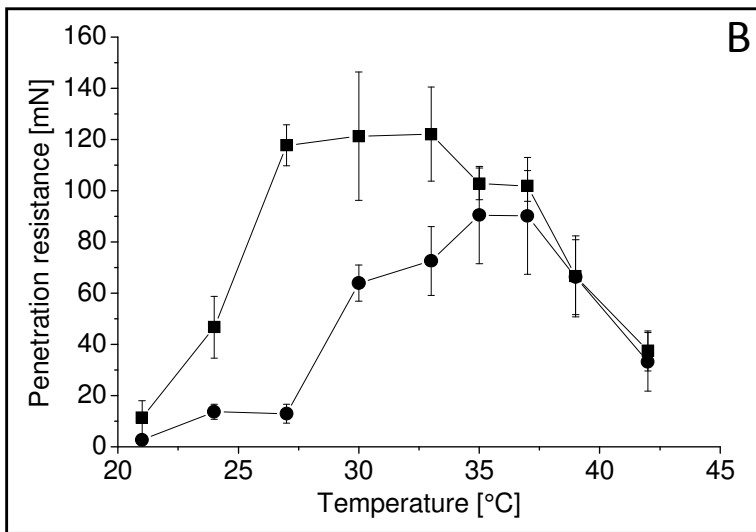
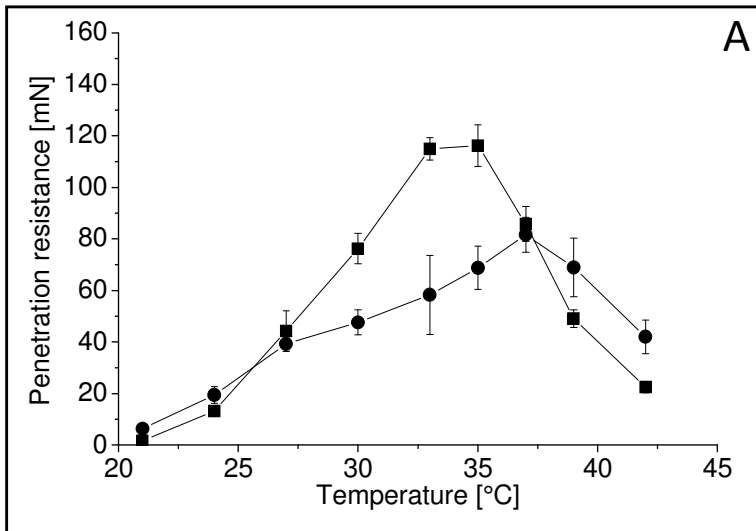


Figure 4.10: Penetration resistance of A: 20 % H6P gels (■) with 80 mg/ml IgG (●); B: 20 % H8P gels (■) with 50 mg/ml Lysozyme (●); C: 20 % H6F gels (■) with 20 mg/ml IgG (●); n=3

4.3. Dissolution of PMT depots

Unmodified poloxamer gels are known to dissolve in physiological media within a few days [17, 98]. Therefore, release is mainly governed by depot erosion [168] and completed within hours to days [17, 98]. To overcome this short release period, PMTs are designed to show decreased solubility and to enable a better release control by matrix diffusion [118, 155]. At the same time, dissolution of the polymer matrix is a key parameter. Hence, dissolution rates of different PMT depots were investigated. PMT gels based on a M_w series of HDI linked poloxamer 403, a concentration series of H6P, PMTs formed by different diisocyanates and from different poloxamer qualities, as well as PMT gels with PEO or protein were pre-formed at 37 °C and overlaid with 37 °C warm PBS. Furthermore, H6P depots were pre-formed and processed at different temperatures (32, 35, 39 or 42 °C) or were in situ-formed by injection of cooled (2-8 °C) gel into 37 °C warm PBS. Depot erosion was monitored visually on a daily basis for 4 days and on weekly base for another 12 weeks and can be caused by either hydrolysis of the urethane linkers and/or dissolution of the polymer molecules in the surrounding medium.

4.3.1. Effect of PMT molecular weight on dissolution of PMT depots

As shown in table 4.1 dissolution time increased with increasing PMT M_w . While unmodified poloxamer 403 was completely dissolved within 4 days, the smallest PMT, H4P with 26 kDa, required approx. 10 weeks. PMTs with even higher M_w showed only incomplete or no dissolution within 88 days. For 36 and 48 kDa PMT depot disintegration and subsequent particle dissolution was observed. These dissolving particles, as well as depots of unmodified poloxamer 403 and H4P, showed a loss in turbidity shortly prior to complete dissolution. At this time point polymer concentration within the depot or particle is too low to maintain clouding. The decreased dissolution rate of high M_w 20 % PMT gels based on poloxamer 403 and HDI is in contrast to the identical gel strength at 37 °C observed for a M_w series of these PMT gels. This can be explained by reducing polymer solubility with increasing M_w .

Polymer name	Poloxamer 403	H4P	H6P	H7P	H8P	H11P
Polymer M _w [kDa]	5.8	26	36	43	48	64
Time point of first visible erosion [d]	< 1	25	60	74	74	> 88
Completely dissolved after [d]	4	67	> 88	> 88	> 88	> 88

Tab. 4.1: Dissolution of pre-formed 20 % gels of poloxamer 403 and a M_w series of poloxamer 403 chain-elongated with HDI; 37 °C; n=1

4.3.2. Effect of gel concentration on dissolution of PMT depots

PMT concentration was found to affect the dissolution time (table 4.2). At 37 °C pre-formed 10 % H6P depots showed first signs of erosion after 32 days, and complete dissolution after 81 days. These gels became transparent after day 74. For 15 % gels it took 46 days until first visible erosion – complete dissolution was not reached within the monitored period of time. 20 % H6P showed first visible dissolution after 60 days that was not completed after 88 days. Increasing the PMT concentration to 25 % did not affect the disintegration behavior any further. For 15 and 20 % gels formation of single smaller particles was observed. These became transparent and dissolved after 14 days each.

PMT concentration [% w/w]	10	15	20	25
Time point of first visible erosion [d]	32	46	60	60
Completely dissolved after [d]	81	> 88	> 88	> 88

Tab. 4.2: Dissolution profiles of 10, 15, 20 and 25 % pre-formed H6P (36 kDa) depots at 37 °C; n=1

The dissolution profiles correlate with gel strengths at 37 °C as the soft 10 % gel dissolves the fastest, while harder gels take more time to dissolve. Differences in both penetration resistance at 37 °C and dissolution at 37 °C between 20 and 25 % H6P gels are only minor. The loss in turbidity shortly to complete dissolution of particles found in 15 and 20 % samples as well as of the entire 10 % gel indicate a continuous loss in polymer concentration to values below the cloud point.

4.3.3. Effect of the diisocyanates on dissolution of PMT depots

Comparing H6P (36 kDa) with M6P (37 kDa) as well as H7P (43 kDa) with B7P (42 kDa) at 20 % gel concentration a strong influence of the employed diisocyanate linker on dissolution rate of pre-formed depots at 37 °C was found (table 4.3). B7P showed no signs of erosion within 88 days. As already mentioned for H6P and H7P gels first erosion effects were found after 60 and 74 days, respectively. Neither of them was completely dissolved within 88 days. In contrast, for M6P gels erosion became first visible by a reduction in gel volume after 18 days, and dissolution was completed after 39 days. Again, opalescence was lost just prior to complete dissolution. Hence, the BDI linked PMT showed the slowest dissolution rate, HDI linked PMTs had intermediate rates, and MDI linked PMT gels dissolved the fastest. This order is in accordance with the penetration resistance (see section 4.2.3): the softer M6P gels dissolves faster, the harder B7P slower than the corresponding H6P and H7P gels. Likely, a reduced interconnectivity of micelles leads to faster dissolution and softer gels.

Linking diisocyanate	HDI	BDI	H ₁₂ MDI
Time point of first visible erosion [d]	60 / 74	> 88	18
Completely dissolved after [d]	> 88 / > 88	> 88	39

Tab. 4.3: Dissolution of pre-formed 20 % PMT depots derived from H6P (36 kDa), H7P (43 kDa), B7P (42 kDa) and M6P (37 kDa) at 37 °C; n=1

4.3.4. Effect of the poloxamer type on dissolution of PMT depots

Variation in the PEO:PPO ratio due to the use of different poloxamer unimers in PMT synthesis were found to strongly affect dissolution rates (table 4.4). 20 % gels of H8P (48 kDa, PEO:PPO ratio of 3:7) showed first signs of erosion after 74 days, but were not completely dissolved within 88 days. In contrast, 20 % H5P2F (51 kDa, PEO:PPO ratio of 3:4) gels started to lose volume immediately after PBS was added and dissolution was completed within 4 days. Gels containing 20 % H2.5P2.5F (48 kDa, PEO:PPO ratio of 1:1) or H4F (55 kDa, PEO:PPO ratio of 7:3) showed an even faster dissolution completed within 2 days. Unmodified poloxamer 407 (12.6 kDa) showed very similar dissolution rates as H4F. 20 % poloxamer 407 gels and 20 % H4F gels became almost transparent when PBS was added,

while 20 % H5P2F and H2.5P2.5F gels became transparent shortly prior to complete dissolution. H8P gels remained turbid throughout the entire timeframe investigated.

Obviously, despite their increased gel strength, the more hydrophilic PMT gels containing poloxamer 407 dissolve faster than PMT gels containing only poloxamer 403. This is in good accordance to [162, 163, 167]: more hydrophilic poloxamer systems form less stable micelles. Although Cohn et al. [112, 114] found that a 30 % gel of a poloxamer 407 tetramer linked with HDI (being nearly identical to H4F as used in this study) sustained in vitro peptide release at 37 °C for several weeks, the PEO rich PMTs H4F, H5P2F and H2.5P2.5F are no candidates for further analysis due to their fast dissolution rate.

PEO:PPO ratio	3:7	3:4	1:1	7:3
Time point of first visible erosion [d]	74	< 1	< 1	< 1 / < 1
Completely dissolved after [d]	> 88	4	2	2 / 3

Tab. 4.4: Dissolution of pre-formed 20 % depots at 37 °C. PEO:PPO ratios represent 48 kDa H8P (3:7), 51 kDa H5P2F (3:4), 48 kDa H2.5P2.5F (1:1), 55 kDa H4F (7:3) and 12.6 kDa unmodified poloxamer 407 (7:3); n=1

4.3.5. Effect of PEO addition on dissolution of PMT depots

In section 4.3.5 addition of PEG to PMT gels was discussed as potential method to adjust gel strength and T_{max} : at 37 °C gel strength was decreased by addition of PEG, being more pronounced the higher the PEG M_w . Analogously, addition of 5 % PEG (1 and 20 kDa) to 20 % H8P gels lead to faster dissolution rate at 37 °C compared to pure H8P systems. For 1 kDa PEG the gel disintegrated into small particles after 4 days and dissolved completely within 46 days. Addition of 20 kDa PEG lead to immediate dissolution into small particles after addition of PBS and complete dissolution within 3 days.

By addition of PEG the micellar network formed by PMTs becomes less dense and less coherent due to a reduced intermicellar interaction. As PEG could be released from the PMT gel over time, matrix healing with newly introduced interconnection of micelles can occur afterwards. For 1 kDa PEG this matrix healing might explain the long timeframe between first visible sign of dissolution and complete dissolution. Thus, small amounts of low M_w PEG might offer a way to accelerate matrix dissolution of PMT gels. For 20 kDa PEG the interference with the gel network is too strong and its addition is not a valuable approach.

4.3.6. Effect of protein load on dissolution of PMT depots

In section 4.3.6 addition of IgG to 20 % H6P gels was shown to shift T_{max} to higher temperatures and reducing the maximal gel strength; at 37 °C both effects canceled each other out, leading to nearly identical gel strength as for protein free gels. Consequently, addition of 20 or 80 mg/ml to 20 % H6P depots had only minor effects on dissolution rates. Without protein, H6P depots took 60 days to show first visible erosion. At 20 mg/ml IgG this time frame was slightly increased to 67 days, but remained 60 days at 80 mg/ml. In each case, erosion was mainly characterized by loss in total volume. Independent of IgG concentration, 20 % H6P gels were not completely dissolved within 88 days. As for addition of PEG, release of IgG from the micellar/gel network might result in identical structures formed in absence of protein. Thus, dissolution rates should become identical to protein free gels once the entire IgG was released.

4.3.7. Effect of temperature on dissolution of PMT depots

Since PMT gels show thermo-reversible hardening, an impact of temperature on dissolution was to be expected. As shown in table 4.5 at 32 °C the onset of erosion of 20 % H6P gels was seen after 46 days, but the gel was not completely dissolved after 88 days. At 35 °C no visible erosion within the investigated time frame occurred at all. For 37 °C and 39 °C the starting erosion was found after 60 and 39 days, respectively, but still gel dissolution was not completed within 88 days. At 42 °C disintegration into numerous small particles occurred after 2 days and these particles became entirely dissolved after 11 days. Near body temperature gels offer sufficient stability to become potential depots for controlled drug release.

Temperature [°C]	32	35	37	39	42
Time point of first visible erosion [d]	46	> 88	60	39	2
Completely dissolved after [d]	> 88	> 88	> 88	> 88	11

Tab. 4.5: Dissolution profiles of pre-formed 20 % H6P depots at varying temperatures; n=1

The closer to T_{max} , the harder 20 % H6P gels become and the slower they dissolve; this correlation between hardening profile and dissolution rate is another proof that increased interconnectivity of micelles reduces dissolution rates. The change in erosion profile from loss in volume by near T_{max} to complete disintegration into particles at 42 °C is in good accordance to the melting of micellar matrices as described in [92].

4.3.8. Dissolution of pre-formed and in situ-formed PMT depots

The aim of this thesis is to develop in situ forming, injectable smart hydrogels for controlled protein delivery. Comparing dissolution behavior of pre-formed and in situ-formed 20 % H6P depots no difference could be seen, although gels were of markedly different shape (see Fig. 4.5). As also gel strength at 37 °C was very similar, matrix formation in injected PMT gels appears to be fast enough to form controlled release depots in situ.

4.4. Cloud point of PMT solutions and gels

All 20 % PMT gels except H4F and H6F become turbid when exposed to ambient or body temperature; H4F and H6F are turbid in the entire temperature range investigated. However, turbidity is notably less for H4F and H6F gels compared to poloxamer 403 based PMTs. Clouding in poloxamer based systems is caused by an increase in micelle concentration (at constant micelle size), leading to strongly pronounced light scattering [161, 167, 170]. The temperature required for clouding is called cloud point (cp) and usually defined as the inflection point of temperature-turbidity or temperature-transmittance graphs [171]. Micelle formation shows a concentration threshold, the critical micellation concentration (CMC), and a temperature threshold, the critical micellation temperature (CMT). As clouding of poloxamer based polymer solutions requires micelles, it can be stated that $CMT \leq cp$ and effects decreasing CMT should also decrease cp. Furthermore, in chapter 4.2 it could be shown that changes in CMT also shift the T_{max} of gel strength.

In situ-formation of PMT gels requires a fast temperature shift; ideally from temperatures that offer low viscosity ($< CMT$) to temperatures close to T_{max} , where the highest gel strength, representing strong micelle interconnectivity, is reached. The closer CMT is to T_{max} , the lower the required heat transfer becomes and the faster and more reproducible gel formation should be. To choose the ideal PMT for controlled protein release from in

situ-formed depots, a CMT close to T_{max} is desired; and c_p values are considered an indirect measure for CMT.

Since at relevant gel concentration most PMT systems investigated reached turbidity values above the detection limit of the applied photometer, inflection points cannot be determined directly. Therefore, in this study, c_p is defined as approximately identical to the temperature with absorbance > 2.0 . As mostly the increase in turbidity is very sharp, the differences between this estimated value and the true inflection point should be minor.

4.4.1. PMT molecular weight effect on c_p

Fig. 4.11 shows temperature-absorbance graphs of 20 % gels of H4P (26 kDa), H6P (36 kDa), H7P (43 kDa) and H11P (64 kDa). Overall, the absorbance increase correlates well with the visual observation of a strong increase in turbidity close to ambient temperatures. Calculated c_p values were 25.4, 25.2, 23.3 and 22.4 °C for 26 (H4P), 36 (H7P), 43 (H7P) and 64 kDa (H11P), respectively. Hence, c_p decreases with increasing M_w , representing a decreasing CMT.

As discussed in chapter 4.2.1 increasing M_w leads to decreasing T_{max} . Independent of PMT M_w c_p appears to be approx. 10 °C lower than T_{max} . Therefore, the difference between CMT and T_{max} can be considered identical for all M_w investigated.

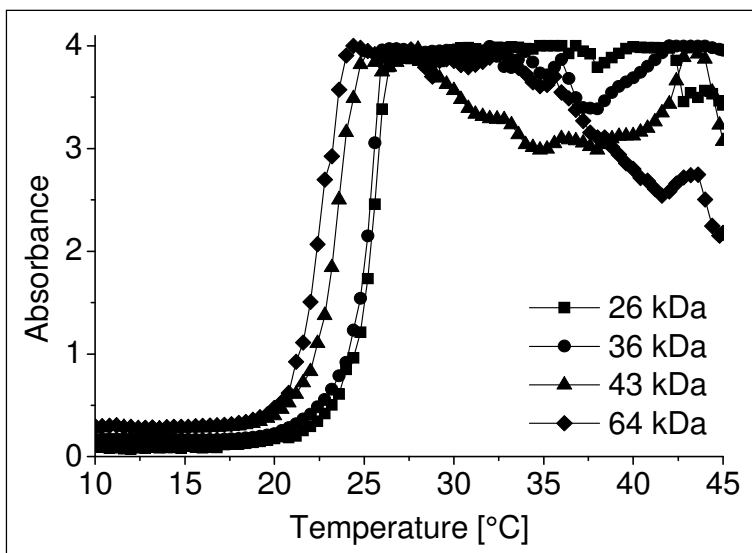


Fig. 4.11: Temperature-absorbance profiles of a H4P (26 kDa, ■), H6P (36 kDa, ●), H7P (43 kDa, ▲) and H11P (64 kDa, ◆); to maintain legibility only every fourth data point collected is indicated; $n=2$

4.4.2. PMT concentration effect on cp

No direct correlation between gel concentration and cp can be seen (Fig. 4.12). Only at the very low concentration of 0.1 % H6P a continuous increase in absorbance was found. For all other concentrations a sharp increase in absorbance at ambient temperatures could be seen. Cp values were 42.8, 23.2, 23.1, 23.2, 24.5 and 25.2 °C for 0.1, 1.0, 5.0, 10, 15 and 20 % samples, respectively. Concentrations of 1.0, 5.0 and 10 % lead to nearly identical cp values, approx. 1-2 °C lower than for 15 and 20 % gels. As shown in chapter 4.2.2 T_{max} is decreasing with increasing gel concentration. Although the observed differences are small, it can be stated that for 20 % gels the difference between cp and T_{max} is smaller than for the other gel concentrations investigated.

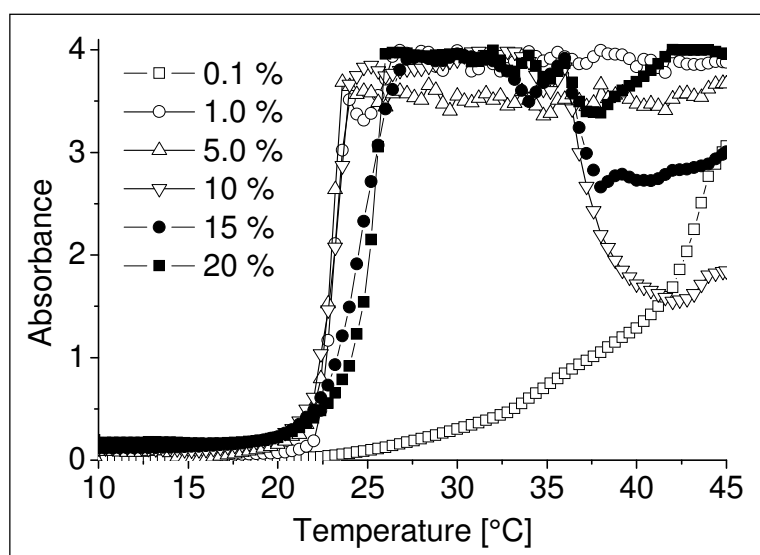


Fig. 4.12: Temperature-absorbance profiles of 0.1 (□), 1.0 (○), 5.0 (Δ), 10 (▽), 15 (●) and 20 % (■) 36 kDa H6P gels; to maintain legibility only every fourth data point collected is indicated; n=2

4.4.3. Effect of diisocyanate structure on cp

As Fig. 4.13 shows absorbance profiles and cp depend strongly on diisocyanate quality. 20 % M6P gels revealed a cp of 20.9 °C, whereas the gels prepared from H6P with corresponding M_w exhibited a cp at 25.2 °C. A similar trend is seen for B7P (42 kDa) vs. H7P (43 kDa): The cp values were 27.3 °C for 20 % B7P and 23.3 °C for 20 % H7P, respectively. Interestingly, M6P showed a lag in absorbance increase close to cp.

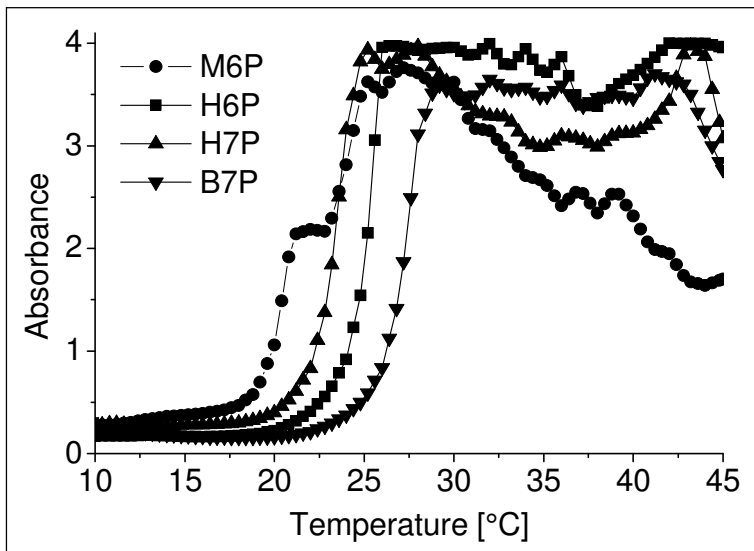


Fig. 4.13: Temperature-absorbance profiles of 20 % M6P (●), H6P (■), H7P (▲) and B7P (▼); to maintain legibility only every fourth data point collected is indicated; n=2

These results correspond to penetration resistance measurements. Compared to HDI based PMTs the more lipophilic MDI induces a slight T_{max} shift to lower temperatures, while the less lipophilic BDI gels show a markedly increased T_{max} . The lag close to c_p for the M6P graph is another hint that either micelle formation is not as linear as expected, or turbidity depends on more processes but micelle formation. Regardless of this effect, M6P shows a reduced c_p but rather similar T_{max} compared to H6P. Thus, the gel network formation requires a stronger temperature shift for M6P gels than for H6P gels and H6P is beneficial in terms of fast sol-gel transition. B7P has increased T_{max} and increased c_p compared to H7P, reflecting similar temperatures shifts required for in situ-hardening and, thus, BDI and HDI based poloxamers can be considered similar in terms of the sol-gel transition.

4.5. Injectability of PMT gels

As discussed in chapter 4.1 cooled (2-8 °C) 20 % H6P gels are easily injectable with 20 G needles as shown by manual observation. Additionally, gels at ambient temperature were tested for injectability with 20 G needles at 100 μ l/sec (Fig. 4.14). For PBS a constant injection force of approx. 3 N was necessary. 10 and 15 % H6P gels revealed an increase in injection force required within the first 50 μ l. Subsequently, a plateau at approx. 8 N was reached. At 20 % gel concentration a continuous increase in injection force for more than 200 μ l was seen, reaching peak force of approx. 25 N followed by a decrease to 20 N at high standard deviation.

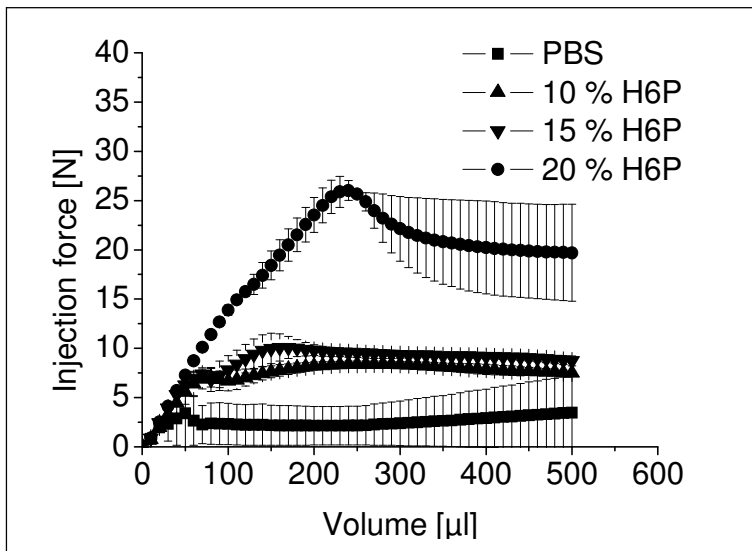


Fig. 4.14: Injection force measurements of PBS (■), 10 (▲), 15 (▼) and 20 % (●) H6P using a 1 ml syringe with 20 G needle at ambient temperature with 100 μl/sec; n=3

For PLGA systems similar forces of 20 N and more are reported for injection into air and a meat model at approx 30 μl/sec [172]. Furthermore, injection forces of up to 25 N are found to correlate with “easy” injection in vivo [172]. Cilurzo et al. report that injection forces of approx. 14 N “went smooth” [173]. Hence, all H6P gels discussed above can be classified as easily syringeable or syringeable using 20 G needles at ambient temperatures.

However, to limit the pain for subcutaneous or intramuscular injection 22 to 25 G or even smaller needles are most common [174]. 20 G needles have an inner diameter of approx. 0.6 mm and an outer diameter of approx. 0.9 mm, whereas e.g. 22 G needles have 0.4 and 0.7 mm, respectively. Injection forces increase with decreasing needle size [174] and increasing injection speed [172]. Thus, to use smaller needles for PMT gel injection, two options are available: (i) reducing the injection speed; (ii) injecting cooled gel with its decreased gel viscosity. Further studies could reveal the ideal compromise between injection volume, injection speed, injection depth, gel concentration, gel temperature and needle size.

As shown in Fig. 4.15 for 20 % PMT gels at ambient temperature the injection force required increases with increasing M_w as T_{max} is shifted closer to ambient temperatures (chapter 4.2.1). 26 kDa H4P reached a plateau of approx. 15 N after 100 μ l. For 36 kDa H6P a peak of 26 N was found after 250 μ l, followed by a plateau at 20 N. At 43 kDa (H7P) the peak force of 42 N was reached at 320 μ l, followed by a decrease to approx. 30 N. 64 kDa H11P gels exceeded the upper detection limit of the system (60 N) immediately after measurement start. Thus, 20 % H6P and H7P gels can be classified as injectable, 20 % H4P gels as easily injectable [172] at the applied conditions, whereas 20 % H11P gels are not injectable.

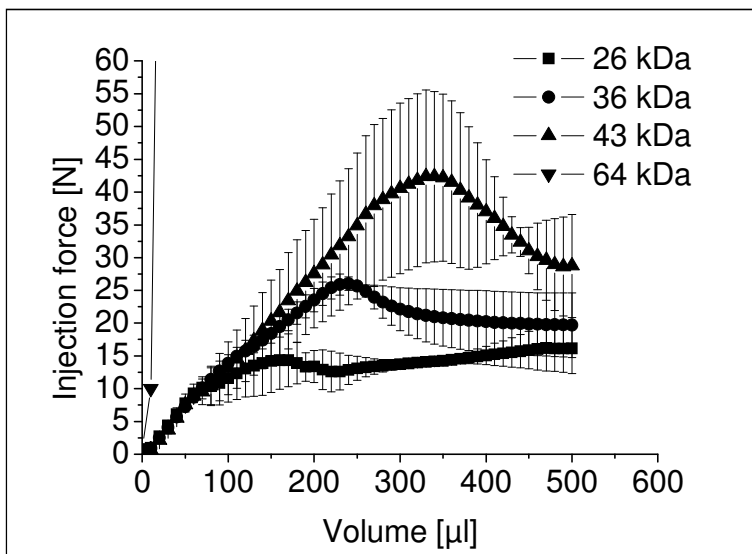


Fig. 4.15: Injection force measurements of 20 % H4P (26 kDa, ■), H6P (36 kDa, ●), H7P (43 kDa, ▲) and H11P (64 kDa, ▼). A 1 ml syringe with 20 G needle was used for injection at ambient temperature and 100 μ l/sec. Injection forces for 64 kDa H11P are above upper detection limit; n=3

Comparing injection forces of PMTs based on different DICs, 20 % H6P, M6P and B7P gels behave very similarly (Fig. 4.16), all showing acceptable peak injection forces of approx. 26 N. The lower injection force found for B7P in comparison with H7P (approx. 42 N) correlates with the higher T_{max} observed for B7P, making injection at ambient temperature easier.

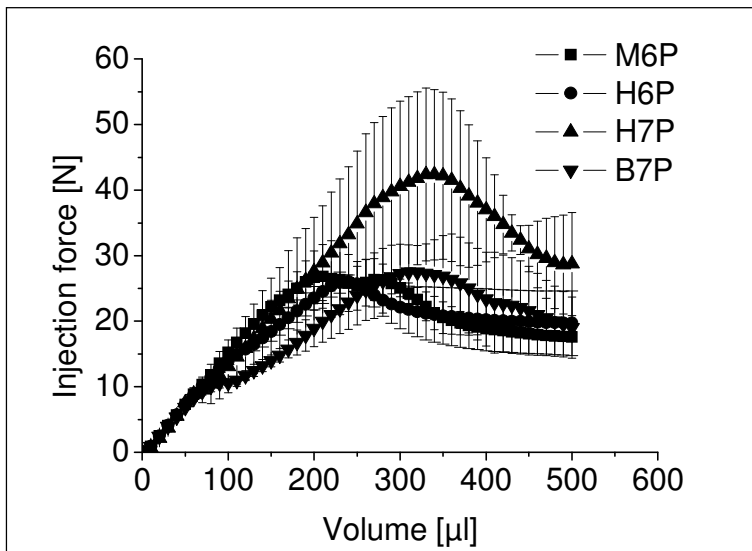


Fig. 4.16: Injection force measurements of 20 % H6P (36 kDa, ●), H7P (43 kDa, ▲), B7P (42 kDa, ▼) and M6P (37 kDa, ■). A 1 ml syringe with 20 G needle was used for injection at ambient temperature and 100 μl/sec; n=3

The addition of protein to H6P gels affected the injectability (Fig. 4.17). 15 % H6P gels with 20 mg/ml IgG showed injection forces of up to 34 N, more than 20 N higher than protein-free 15 % H6P. For 20 % H6P injection forces exceeded the detection limit when 20 mg/ml IgG were added.

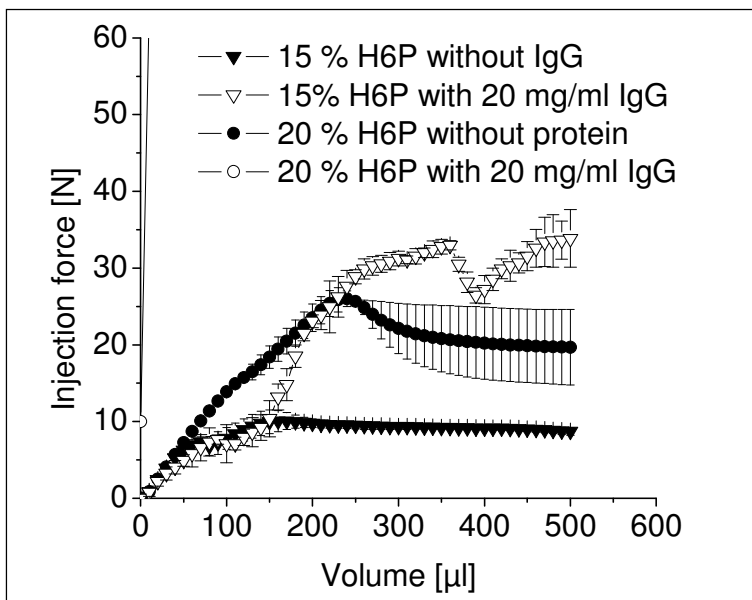


Fig. 4.17: Injection force measurements of 15 % H6P (36 kDa) gels with (▽) and without (▼) 20 mg/ml IgG and 20 % H6P gels with (○) and without (●) 20 mg/ml IgG. A 1 ml syringe with 20 G needle was used for injection at ambient temperature and 100 μl/sec. Injection forces for 20 % H6P with 20 mg/ml IgG are above upper detection limit; n=3

The strong increase in injection force cannot be explained by increased viscosity at ambient temperature as penetration resistance did not change at 21 °C (chapter 4.2.6). However, as will be discussed in chapter 5.1, IgG tends to precipitate in H6P gels at low and ambient temperatures. Hence, protein particles may block the needle, leading to increased injection force, but in situ-formed release samples generated from cooled (2-8 °C) gels (chapter 5.2.5) were injectable.

5. PMT depots for controlled protein delivery

In chapter 4 the physico-chemical properties of PMT gels are described. Chain-elongated poloxamer 403 derivatives such as H4P to H11P, B7P and M6P exhibited enhanced mechanical stability and decreased solubility compared to unmodified poloxamer 403. In a preliminary test pre-formed 20 % H6P gels sustained the release of Lysozyme and FITC-Dextran 150 kDa. With the exception of H11P, 20 % PMT gels were injectable through a 20 G needle at ambient temperatures. However, protein precipitation was observed, indicating a risk of needle clogging as well as potential protein instability. To identify the most promising PMT for controlled protein release, deeper analysis of protein precipitation, release and integrity, followed by studies on polymer stability, were carried out.

5.1. Protein precipitation in PMT systems

Fig. 5.1 illustrates particle formation and subsequent precipitation for lysozyme loaded gels. 20 % H6P gels with increasing lysozyme concentration, as well as a concentration series of H6P with 25 mg/ml lysozyme were chosen. The higher PMT and/or the protein concentration, the more pronounced the formation of visible particles became.



Fig. 5.1: PMT systems with visible lysozyme precipitation (at the bottom of lower syringes). From left to right: 20 % H6P gel with 5, 15, 25 or 35 mg/ml lysozyme, respectively, and H6P gel with 25 mg/ml lysozyme and 10, 15, 20 or 25 % gel concentration, respectively.

After centrifugation protein was detected in both supernatant and precipitate, revealing 100 % of the initial protein amount and, thus, indicating that precipitation is fully reversible. The supernatant has maintained thermo-responsive properties, but at 2-8 °C further particle formation could be seen. This indicates that the supernatant consists of a PMT-protein mixture. The precipitate was gel like from 2-8 °C to 42 °C, but dissolved within one hour when 0.5 ml cooled (2-8 °C) PBS were added. This dissolved precipitate showed thermo-responsive hardening as well, indicating an initial co-precipitation of PMT and protein.

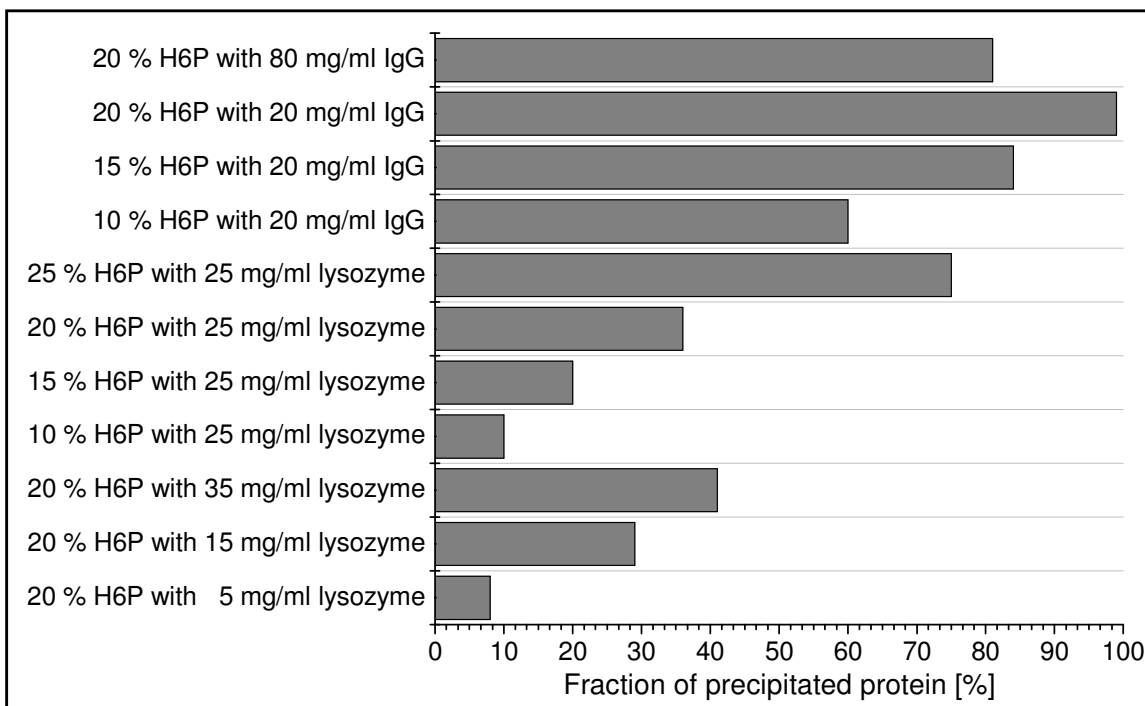


Fig. 5.2: Fraction of protein found in the precipitate after centrifugation at 4 °C and re-dissolving in PBS at 2-8 °C for 1 h; n=1

For increasing lysozyme concentration from 5 to 35 mg/ml in 20 % H6P gels increasing amounts of precipitated protein with approx. 8 % at 5 mg/ml and 41 % at 35 mg/ml were found (Fig. 5.2). In 20 % H6P 99 % of 20 and 81 % of 80 mg/ml IgG precipitated. The precipitated fraction of 25 mg/ml lysozyme increased with increasing H6P concentration from 10 to 25 %, yielding 10 and 75 %, respectively. For 20 mg/ml IgG 60 % precipitation were found at 10 % gel concentration, and 99 % at 20 % H6P. Hence, the precipitated protein fraction increases with increasing lysozyme concentration, but decreases with increasing IgG concentration. For both proteins, increasing gel concentration increases the precipitated fraction.

This protein precipitation can be both beneficial and disadvantageous at the same time. In general, protein precipitates need to dissolve prior to distribution in the human body, inducing potential sustained release properties [118]. The stability of a precipitated IgG after re-dissolution is already shown in literature [175]. However, precipitated protein can clog injection needles and hinder parenteral application (as seen in chapter 4.5). Furthermore, protein precipitation introduces potential quality issues: parenteral products have to maintain low number of particles matching pharmacopeia standards. If protein precipitates were insoluble, immunogenic, or simply inactive, they were a major drawback for the desired purpose of controlled protein release. This aspect will be discussed in more detail in chapter 5.3

5.2. Release of IgG from PMT gels

In literature, for e.g. poloxamer 407 [24, 106], different kinds of pNiPAAm co-polymers [120, 179] as well as stearyl-alanine oleogels [180] sustaining for some hours can be achieved. In other systems, e.g. photo-cross-linked HA-PEG co-polymers [181], PLGA-PEG-PLGA “ReGel®” [182] and pNiPAAm-PEG co-polymers [107], release periods can be prolonged to several days. Sustained release for up to several weeks is e.g. reported for PLGA-PEG-PLGA copolymers similar to ReGel® [108] as well as for photo-cross-linked thiol-PEG derivatives [183]. Bursts within 24 h as low as approx. 5 % using chain-elongated poloxamer 205 and 304 systems [102] and PLGA-PEG-PLGA “ReGel®” systems [182] are reported. On the other hand, e.g. Zhuo et al. report 40 % BSA release within the first 24 h from their pNiPAAm-PEG gels [107]. Gong et al. found up to 80 % release within 24 h for a PEG-PCL-PEG system [176], and poloxamer 407 mixed with polysorbate 80 shows 40 % burst within 24 h as well [177].

However, this release data from literature is based on different drugs (some proteins, some peptides, some small molecules), different gel concentrations (ranging from approx. 10 to 40 %), and different release conditions (different in vitro systems as well as in vivo experiments in rats, rabbits, etc.), leading to limited comparability in general. Furthermore, burst is an important feature in many controlled release platforms to initialize therapeutic levels in the first place [184].

In this thesis series of release experiments to determine the impact of PMT M_w , concentration, employed diisocyanate, protein concentration, release temperature, depot formation technique and gel shelf-life were carried out. To compare release profiles, burst release after 24 h and time point of complete IgG release were determined.

5.2.1. Impact of PMT molecular weight on IgG release

20 % gels of poloxamer 403 (5.8 kDa), H4P (26 kDa), H6P (36 kDa), H7P (43 kDa) and H11P (64 kDa), representing a M_w series of PMTs, with 20 mg/ml IgG were prepared and depots were pre-formed as described in chapter 2.2.11. Release from unmodified poloxamer 403 was completed within 8 h (Fig. 5.3). 26 kDa H4P and 64 kDa H11P gels showed bursts of 34 and 62 % after 24 h, respectively, and complete release at 7 d. 43 kDa H7P showed 33 % burst after 24 h with subsequent complete release within 21 d. The most pronounced sustaining of IgG release was achieved by 36 kDa H6P, as the burst was 29 %, and complete release was reached after 46 d.

The lack of sustaining properties for unmodified poloxamer 403 correlates well with its fast dissolution rate and low mechanical strength. Poloxamer 403 gels are too soft and dissolve too rapidly to sustain IgG. Interestingly, although their gel strengths were very similar at 37 °C (approx. 80 mN), substantial differences in IgG release were observed for the different PMTs. For H4P release time correlates with the gel dissolution time of one week. For H11P a similar release period but increased burst was observed, although H11P gels did not dissolve within the investigated time frame. H6P and H7P gels showed further prolonged IgG release, and did not dissolve. This indicates that IgG was less efficiently entrapped in the gel matrix of H11P than in H6P or H7P. As already discussed in chapter 4, matrix formation and density are closely correlated to micelle interconnection and the most ordered and most densely packed matrix can be found at T_{max} as analysed by penetration resistance. Considering that IgG leads to a decrease in T_{max} for 20 % PMT gels, the following order of T_{max} was found: H11P < H7P < H6P = 37 °C < H4P.

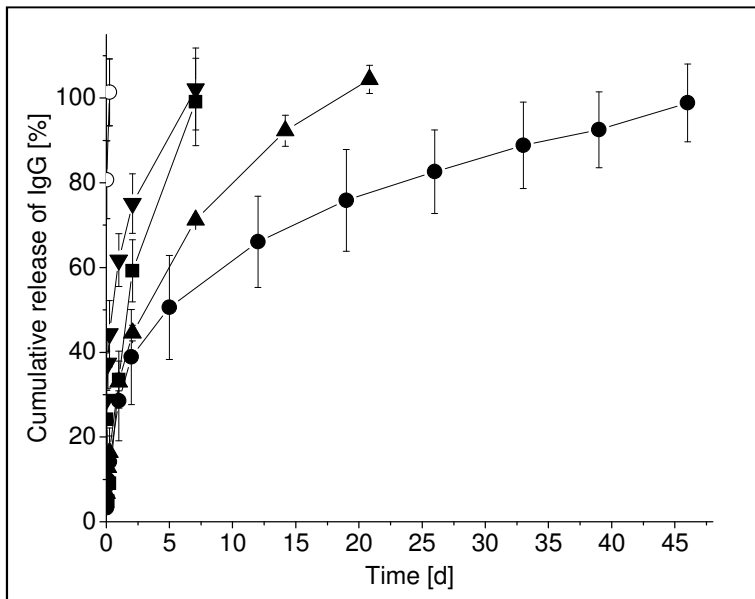


Fig. 5.3: Cumulative release of 20 mg/ml IgG from pre-formed 20 % depots of Poloxamer 403 (5.8 kDa, ○), H4P (26 kDa, ■), H6P (36 kDa, ●), H7P (43 kDa, ▲) or H11P (64 kDa, ▼) at 37 °C; n = 3

Thus, H4P gels with $T_{max} > 37\text{ °C}$ have a less complete micelles network, triggering lower gel strength and faster dissolution. For H7P and most pronounced for H11P gels ($T_{max} < 37\text{ °C}$) interconnected micelle networks were already partly molten at 37 °C, leading to less efficient protein entrapment than in H6P gels ($T_{max} = 37\text{ °C}$). PMT M_w could therefore serve as trigger to set release periods on demand for days to weeks.

5.2.2. Impact of PMT concentration on IgG release

Pre-formed depots with 20 mg/ml IgG from H6P gels with PMT concentration of 10, 15 and 20 %, respectively, were generated and analysed. A strong dependency of release rates on PMT concentration was found (Fig. 5.4). As already discussed above, for 20 % H6P a burst of 29 % and complete IgG release within 46 d were achieved. At lower gel concentration, IgG release was accelerated to 53 and 100 % burst for 15 and 10 % gels, respectively. IgG release was completed within 28 d for 15 % H6P gels, although gels were not dissolved at this time point.

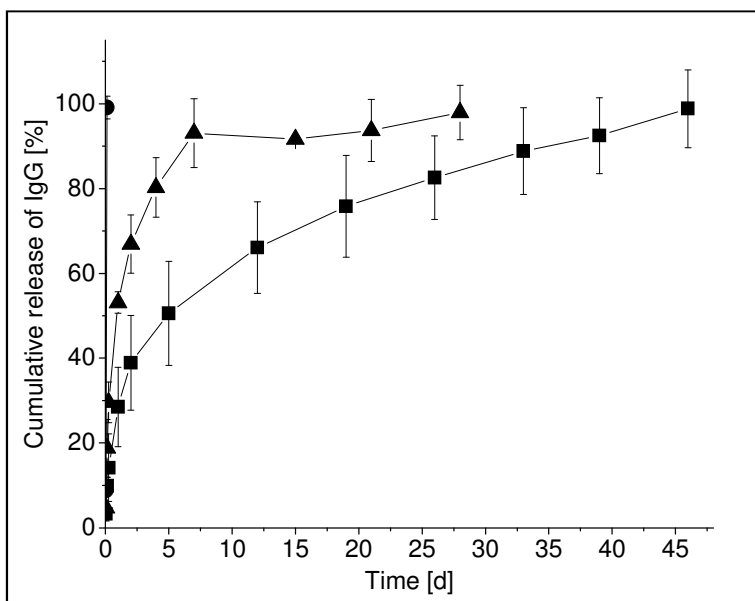


Fig. 5.4: Cumulative release of 20 mg/ml IgG from pre-formed H6P depots with 10 (●), 15 (▲) or 20 (■) % gel concentration at 37 °C; n = 3

Interestingly, there was no notable difference in gel volume between the different H6P concentrations and, thus, matrix density is lower for 10 and 15 % compared to 20 % gels. Furthermore, T_{max} of H6P gels is shifted to higher temperatures by decreasing gel concentration and addition of IgG, being 37 °C at 20 % but > 37 °C for 15 and 10 % H6P gels. This results in further reduced matrix density for 10 and 15 % compared to 20 % gels, leading to faster IgG release and faster gel dissolution. For gels with $T_{max} < 37$ °C, e.g. 20 % H7P and H11P, reducing gel concentration might lead to shift in T_{max} closer to 37 °C and gel concentration may affect IgG release differently.

5.2.3. Impact of IgG concentration on release from PMT gels

Drug concentration is reported to affect release rates of depot formulations [117, 154, 155]. At 5, 20 and 80 mg/ml IgG nearly identical release profiles with complete protein release after 46 d were observed (Fig. 5.5A). This corresponds to a total released protein mass of approx. 2.5, 10 and 40 mg (Fig. 5.5B) for the three different IgG concentrations, respectively. At 5 mg/ml a 24 h burst of 57 % (1.4 mg) was observed. For 20 mg/ml 29 % (2.9 mg) IgG, were found. Increasing protein concentration to 80 mg/ml the burst after 24 h was 19 % (7.6 mg).

Interestingly, the fraction released within the first 24 h decreased with increasing IgG concentration. In chapter 4.2.6 for H6P a T_{\max} of 37 °C at 80 mg/ml IgG was found, leading to a more pronounced protein entrapment and, consequently, reduced burst release. As discussed in chapter 4.10, all PMT gels showed reversible protein precipitation. With increasing IgG concentration the precipitated fraction became smaller (99 % at 20 mg/ml and 81 % at 80 mg/ml). Therefore, if this precipitation was the main sustaining mechanism, for 20 mg/ml a more pronounced sustaining than for 80 mg/ml was to be expected. It can be concluded that IgG release is less governed by protein concentration and/or precipitation than by gel matrix structure. In contrast, many other hydrogel systems like pNiPAAm co-polymers offer limited protein loading (e.g. 90 to 95 % loading efficacy for 2 mg/ml insulin and even less for Angiotensin II, [120]) and a concentration dependent release within hours to days [9].

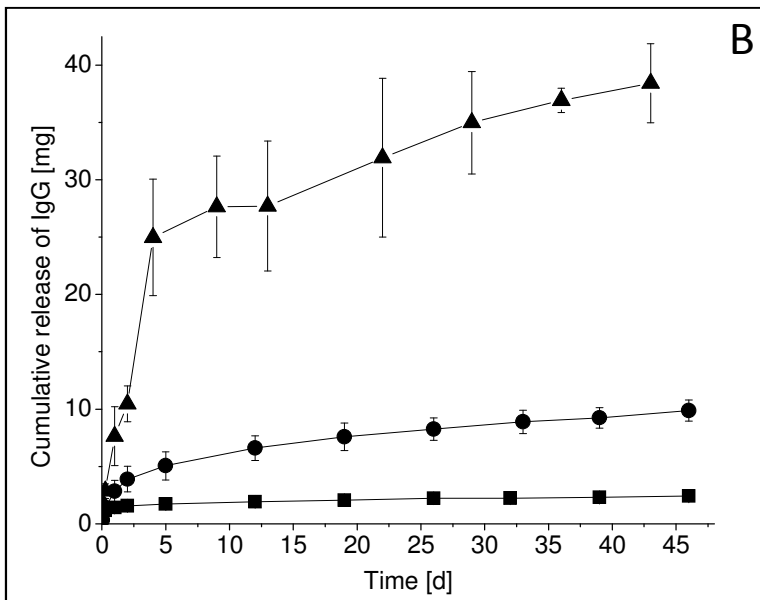
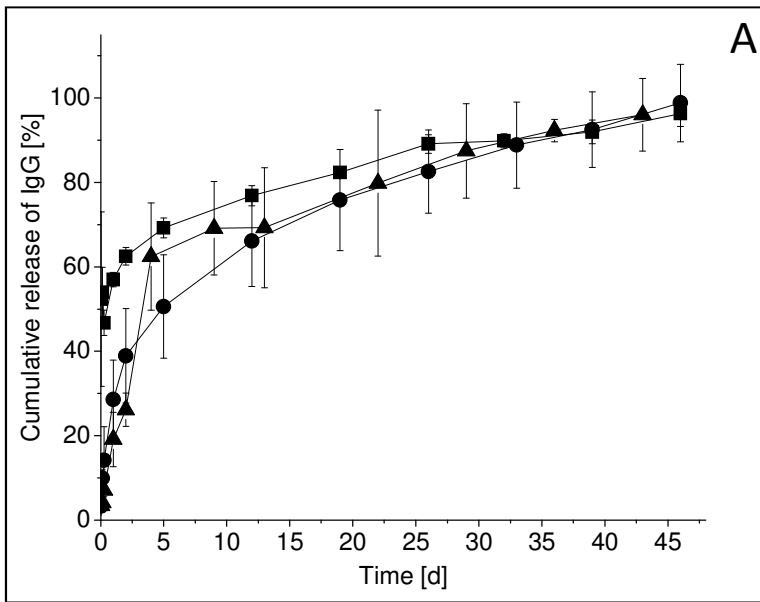


Fig. 5.5: Cumulative release of 5 (■), 20 (●) or 80 (▲) mg/ml IgG from pre-formed 20 % H6P depots at 37 °C; A: released protein fraction; B: total protein mass released; n = 3

5.2.4. Impact of diisocyanate structure on IgG release

Diisocyanate quality was found to strongly alter gel strength (chapter 4.2.3). Comparing 36 kDa H6P and 37 kDa M6P at gel concentrations of 20 % with 20 mg/ml IgG each, M6P showed higher burst (37 vs. 29 %), and faster complete release (35 vs. 46 d) (Fig. 5.6). Comparing 42 kDa B7P and 43 kDa H7P, again at 20 % gel concentration and 20 mg/ml IgG each, B7P had lower burst (24 vs. 29 %) and longer overall release time (35 vs. 19 d).

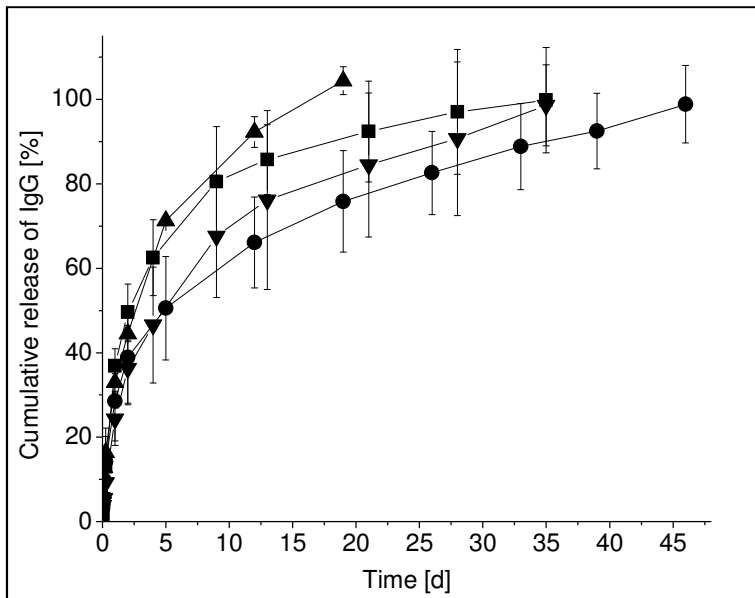


Fig. 5.6: Cumulative release of 20 mg/ml IgG from pre-formed 20 % H6P (●), M6P (■), H7P (▲) or B7P (▼) depots at 37 °C; in % of total IgG mass; n = 3

More hydrophilic (smaller) diisocyanates led to higher T_{max} and higher overall penetration resistance than more lipophilic (bigger) diisocyanates (chapter 4.2.3). Thus, compared to HDI systems, gels based on BDI linked PMTs have increased strength, and their T_{max} is shifted to higher temperatures. In contrast, MDI based gels have reduced gel strength. As discussed in chapter 4.6.8, hardening profiles were furthermore affected by IgG as T_{max} increased and overall penetration resistance decreased with protein load.

For 20 % H6P gels IgG load shifted T_{max} from approx. 34 °C to 37 °C, leading to a strong gel network, resulting in pronounced sustaining of protein release. 20 % M6P gels were found to have very similar T_{max} values as H6P gels, but reduced overall gel strength, representing matrix density, leading to a slightly faster protein release compared to H6P gels. Protein-free 20 % B7P gels showed a T_{max} of 37 °C, but addition of IgG led to a shift in $T_{max} > 37$ °C and therefore incomplete matrix formation at 37 °C. Compensation of this T_{max} shift by reducing the gel concentration, B7P gels might offer enhanced sustaining properties.

5.2.5. In situ-formed PMT depots for controlled IgG delivery

The aim of this thesis is to develop injectable in situ-forming depots for controlled protein delivery. Hence, release profiles of in situ-formed depots were investigated. As discussed in chapter 4.1, a rod-like structure was formed. As shown in Fig. 5.7 burst release of IgG within the first 24 h was approx. 30 % for both in situ-formed and pre-formed depots. IgG release from in situ-formed depots was completed after 26 d, compared to 46 d for pre-formed counterparts.

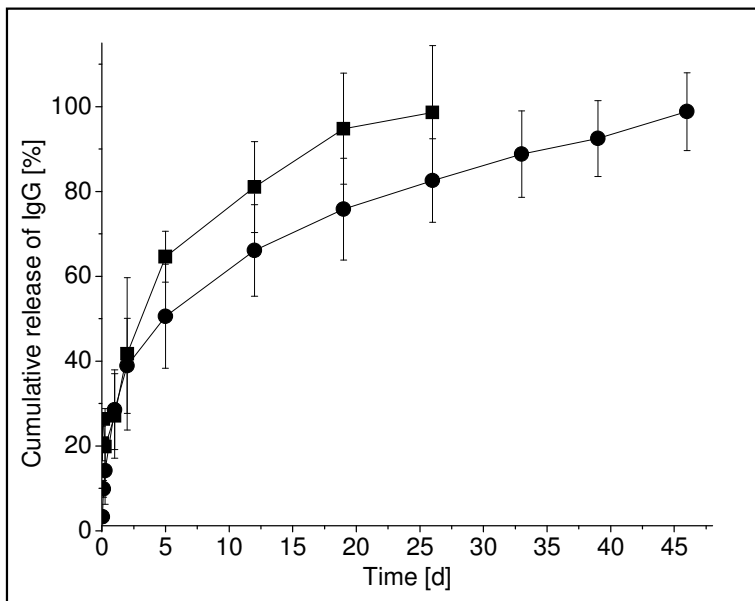


Fig. 5.7: Cumulative release of 20 mg/ml IgG from pre-formed (●) or in situ-formed (■) 20 % H6P depots at 37 °C; n = 3

No relevant difference in dissolution rate could be found comparing in situ-formed and pre-formed depots (chapter 4.3.8). This indicates that mechanical properties are independent of formation strategy. Increased IgG release rates could be explained by increased surface area of the worm-like structure compared to the condensed block structure of pre-formed depots. Interestingly, there is no increase in burst release upon in situ hardening. Hardening appears to be fast enough to prevent significant solution of drug and/or thermo-polymer immediately after injection into 37 °C warm media. This is an outstanding property of PMT gels, as other hydrogels with a hardening upon injection principle show higher bursts and overall faster release. E.g. pNiPAAm-PEG gels with 40 % BSA burst release, [107]. A PEG-PCL-PEG system with up to 80 % burst release [176], and poloxamer 407 mixed with polysorbate 80 showing 40 % burst within 24 h [177].

5.2.6. IgG release from PMT depots at different temperatures

PMT gels undergo thermo-reversible hardening and melting. This is caused by formation and subsequent deformation of a coherent micellar network. Network density and/or micelle interconnectivity are highest at a specific T_{max} values. T_{max} depends on PMT M_w , concentration and hydrophilicity, as well as on protein load. For concentration and M_w series of PMT IgG release was slowest for systems with T_{max} of, or at least close to, 37 °C. For 20 % H6P gels with 20 mg/ml IgG mechanical strength decreased at temperatures below or above 37 °C (= T_{max}). As shown in Fig. 5.8 this also affected IgG release: at 35 °C and 39 °C the 24 h burst was increased to 38 % and 47 %, with completed IgG release after 40 or 26 d, respectively.

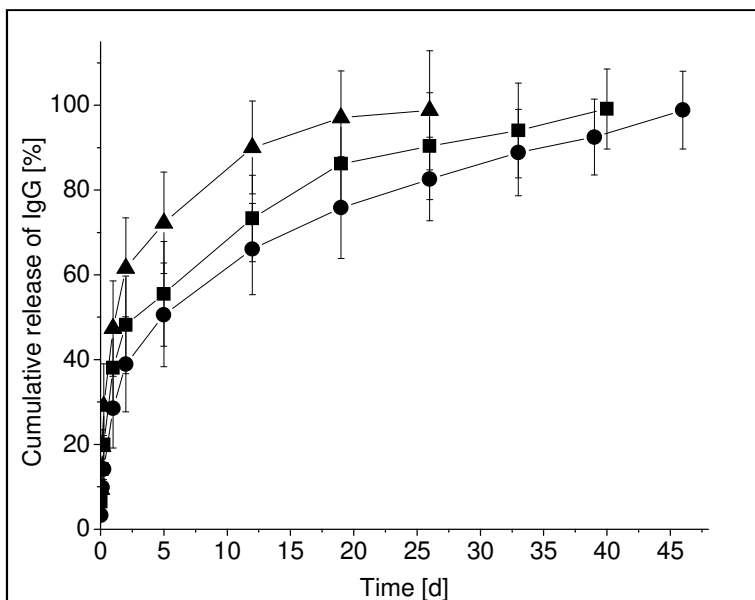


Fig. 5.8: Cumulative release of 20 mg/ml IgG from pre-formed 20 % H6P depots at 35 (■), 37 (●) or 39 (▲) °C; n = 3

As shown before, IgG release was most effectively sustained at or close to T_{max} of the corresponding gel system. Release at temperatures higher than T_{max} is faster than for temperatures below T_{max} , indicating that matrix melting affects matrix density more than yet incomplete matrix formation.

Overall, increased body temperature, e.g. due to local inflammation, may accelerate IgG release from 20 % H6P depots with their T_{max} of 37 °C. At the same time increased body temperature could slow down protein release for lower M_w PMT depots or less concentrated H6P gels with T_{max} values < 37 °C .

5.2.7. Impact of PMT gel shelf-life on IgG release

As discussed in chapter 1.3.2 PMTs contain urethane groups. These urethane groups can be hydrolyzed, generating smaller PMT derivatives and/or poloxamer. In vivo, this mechanism should lead to depot dissolution and subsequent polymer extraction by the kidneys. Also, a potential degradation of PMTs prior to depot formation may affect M_w and, hence, both dissolution and release rate. Therefore, a 20 % H6P gel with 20 mg/ml IgG was prepared and stored at 2-8 °C for 15 weeks and subsequently IgG release from a pre-formed depot was monitored at 37 °C. As seen in Fig. 5.9 the release was not significantly changed ($p = 0.05$), and potential H6P hydrolysis upon storage appears to have no impact on the sustaining properties of the derived hydrogels.

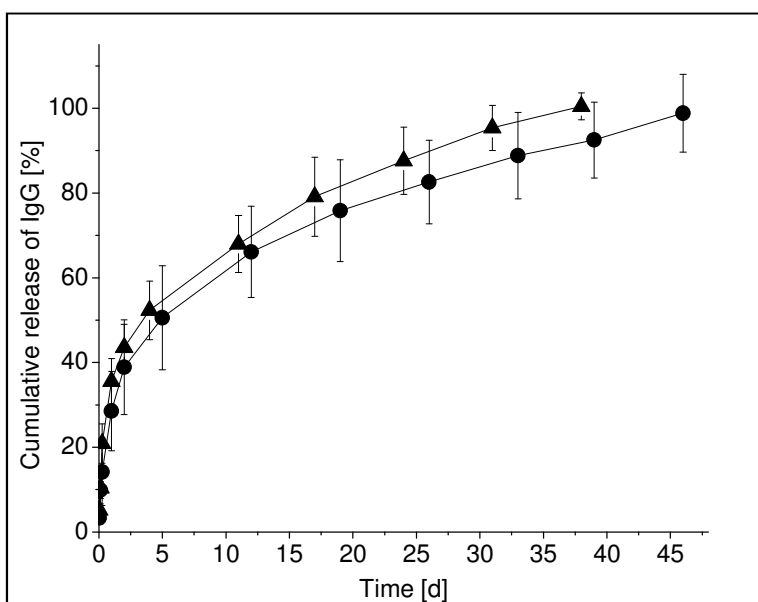


Fig. 5.9: Cumulative release release at 37 °C of 20 mg/ml IgG from approx. 0.5 g pre-formed 20 % H6P depots from freshly prepared gel (■) or gel stored for 15 weeks at 2-8 °C (▲); $n = 3$

IgG almost completely precipitated in 20 % H6P gels at 2-8 °C, and the protein was actually stored in a precipitated state for 15 weeks. Interestingly, still complete IgG release was observed and HPSEC analysis showed no indication for the formation of protein aggregates. It can be concluded that IgG precipitation in PMT gels is reversible, even after 15 weeks.

5.3. Integrity of released IgG

In order to serve as controlled release system PMT gels and depots have to maintain protein integrity. Chapter 5.1 already discussed protein precipitation in PMT systems. Depending on several parameters, including protein quality and concentration of both protein and PMT, up to 99 % protein were found in the precipitate. However, all precipitates redissolved upon mixing with PBS. Despite initial precipitation, IgG was released completely for all PMT systems investigated. In HPSEC, neither soluble aggregates nor fragments were found. Even storing the precipitate for 15 weeks in an aqueous system at 2-8 °C led to the same results (chapter 5.2.7).

To further proof the integrity of released IgG this chapter summarizes results from visual inspection, HPSEC, and light obscuration, turbidity and intrinsic fluorescence. Pre-formed 20 % H7P depots with 20 mg/ml IgG were chosen as candidates as they released approx. 3.3 mg IgG within the final 13 days of the release period and the shortened time frame for H7P release compared to H6P reduced measurement time. Furthermore, two controls were tested (i) pre-formed placebo 20 % H7P depots, representing particles and noise generated by the thermo-polymer itself; (ii) pre-formed placebo 20 % H7P depots with additional IgG spiked at 0.5 mg/ml immediately after PBS addition, representing particles and other species formed by IgG under the given release conditions in presence of PMT, but without initial protein precipitation and release from a gel depot.

5.3.1. Visible particles

Release samples as well as all control samples were free of visible particles after 1 d, 1 week and 3 weeks. After three weeks in one sample and one control sample particles deriving from disintegration of the PMT depots were noticeable.

5.3.2. Turbidity

For IgG release samples a turbidity of 0.77 ± 0.27 FNU was found after 3 weeks. At the same time point control samples showed a turbidity of 0.72 ± 0.52 (IgG spiked) and 0.28 ± 0.07 (H7P placebo) FNU, respectively. Overall, turbidity values were low, and IgG release as well as spiked IgG samples showed no significant difference ($p = 0.01$). The overall low turbidity correlates well with visual observation of clear, nearly particle free solutions and indicates the absence of IgG aggregates.

5.3.3. SEC analysis

All IgG peaks detected for release and control samples represent monomers. They are symmetrical with no relevant tailing or fronting. No fragment or aggregate peaks can be seen. Of course, placebo samples show no protein peak at all.

5.3.4. Subvisible particles

In all samples subvisible particles were formed. For release samples $61,820 \pm 1,220$ particles $> 1 \mu\text{m}$ were found in the 20 ml release medium, with $1,440 \pm 1,740$ (2.3 %) of them $> 10 \mu\text{m}$ and 260 ± 280 (0.4 %) $> 25 \mu\text{m}$. In IgG spiked samples $36,880 \pm 800$ particles $> 1 \mu\text{m}$, 140 ± 60 (0.4 %) $> 10 \mu\text{m}$ and 40 ± 20 (0.1 %) $> 25 \mu\text{m}$ were detected. In H7P placebo samples $9,800 \pm 540$ particles $> 1 \mu\text{m}$ were detected, among them 120 ± 20 (1.2 %) $> 10 \mu\text{m}$ and 40 ± 0 (0.4 %) $> 25 \mu\text{m}$.

Subvisible particles were detected by HPSEC and light obscuration, as described in chapters 2.2.5 and 2.2.8. For both measurements portions of turbidity samples (chapter 2.2.14) were used. Furthermore, all IgG release data was derived from HPSEC; but only these special samples were generated under continuous laminar air-flow conditions.

Table 5.1 shows subvisible particles as analysed by light obscuration. Numbers represent calculated total particle counts in the entire PBS volume of 20 ml. It can be seen that for

Particle fraction [μm]	>1	>10	>25
Release sample medium	61820 \pm 1220	1440 \pm 1740	260 \pm 280
IgG spiked control medium	36880 \pm 800	140 \pm 60	40 \pm 20
H7P placebo control medium	9800 \pm 540	120 \pm 20	40 \pm 0

Table 5.1: Subvisible particles as determined by light obscuration of samples drawn after 3 weeks release under LAF conditions. Numbers represent extrapolated values for the entire 20 ml release medium. Release sample is 0.5 g pre-formed 20 % H7P with 20 mg/ml IgG in 20 ml PBS at 37 °C, control samples are analogous H7P placebo gels, one of them with additional IgG spiking to yield protein concentration of 0.5 mg/ml; n = 3

Total numbers of particles > 1 μm as well as > 10 μm were significantly higher for release samples than for IgG spiked controls ($p = 0.01$). The same holds true for particles > 1 μm in IgG spiked controls compared with H7P placebo samples ($p = 0.01$). All other differences are non-significant ($p = 0.05$). The increased particle numbers compared to placebo correspond to increased turbidity values. Considering H7P derived particles nearly identical in all samples (justified by the very low sd for placebo samples), the number of proteinaceous particles can be estimated: in release samples approx. 52,000 particles > 1 μm , 1,300 > 10 μm and 200 > 25 μm might originate from IgG. In IgG spiked control samples approx. 27,000 particles > 1 μm , but none > 10 or 25 μm might be proteinaceous.

As proteinaceous particles have to be considered potentially immunogenic [178], according to Ph.Eur. 2.9.19 liquids for injection may contain only up to 6,000 particles > 10 μm . Hence, even if all particles were to be released simultaneously, 20 % H7P depots with 20 mg/ml IgG meet Ph.Eur. criteria. Thus, protein aggregation is no relevant issues for IgG release from H7P gels. As all gels showed similar protein precipitation as well as complete IgG release, this trend is well generalized for other PMTs.

5.3.5. Intrinsic fluorescence

Measuring intrinsic fluorescence no differences between freshly diluted IgG stock solution (0.5 mg/ml) and release medium after 3 weeks could be seen (Fig. 5.10), representing maintained secondary protein structure. FTIR as orthogonal method could not be used due to interference of the urethane signals of dissolved PMT.

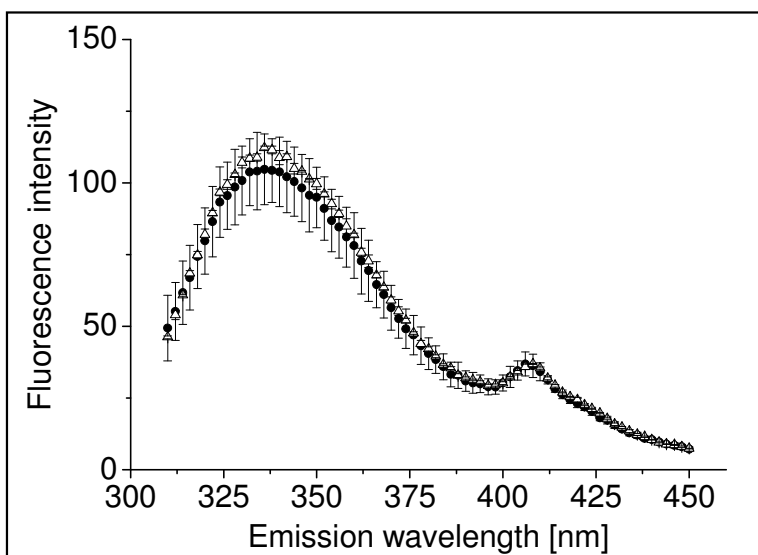


Fig. 5.10: Intrinsic fluorescence of freshly prepared 0.5 mg/ml IgG solution (Δ) and release samples of 20 mg/ml IgG from pre-formed 20 % H6P depots after three weeks (\bullet); $n = 3$. To render graphs visible, not all data points are shown.

5.4. Chemical stability of H7P

Dissolution experiments showed that H7P depots are stable at physiological pH and temperature for several months (chapter 4.3). Gels can be prepared several weeks prior to application and stored at 2-8 °C without negative impact on release properties (chapter 5.2.7). To further characterize the polymer stability, GPC analysis was performed. Dry H7P and autoclaved H7P, H7P dissolved in either PBS, 0.5 M HCl or 0.5 M NaOH after 7 d at 40 °C and after 3 d at 90 °C were analysed.

Naive H7P yielded a M_w of 43.8 kDa (table 5.2), which is in good accordance to 43 kDa as specified by the provider. Approx. 80 % material was lost from the autoclaving bag during the autoclaving process of H7P, leaving polymers with an increased M_w of 51.5 kDa as smaller M_w fractions of H7P dissolve and hydrolyse more readily. Incubation at 40 °C for one

week showed no impact on M_w as 44.1, 45.6 and 43.1 kDa were found in PBS, HCl and NaOH, respectively. Increasing incubation temperature to 90 °C, however, led to strong M_w losses to 27.2 kDa in PBS, 3.3 kDa in HCl and a M_w below the detection limit for NaOH samples.

H7P manipulation	M_w [kDa]
-	43.8
autoclaving	51.5
7 d incubation at 40 °C in PBS	44.1
7 d incubation at 40 °C in 0.5 M HCl	45.7
7 d incubation at 40 °C in 0.5 M NaOH	43.1
3 d incubation at 90 °C in PBS	27.3
3 d incubation at 90 °C in 0.5 M HCl	3.3
3 d incubation at 90 °C in 0.5 M NaOH	-

Table 5.2: M_w of naive and temperature-treated H7P as determined by GPC.; n = 1

The decrease in M_w is mainly induced by hydrolysis of urethane groups, forming poloxamer unimers [123]. Even after 121 °C for 15 min a high M_w fraction remained, suggesting that small M_w fractions hydrolyse more readily. Incubation at 40 °C for 7 d indicates good PMT stability, even at extreme pH values of 0.3 (HCl) and 13.7 (NaOH). This is in accordance to the dissolution experiments as PMT depots remain stable for months rather than weeks. At 90 °C PMT degrade substantially and, as expected for urethane groups, this cleavage was much more pronounced at pH 0.3 and 13.7 than at 7.2 [123]. Hence, PMTs are fairly stable under relevant storage, application and release conditions.

6. Summary and outlook

6.1. In situ cross-linked HA gels

Several chemically cross-linked hydrogels are reported as promising controlled release platforms [5, 21, 55, 150, 151]. Among these, the derivatization and cross-linking of HA by means of azide-alkyne cycloaddition is specifically interesting [49, 81, 82]. In an effort to test this approach for protein delivery the degree of HA substitution achieved was below the values reported in literature. Formation of high-molecular weight species could be shown by HPSEC and centrifugation experiments. At the same time, a significant amount of unreacted small M_w species remains due to the low DoS. Furthermore, the cross-linking achieved is not sufficient to form a gel structure with increased viscosity and reduced water solubility compared to unmodified HA. The impact of linker size and concentration, as well as the actual release profiles of proteins from the cross-linked HA could not be investigated as no functioning controlled release system is generated. Possibly, simultaneous cleavage of HA by the Cu-(II)/ascorbic acid system [134] competes with cross-linking.

To make the system suitable for the task of in situ formation of controlled release systems for protein pharmaceuticals the DoS of the derivatized HA and the degree of cross-linking have to be increased. With this new material an increase in viscosity and a decrease in water solubility should be possible. A more water soluble linker could introduce more flexibility in the experimental design. Transition to copper-(I) or, preferably, copper-free protocols is highly recommended to sustain protein integrity within the in situ gelling system. This would, at the same time, entirely prevent HA cleavage by Cu-(II)/Ascorbic acid. Also other click reactions to cross-link HA are interesting alternatives [152].

Overall, the discussed system of cross-linking HA by the azide-alkyne cycloaddition offers great potential. However, there are many complex parameters to be set and characterized: the initial M_w and concentration of the HA, the derivatization procedure, the catalytic system used, linker concentration, size and solubility, as well as potential cleavage reactions and protein integrity. Setting all these parameters correctly, to achieve a functional controlled release system for protein pharmaceuticals, requires a deeper understanding of the entire system.

6.2. Thermo-responsive PMT gels

PMTs are amphiphilic block-co-polymers generated by chain-elongation of poloxamers with diisocyanates. Similar to unmodified poloxamer, PMTs form micelles. These micelles interconnect and rearrange into higher molecular structures to form defined hydrogel networks. This sol-gel transition occurs over approx. 10 °C between 25 to 35 °C, for e.g. 20 % H6P (36 kDa M_w).

A series of different PMTs with different M_w , poloxamer quality and diisocyanate quality are studied, introducing different hydrophilicity, gel formation, clouding and dissolution properties. PMT gels offer promising thermo-responsive hardening profiles in the desired temperature range between ambient temperature and body temperature. Gels are generally injectable using 20 G needles at ambient temperature and offer acceptable mechanical strength > 1 kPa by many PMT qualities at concentrations higher than 10 %. Gels of poloxamer 403 based PMTs remain stable in PBS at 37 °C for several weeks, followed by slow dissolution. Poloxamer 407 based PMTs dissolve within hours to days. Increasing M_w or PMT concentration lead to increased gel hardness, shifting gel formation to lower temperatures. Using BDI as linking diisocyanate leads to harder gels and shifts in hardening profiles to higher temperatures compared to HDI based PMTs. MDI linkage reduces gel strength, but does not lead to similar temperature shifts as BDI. In general, with higher gel strength the dissolution rate for poloxamer 403 PMTs decreases. Addition of PEG can be used to adjust hardening and gel dissolution. Addition of high protein amounts increases the temperature of highest mechanical strength, T_{max} , but does not negatively impact the gel strength at 37 °C.

Several PMTs showed promising release profiles for IgG over several days to weeks with a burst release of up to 30 % within 24 h. The delay in release at body temperature was most pronounced for systems with T_{max} values close to 37 °C. This target was matched by 20 % H6P gels with 20 mg/ml IgG. Other potential candidates include H4P, H7P, B7P and M6P gels at 20 %. Also other gel concentrations might be applicable, esp. for high M_w PMTs like H7P, H8P or even H11P. For H6P systems manual injection through 20 G needles could be easily performed, leading to in situ-formed depots with also strongly pronounced sustaining properties. Very high protein concentrations of up to 80 mg/ml IgG could be effectively

delivered. Furthermore, for H6P, sustained release of Lysozyme and 150 kDa FITC-Dextran were shown as well. These latter two substances were released faster than IgG and other PMTs at different concentrations might be beneficial. This makes PMT gels a very promising and competitive sustained release system.

Both proteins showed marked but reversible precipitation in all PMT gels tested, while FITC-Dextran remained soluble. This precipitation might add to the sustaining properties of PMT depots, but matrix diffusion remains the key parameter as indicated by the strong impact of T_{max} shifts. As the PMT depots dissolved slowly under physiological conditions, depot erosion played only a minor role in release profiles. Lasting months rather than weeks at 37 °C in vitro, 20 % PMT depots might actually be too stable as their half-life in the body might be months to years. Optimizing gel concentration, PMT M_w and additives like PEG can be used to increase dissolution rates.

Throughout all release experiments, despite the initial protein precipitation in PMT gels, no indication for instability of IgG in PMT gels or upon release was found. No proteinaceous visible particles and only a minimal number of subvisible particles were released from the gel matrix. Neither increased turbidity, nor soluble aggregates or fragments as determined by HPSEC, nor changes in intrinsic fluorescence were observed. At the same time, PMT polymers and gels were fairly stable at 2-8 °C, under relevant physiological conditions and at 40 °C.

All in all, PMTs are a promising system for injectable in situ hardening hydrogels for controlled protein delivery. As release periods can be set between days to weeks by choosing the correct PMT system, both local and systemic sustained release should be possible.

7. References

1. Rader, R.A., *(Re)defining biopharmaceutical*. Nat Biotech, 2008. **26**(7): p. 743-751.
2. Sommerfeld, S. and J. Strube, *Challenges in biotechnology production—generic processes and process optimization for monoclonal antibodies*. Chemical Engineering and Processing: Process Intensification, 2005. **44**(10): p. 1123-1137.
3. Manning, M., et al., *Stability of Protein Pharmaceuticals: An Update*. Pharmaceutical Research, 2010. **27**(4): p. 544-575.
4. Wang, W., *Instability, stabilization, and formulation of liquid protein pharmaceuticals*. International Journal of Pharmaceutics, 1999. **185**(2): p. 129-188.
5. Vermonden, T., R. Censi, and W.E. Hennink, *Hydrogels for Protein Delivery*. Chemical Reviews (Washington, DC, United States), 2012. **112**: p. 2853-2888.
6. Tang, L., et al., *Pharmacokinetic aspects of biotechnology products*. Journal of Pharmaceutical Sciences, 2004. **93**(9): p. 2184-2204.
7. Saks, S.R. and L.B. Gardner, *The pharmacoeconomic value of controlled-release dosage forms*. Journal of Controlled Release, 1997. **48**(2–3): p. 237-242.
8. Adams, S.B., et al., *Effect of needle size and type, reuse of needles, insertion speed, and removal of hair on contamination of joints with tissue debris and hair after arthrocentesis*. Vet Surg, 2010. **39**(Copyright (C) 2011 U.S. National Library of Medicine.): p. 667-73.
9. Shi, Y. and L. Li, *Current advances in sustained-release systems for parenteral drug delivery*. Expert Opinion on Drug Delivery, 2005. **2**(6): p. 1039-1058.
10. Malik, D.K., et al., *Recent advances in protein and peptide drug delivery systems*. Curr Drug Deliv, 2007. **4**(2): p. 141-51.
11. Degim, I.T. and N. Celebi, *Controlled delivery of peptides and proteins*. Curr Pharm Des, 2007. **13**(1): p. 99-117.
12. Sinha, V.R. and A. Trehan, *Biodegradable microspheres for protein delivery*. Journal of Controlled Release, 2003. **90**(3): p. 261-280.
13. Bysell, H., et al., *Microgels and microcapsules in peptide and protein drug delivery*. Advanced Drug Delivery Reviews, 2011. **63**(13): p. 1172-1185.
14. Kim, K. and D. Pack, *Microspheres for Drug Delivery*, in *BioMEMS and Biomedical Nanotechnology*, M. Ferrari, A. Lee, and L.J. Lee, Editors. 2006, Springer US. p. 19-50.
15. Crofts, G. and T.G. Park, *Protein delivery from poly(lactic-co-glycolic acid) biodegradable microspheres: release kinetics and stability issues*. J Microencapsul, 1998. **15**(6): p. 699-713.
16. Lin, C.-C. and A.T. Metters, *Hydrogels in controlled release formulations: Network design and mathematical modeling*. Advanced Drug Delivery Reviews, 2006. **58**(12–13): p. 1379-1408.
17. Kempe, S. and K. Mäder, *In situ forming implants — an attractive formulation principle for parenteral depot formulations*. Journal of Controlled Release, 2012. **161**(2): p. 668-679.
18. Hoare, T.R. and D.S. Kohane, *Hydrogels in drug delivery: Progress and challenges*. Polymer, 2008. **49**(8): p. 1993-2007.
19. Singh, A., et al., *Hydrogels: A review*. International Journal of Pharmaceutical Sciences Review and Research, 2010. **4**(2): p. 97-105.
20. Kamath, K.R. and K. Park, *Biodegradable hydrogels in drug delivery*. Advanced Drug Delivery Reviews, 1993. **11**(1–2): p. 59-84.
21. Chung, H.J. and T.G. Park, *Self-assembled and nanostructured hydrogels for drug delivery and tissue engineering*. Nano Today, 2009. **4**(5): p. 429-437.
22. Gupta, P., K. Vermani, and S. Garg, *Hydrogels: from controlled release to pH-responsive drug delivery*. Drug Discovery Today, 2002. **7**(10): p. 569-579.
23. Hoffman, A.S., *Hydrogels for biomedical applications*. Advanced Drug Delivery Reviews, 2002. **54**(1): p. 3-12.
24. Packhaeuser, C.B., et al., *In situ forming parenteral drug delivery systems: an overview*. European Journal of Pharmaceutics and Biopharmaceutics, 2004. **58**(2): p. 445-455.

25. Chaterji, S., I.K. Kwon, and K. Park, *Smart polymeric gels: Redefining the limits of biomedical devices*. Progress in Polymer Science, 2007. **32**(8-9): p. 1083-1122.
26. Shibayama, M., *Structure-mechanical property relationship of tough hydrogels*. Soft Matter, 2012. **8**(31): p. 8030-8038.
27. Silberberg, A., *Gelled Aqueous Systems*, in *Polymers in Aqueous Media*. 1989, American Chemical Society. p. 3-14.
28. Ganji, F., S. Vasheghani-Farahani, and E. Vasheghani-Farahani, *Theoretical description of hydrogel swelling: a review*. Iranian Polymer Journal, 2010. **19**(5): p. 375-398.
29. Bromberg, L., *Scaling of Rheological Properties of Hydrogels from Associating Polymers*. Macromolecules, 1998. **31**: p. 6148-6156.
30. Prestwich, G.D., *Hyaluronic acid-based clinical biomaterials derived for cell and molecule delivery in regenerative medicine*. J. Controlled Release, 2011. **155**(2): p. 193-199.
31. Price, R.D., M.G. Berry, and H.A. Navsaria, *Hyaluronic acid: the scientific and clinical evidence*. Journal of Plastic, Reconstructive & Aesthetic Surgery, 2007. **60**(10): p. 1110-1119.
32. Lapčik, L., et al., *Hyaluronan: Preparation, Structure, Properties, and Applications†*. Chemical Reviews, 1998. **98**(8): p. 2663-2684.
33. Hargittai, I. and M. Hargittai, *Molecular structure of hyaluronan: an introduction*. Structural Chemistry, 2008. **19**(5): p. 697-717.
34. Chytil, M., et al., *Calorimetric and light scattering study of interactions and macromolecular properties of native and hydrophobically modified hyaluronan*. Carbohydrate Polymers, 2010. **81**: p. 855-863.
35. Choi, K.Y., et al., *Hyaluronic acid-based nanocarriers for intracellular targeting: Interfacial interactions with proteins in cancer*. Colloids Surf., B, 2012. **99**: p. 82-94.
36. Collins, M.N. and C. Birkinshaw, *Hyaluronic acid based scaffolds for tissue engineering-A review*. Carbohydr. Polym., 2013. **92**(2): p. 1262-1279.
37. Soltés, L., et al., *Molecular characteristics of some commercial high-molecular-weight hyaluronans*. Biomedical Chromatography, 2002. **16**(7): p. 459-462.
38. Šoltés, L., et al., *Solution properties of high-molar-mass hyaluronans: the biopolymer degradation by ascorbate*. Carbohydrate Research, 2007. **342**(8): p. 1071-1077.
39. Gaffney, J., et al., *Therapeutic applications of hyaluronan*. Molecular BioSystems, 2010. **6**(3): p. 437-443.
40. Ghosh, P., *The role of hyaluronic acid (hyaluronan) in health and disease: interactions with cells, cartilage and components of synovial fluid*. Clinical and experimental rheumatology, 1994. **12**(1): p. 75-82.
41. Ferguson, E.L., et al., *Evaluation of the physical and biological properties of hyaluronan and hyaluronan fragments*. International Journal of Pharmaceutics, 2011. **420**(1): p. 84-92.
42. Meyer, J., et al., *Sustained in vivo activity of recombinant human granulocyte colony stimulating factor (rHG-CSF) incorporated into hyaluronan*. Journal of Controlled Release, 1995. **35**(1): p. 67-72.
43. Larsen, N.E. and E.A. Balazs, *Drug delivery systems using hyaluronan and its derivatives*. Advanced Drug Delivery Reviews, 1991. **7**(2): p. 279-293.
44. Prisell, P.T., et al., *Evaluation of hyaluronan as a vehicle for peptide growth factors*. International Journal of Pharmaceutics, 1992. **85**(1-3): p. 51-56.
45. Schanté, C.E., et al., *Chemical modifications of hyaluronic acid for the synthesis of derivatives for a broad range of biomedical applications*. Carbohydrate Polymers, 2011. **85**(3): p. 469-489.
46. Simon, L.D., et al., *Mechanisms controlling diffusion and release of model proteins through and from partially esterified hyaluronic acid membranes*. Journal of Controlled Release, 1999. **61**(3): p. 267-279.
47. Oh, E.J., et al., *Target specific and long-acting delivery of protein, peptide, and nucleotide therapeutics using hyaluronic acid derivatives*. Journal of Controlled Release, 2010. **141**(1): p. 2-12.

48. Zhang, M. and S.P. James, *Synthesis and properties of melt-processable hyaluronan esters*. Journal of Materials Science Materials in Medicine, 2005. **16**(6): p. 587-593.
49. Crescenzi, V., C. Di Meo, and D. Galesso, *Hyaluronic acid derivatives obtained via "click chemistry" crosslinking*. 2008: WO 2008031525. p. 99 pp.
50. Crescenzi, V., et al., *New bioactive products and biomaterials from hyaluronic acid*. Chimica e l'Industria (Milan, Italy), 2002. **84**(2): p. 46.
51. Matricardi, P., et al., *Interpenetrating Polymer Networks polysaccharide hydrogels for drug delivery and tissue engineering*. Advanced Drug Delivery Reviews, 2013. **65**(9): p. 1172-1187.
52. Bodnar, M., et al., *Preparation and characterization of cross-linked hyaluronan nanoparticles*. Colloid and Polymer Science, 2009. **287**(8): p. 991-1000.
53. Crescenzi, V., et al., *Hyaluronan networking via Ugi's condensation using lysine as cross-linker diamine*. Carbohydrate Polymers, 2003. **53**(3): p. 311-316.
54. Crescenzi, V., et al., *Hyaluronan linear and crosslinked derivatives as potential/actual biomaterials*. Hyaluronan, [Proceedings of the International Cellucon Conference], 12th, Wrexham, United Kingdom, 2000, 2002. **1**: p. 261-268.
55. Hahn, S.K., et al., *Sustained release formulation of erythropoietin using hyaluronic acid hydrogels crosslinked by Michael addition*. International Journal of Pharmaceutics, 2006. **322**(1-2): p. 44-51.
56. Bulpitt, P. and D. Aeschlimann, *New strategy for chemical modification of hyaluronic acid: preparation of functionalized derivatives and their use in the formation of novel biocompatible hydrogels*. Journal of Biomedical Materials Research, 1999. **47**(2): p. 152-169.
57. Huisgen, R., G. Szeimies, and L. Moebius, *1,3-Dipolar cycloadditions. XXXII. Kinetics of the addition of organic azides to carbon-carbon multiple bonds*. Chemische Berichte, 1967. **100**(8): p. 2494-507.
58. Lutz, J.-F., *1,3-Dipolar cycloadditions of azides and alkynes: a universal ligation tool in polymer and materials science*. Angewandte Chemie, International Edition, 2007. **46**(7): p. 1018-1025.
59. Gil, M.V., M.J. Arevalo, and O. Lopez, *Click chemistry - what's in a name? Triazole synthesis and beyond*. Synthesis, 2007(11): p. 1589-1620.
60. Moses, J.E. and A.D. Moorhouse, *The growing applications of Click chemistry*. Chemical Society Reviews, 2007. **36**(8): p. 1249-1262.
61. Binder, W.H. and R. Sachsenhofer, *'Click' chemistry in polymer and material science: an update*. Macromolecular Rapid Communications, 2008. **29**(12-13): p. 952-981.
62. Diaz, D.D., et al., *Click chemistry in materials synthesis. 1. Adhesive polymers from copper-catalyzed azide-alkyne cycloaddition*. Journal of Polymer Science, Part A Polymer Chemistry, 2004. **42**(17): p. 4392-4403.
63. Meldal, M., *Polymer "clicking" by CuAAC reactions*. Macromolecular Rapid Communications, 2008. **29**(12-13): p. 1016-1051.
64. Bock, V.D., H. Hiemstra, and J.H. van Maarseveen, *Cu(I)-catalyzed alkyne-azide click cycloadditions from a mechanistic and synthetic perspective*. European Journal of Organic Chemistry, 2005(1): p. 51-68.
65. Chen, L. and C.-J. Li, *Catalyzed reactions of alkynes in water*. Advanced Synthesis & Catalysis, 2006. **348**(12+13): p. 1459-1484.
66. Clark, M. and P. Kiser, *In situ crosslinked hydrogels formed using Cu(I)-free Huisgen cycloaddition reaction*. Polymer International, 2009. **58**(10): p. 1190-1195.
67. Ess, D.H., G.O. Jones, and K.N. Houk, *Transition States of Strain-Promoted Metal-Free Click Chemistry: 1,3-Dipolar Cycloadditions of Phenyl Azide and Cyclooctynes*. Organic Letters, 2008. **10**(8): p. 1633-1636.
68. Golas, P.L., N.V. Tsarevsky, and K. Matyjaszewski, *Structure-reactivity correlation in "click" chemistry: substituent effect on azide reactivity*. Macromolecular Rapid Communications, 2008. **29**(12-13): p. 1167-1171.

69. Golas, P.L., et al., *Catalyst Performance in "Click" Coupling Reactions of Polymers Prepared by ATRP: Ligand and Metal Effects*. *Macromolecules*, 2006. **39**(19): p. 6451-6457.
70. Meldal, M. and C.W. Tornøe, *Cu-Catalyzed Azide-Alkyne Cycloaddition*. *Chemical Reviews* (Washington, DC, United States), 2008. **108**(8): p. 2952-3015.
71. Becer, C.R., R. Hoogenboom, and U.S. Schubert, *Click Chemistry beyond Metal-Catalyzed Cycloaddition*. *Angewandte Chemie, International Edition*, 2009. **48**(27): p. 4900-4908.
72. Binauld, S., et al., *Kinetic study of copper(I)-catalyzed click chemistry step-growth polymerization*. *Journal of Polymer Science, Part A Polymer Chemistry*, 2008. **46**(16): p. 5506-5517.
73. Prescher, J.A. and C.R. Bertozzi, *Chemistry in living systems*. *Nature Chemical Biology*, 2005. **1**(1): p. 13-21.
74. Speers, A.E., G.C. Adam, and B.F. Cravatt, *Activity-based protein profiling in vivo using a copper(I)-catalyzed azide-alkyne [3 + 2] cycloaddition*. *Journal of the American Chemical Society*, 2003. **125**(16): p. 4686-4687.
75. Agard, N.J., J.A. Prescher, and C.R. Bertozzi, *A strain-promoted [3+2] azide-alkyne cycloaddition for covalent modification of biomolecules in living systems*. *Journal of the American Chemical Society*, 2004. **126**(46): p. 15046-15047.
76. Baskin, J.M., et al., *Copper-free click chemistry for dynamic in vivo imaging*. *Proceedings of the National Academy of Sciences of the United States of America*, 2007. **104**(43): p. 16793-16797.
77. Fokin, V.V., *Click Imaging of Biochemical Processes in Living Systems*. *ACS Chemical Biology*, 2007. **2**(12): p. 775-778.
78. Ning, X., et al., *Visualizing metabolically labeled glycoconjugates of living cells by copper-free and fast Huisgen cycloadditions*. *Angewandte Chemie, International Edition*, 2008. **47**(12): p. 2253-2255.
79. Lutz, J.-F., *Copper-free azide-alkyne cycloadditions: new insights and perspectives*. *Angewandte Chemie, International Edition*, 2008. **47**(12): p. 2182-2184.
80. Brik, A., et al., *1,2,3-triazole as a peptide surrogate in the rapid synthesis of HIV-1 protease inhibitors*. *ChemBioChem*, 2005. **6**(7): p. 1167-1169.
81. Crescenzi, V., et al., *Novel Hydrogels via Click Chemistry: Synthesis and Potential Biomedical Applications*. *Biomacromolecules*, 2007. **8**(6): p. 1844-1850.
82. Testa, G., et al., *Influence of dialkyne structure on the properties of new click-gels based on hyaluronic acid*. *International Journal of Pharmaceutics*, 2009. **378**(1-2): p. 86-92.
83. Tabatabaei, F., O. Lenz, and C. Holm, *Simulation study of anomalous tracer diffusion in hydrogels*. *Colloid & Polymer Science*, 2011. **289**(5-6): p. 523-534.
84. Brandl, F., et al., *Hydrogel-based drug delivery systems: Comparison of drug diffusivity and release kinetics*. *Journal of Controlled Release*. **142**(2): p. 221-228.
85. Voit, B., *The potential of cycloaddition reactions in the synthesis of dendritic polymers*. *New Journal of Chemistry*, 2007. **31**(7): p. 1139-1151.
86. Di Meo, C., et al., *Novel types of carborane-carrier hyaluronan derivatives via "click chemistry"*. *Macromolecular Bioscience*, 2008. **8**(7): p. 670-681.
87. Ruel-Gariépy, E. and J.-C. Leroux, *In situ-forming hydrogels—review of temperature-sensitive systems*. *European Journal of Pharmaceutics and Biopharmaceutics*, 2004. **58**(2): p. 409-426.
88. Hennink, W.E. and C.F. van Nostrum, *Novel crosslinking methods to design hydrogels*. *Advanced Drug Delivery Reviews*, 2002. **54**(1): p. 13-36.
89. Zentner, G.M., et al., *Biodegradable block copolymers for delivery of proteins and water-insoluble drugs*. *Journal of Controlled Release*, 2001. **72**: p. 203-215.
90. Constantin, M., et al., *Lower critical solution temperature versus volume phase transition temperature in thermoresponsive drug delivery systems*. *eXPRESS Polym. Lett.*, 2011. **5**(10): p. 839-848.
91. Alexandridis, P., *Amphiphilic copolymers and their applications*. *Current Opinion in Colloid & Interface Science*, 1996. **1**(4): p. 490-501.

92. Mortensen, K. and J.S. Pedersen, *Structural study on the micelle formation of poly(ethylene oxide)-poly(propylene oxide)-poly(ethylene oxide) triblock copolymer in aqueous solution*. *Macromolecules*, 1993. **26**: p. 805-12.
93. Bromberg, L.E. and E.S. Ron, *Temperature-responsive gels and thermogelling polymer matrices for protein and peptide delivery*. *Advanced Drug Delivery Reviews*, 1998. **31**(3): p. 197-221.
94. Brown, W., K. Schillen, and S. Hvidt, *Triblock copolymers in aqueous solution studied by static and dynamic light scattering and oscillatory shear measurements: influence of relative block sizes*. *J. Phys. Chem.*, 1992. **96**: p. 6038-44.
95. Kabanov, A.V., E.V. Batrakova, and V.Y. Alakhov, *Pluronic® block copolymers as novel polymer therapeutics for drug and gene delivery*. *Journal of Controlled Release*, 2002. **82**(2-3): p. 189-212.
96. Walz, M., et al., *Micellar Crystallization with a Hysteresis in Temperature*. *Langmuir*, 2010. **26**: p. 14391-14394.
97. Jeong, B., S.W. Kim, and Y.H. Bae, *Thermosensitive sol-gel reversible hydrogels*. *Advanced Drug Delivery Reviews*, 2002. **54**(1): p. 37-51.
98. Ahn, J.S., et al., *Slow eroding biodegradable multiblock poloxamer copolymers*. *Polymer International*, 2005. **54**(5): p. 842-847.
99. Fusco, S., A. Borzacchiello, and P.A. Netti, *Perspectives on: PEO-PPO-PEO Triblock Copolymers and their Biomedical Applications*. *Journal of Bioactive and Compatible Polymers*, 2006. **21**(2): p. 149-164.
100. Wanka, G., H. Hoffmann, and W. Ulbricht, *Phase Diagrams and Aggregation Behavior of Poly(oxyethylene)-Poly(oxypropylene)-Poly(oxyethylene) Triblock Copolymers in Aqueous Solutions*. *Macromolecules*, 1994. **27**: p. 4145-9.
101. Chung, Y.-M., et al., *Sol-Gel Transition Temperature of PLGA-g-PEG Aqueous Solutions*. *Biomacromolecules*, 2002. **3**(3): p. 511-516.
102. Garripelli, V.K., et al., *A novel thermosensitive polymer with pH-dependent degradation for drug delivery*. *Acta Biomaterialia*, 2010. **6**(2): p. 477-485.
103. He, C., S.W. Kim, and D.S. Lee, *In situ gelling stimuli-sensitive block copolymer hydrogels for drug delivery*. *Journal of Controlled Release*, 2008. **127**(3): p. 189-207.
104. He, L., et al., *Intelligent hydrogels for drug delivery system*. *Recent Pat. Drug Delivery Formulation*, 2011. **5**: p. 265-274.
105. Censi, R., et al., *Hydrogels for protein delivery in tissue engineering*. *Journal of Controlled Release*, 2012. **161**(2): p. 680-692.
106. Johnston, T.P., M.A. Punjabi, and C.J. Froelich, *Sustained delivery of interleukin-2 from a poloxamer 407 gel matrix following intraperitoneal injection in mice*. *Pharm Res*, 1992. **9**: p. 425-34.
107. Zhuo, R.-X. and W. Li, *Preparation and characterization of macroporous poly(N-isopropylacrylamide) hydrogels for the controlled release of proteins*. *Journal of Polymer Science Part A: Polymer Chemistry*, 2003. **41**(1): p. 152-159.
108. Chen, S. and J. Singh, *Controlled release of growth hormone from thermosensitive triblock copolymer systems: In vitro and in vivo evaluation*. *International Journal of Pharmaceutics*, 2008. **352**(1-2): p. 58-65.
109. Hatefi, A. and B. Amsden, *Biodegradable injectable in situ forming drug delivery systems*. *Journal of Controlled Release*, 2002. **80**(1-3): p. 9-28.
110. Bromberg, L., *Novel Family of Thermogelling Materials via C-C Bonding between Poly(acrylic Acid) and Poly(ethylene oxide)-b-poly(propylene oxide)-b-poly(ethylene oxide)*. *J. Phys. Chem. B*, 1998. **102**: p. 1956-1963.
111. Bromberg, L., *Properties of Aqueous Solutions and Gels of Poly(ethylene oxide)-b-poly(propylene oxide)-b-poly(ethylene oxide)-g-poly(acrylic acid)*. *J. Phys. Chem. B*, 1998. **102**: p. 10736-10744.

112. Cohn, D., A. Sosnik, and A. Levy, *Improved reverse thermo-responsive polymeric systems*. *Biomaterials*, 2003. **24**(21): p. 3707-3714.
113. Garripelli, V.K., et al., *Drug Release from a pH-Sensitive Multiblock Co-Polymer Thermogel*. *J Biomater Sci Polym Ed*, 2011.
114. Cohn, D., et al., *PEO-PPO-PEO-based poly(ether ester urethane)s as degradable reverse thermo-responsive multiblock copolymers*. *Biomaterials*, 2006. **27**(9): p. 1718-1727.
115. Sosnik, A. and D. Cohn, *Reverse thermo-responsive poly(ethylene oxide) and poly(propylene oxide) multiblock copolymers*. *Biomaterials*, 2005. **26**(4): p. 349-357.
116. Vermonden, T., et al., *Macromolecular Diffusion in Self-Assembling Biodegradable Thermosensitive Hydrogels*. *Macromolecules (Washington, DC, United States)*, 2010. **43**: p. 782-789.
117. Bodmer, D., T. Kissel, and E. Traechslin, *Factors influencing the release of peptides and proteins from biodegradable parenteral depot systems*. *Journal of Controlled Release*, 1992. **21**(1-3): p. 129-137.
118. Siegel, R.A. and M. Rathbone, *Overview of Controlled Release Mechanisms*. Book Chapter in *Fundamentals and Applications of Controlled Release Drug Delivery*, 2012. **Chapter 2**: p. 19-43.
119. Giacomelli, F.C., et al., *Aggregation Behavior of a New Series of ABA Triblock Copolymers Bearing Short Outer A Blocks in B-Selective Solvent: From Free Chains to Bridged Micelles*. *Langmuir*, 2008. **25**(2): p. 731-738.
120. Ramkissoon-Ganorkar, C., et al., *Modulating insulin-release profile from pH/thermosensitive polymeric beads through polymer molecular weight*. *Journal of Controlled Release*, 1999. **59**(3): p. 287-298.
121. Barichello, J.M., et al., *Absorption of insulin from pluronic F-127 gels following subcutaneous administration in rats*. *Int J Pharm*, 1999. **184**: p. 189-98.
122. Tessmar, J.K. and A.M. Göpferich, *Matrices and scaffolds for protein delivery in tissue engineering*. *Advanced Drug Delivery Reviews*, 2007. **59**(4-5): p. 274-291.
123. Pegoretti, A., et al., *Hydrolytic resistance of model poly(ether urethane ureas) and poly(ester urethane ureas)*. *Journal of Applied Polymer Science*, 1998. **70**(3): p. 577-586.
124. Dische, Z., *A SPECIFIC COLOR REACTION FOR GLUCURONIC ACID*. *Journal of Biological Chemistry*, 1947. **171**(2): p. 725-730.
125. Dische, Z., *A NEW SPECIFIC COLOR REACTION OF HEXURONIC ACIDS*. *Journal of Biological Chemistry*, 1947. **167**(1): p. 189-198.
126. Dische, Z. and C. Rothschild, *Two modifications of the carbazole reaction of hexuronic acids for the differentiation of polyuronides*. *Analytical Biochemistry*, 1967. **21**(1): p. 125-130.
127. Chytil, M., et al., *Calorimetric and light scattering study of interactions and macromolecular properties of native and hydrophobically modified hyaluronan*. *Carbohydrate Polymers*, 2010. **81**(4): p. 855-863.
128. Kogan, G., et al., *Hyaluronic acid: its function and degradation in in vivo systems*. *Studies in Natural Products Chemistry*, 2008. **34**(Bioactive Natural Products (Part N)): p. 789-882.
129. Stern, R., et al., *The many ways to cleave hyaluronan*. *Biotechnology Advances*, 2007. **25**(6): p. 537-557.
130. Tokita, Y. and A. Okamoto, *Hydrolytic degradation of hyaluronic acid*. *Polymer Degradation and Stability*, 1995. **48**(2): p. 269-273.
131. Cowman, M.K. and S. Matsuoka, *Experimental approaches to hyaluronan structure*. *Carbohydrate Research*, 2005. **340**(5): p. 791-809.
132. Furlan, S., et al., *Hyaluronan chain conformation and dynamics*. *Carbohydrate Research*, 2005. **340**(5): p. 959-970.
133. Maleki, A., A.-L. Kjøniksen, and B. Nyström, *Characterization of the chemical degradation of hyaluronic acid during chemical gelation in the presence of different cross-linker agents*. *Carbohydrate Research*, 2007. **342**(18): p. 2776-2792.

134. Valachova, K., et al., *Free-radical degradation of high-molecular-weight hyaluronan induced by ascorbate plus cupric ions. Testing of buccillamine and its SA981-metabolite as antioxidants*. Journal of Pharmaceutical and Biomedical Analysis, 2011. **56**: p. 664-670.
135. Šoltés, L., et al., *Degradation of high-molar-mass hyaluronan by an oxidative system comprising ascorbate, Cu(II), and hydrogen peroxide: Inhibitory action of antiinflammatory drugs—Naproxen and acetylsalicylic acid*. Journal of Pharmaceutical and Biomedical Analysis, 2007. **44**(5): p. 1056-1063.
136. Mendichi, R., et al., *Characterization of ultra-high molar mass hyaluronan: 1. Off-line static methods*. Polymer, 1998. **39**(25): p. 6611-6620.
137. Mendichi, R. and A. Giacometti Schieron, *Fractionation and characterization of ultra-high molar mass hyaluronan. 2. Online size exclusion chromatography methods*. Polymer, 2002. **43**(23): p. 6115-6121.
138. Baggenstoss, B.A. and P.H. Weigel, *Size exclusion chromatography—multiangle laser light scattering analysis of hyaluronan size distributions made by membrane-bound hyaluronan synthase*. Analytical Biochemistry, 2006. **352**(2): p. 243-251.
139. Stirpe, A., et al., *Early stage aggregation of human serum albumin in the presence of metal ions*. International Journal of Biological Macromolecules, 2011. **49**(3): p. 337-342.
140. Rosell, F.I., M.R. Mauk, and A.G. Mauk, *pH- and Metal Ion-Linked Stability of the Hemopexin–Heme Complex†*. Biochemistry, 2005. **44**(6): p. 1872-1879.
141. Rezaei Behbehani, G., et al., *Thermodynamic Study on the Interaction of Copper Ion with Human Growth Hormone*. Journal of Solution Chemistry, 2010. **39**(2): p. 153-164.
142. Sereikaite, J., et al., *Protein Scission by Metal Ion–Ascorbate System*. The Protein Journal, 2006. **25**(6): p. 369-378.
143. Khossravi, M., S.J. Shire, and R.T. Borchardt, *Evidence for the Involvement of Histidine A(12) in the Aggregation and Precipitation of Human Relaxin Induced by Metal-Catalyzed Oxidation†*. Biochemistry, 2000. **39**(19): p. 5876-5885.
144. Deiters, A. and P.G. Schultz, *In vivo incorporation of an alkyne into proteins in Escherichia coli*. Bioorganic & Medicinal Chemistry Letters, 2005. **15**(5): p. 1521-1524.
145. Wang, Q., et al., *Bioconjugation by copper(I)-catalyzed azide-alkyne [3 + 2] cycloaddition*. Journal of the American Chemical Society, 2003. **125**(11): p. 3192-3193.
146. Le Droumaguet, B. and K. Velonia, *Click chemistry: a powerful tool to create polymer-based macromolecular chimeras*. Macromolecular Rapid Communications, 2008. **29**(12-13): p. 1073-1089.
147. Thordarson, P., B. Droumaguet, and K. Velonia, *Well-defined protein-polymer conjugates-synthesis and potential applications*. Applied Microbiology and Biotechnology, 2006. **73**(2): p. 243-254.
148. Mindt, T.L., et al., *A "Click Chemistry" Approach to the Efficient Synthesis of Multiple Imaging Probes Derived from a Single Precursor*. Bioconjugate Chemistry: p. ACS ASAP.
149. Han, Y., et al., *Grafting BSA onto poly[(L-lactide)-co-carbonate] microspheres by click chemistry*. Macromolecular Bioscience, 2008. **8**(7): p. 638-644.
150. Van Tomme, S.R., G. Storm, and W.E. Hennink, *In situ gelling hydrogels for pharmaceutical and biomedical applications*. Int J Pharm, 2008. **355**(1-2): p. 1-18.
151. Hahn, S.K., J.S. Kim, and T. Shimobouji, *Injectable hyaluronic acid microhydrogels for controlled release formulation of erythropoietin*. Journal of Biomedical Materials Research Part A, 2007. **80A**(4): p. 916-924.
152. Nimmo, C.M., S.C. Owen, and M.S. Shoichet, *Diels–Alder Click Cross-Linked Hyaluronic Acid Hydrogels for Tissue Engineering*. Biomacromolecules, 2011. **12**(3): p. 824-830.
153. Jorgensen, E.B., et al., *Effects of Salts on the Micellization and Gelation of a Triblock Copolymer Studied by Rheology and Light Scattering*. Macromolecules, 1997. **30**: p. 2355-2364.
154. Maderuelo, C., A. Zarzuelo, and J.M. Lanao, *Critical factors in the release of drugs from sustained release hydrophilic matrices*. Journal of Controlled Release, 2011. **154**(1): p. 2-19.

155. Siepmann, J., F. Lecomte, and R. Bodmeier, *Diffusion-controlled drug delivery systems: calculation of the required composition to achieve desired release profiles*. Journal of Controlled Release, 1999. **60**(2–3): p. 379-389.
156. Okay, O., *General Properties of Hydrogels*. Book Chapter in Hydrogel Sensors and Actuators (part 6 of the Springer Series on Chemical Sensors and Biosensors), 2009. **1**: p. 1-14.
157. Hu, Y., et al., *Indentation: a simple, nondestructive method for characterizing the mechanical and transport properties of pH-sensitive hydrogels*. J. Mater. Res., 2012. **27**(1): p. 152-160.
158. Drury, J.L. and D.J. Mooney, *Hydrogels for tissue engineering: scaffold design variables and applications*. Biomaterials, 2003. **24**(24): p. 4337-4351.
159. Monti, R.J., et al., *Transmission of forces within mammalian skeletal muscles*. Journal of Biomechanics, 1999. **32**(4): p. 371-380.
160. Boutris, C., E.G. Chatzi, and C. Kiparissides, *Characterization of the LCST behaviour of aqueous poly(N-isopropylacrylamide) solutions by thermal and cloud point techniques*. Polymer, 1997. **38**(10): p. 2567-2570.
161. Attwood, D., J.H. Collett, and C.J. Tait, *The micellar properties of the poly(oxyethylene)-poly(oxypropylene) copolymer Pluronic F127 in water and electrolyte solution*. International Journal of Pharmaceutics, 1985. **26**: p. 25-33.
162. Alexandridis, P., J.F. Holzwarth, and T.A. Hatton, *Micellization of Poly(ethylene oxide)-Poly(propylene oxide)-Poly(ethylene oxide) Triblock Copolymers in Aqueous Solutions: Thermodynamics of Copolymer Association*. Macromolecules, 1994. **27**: p. 2414-25.
163. Alexandridis, P., J.F. Holzwarth, and T.A. Hatton, *A correlation for the estimation of critical micellization concentrations and temperatures of polyols in aqueous solutions*. J. Am. Oil Chem. Soc., 1995. **72**: p. 823-6.
164. Jeong, B., et al., *Biodegradable block copolymers as injectable drug-delivery systems*. Nature, 1997. **388**(6645): p. 860-862.
165. Bhardwaj, R. and J. Blanchard, *Controlled-release delivery system for the alpha-MSH analog melanotan-I using poloxamer 407*. J Pharm Sci, 1996. **85**: p. 915-9.
166. Bivigou-Koumba, A., et al., *Thermoresponsive amphiphilic symmetrical triblock copolymers with a hydrophilic middle block made of poly(N-isopropargylacrylamide): synthesis, self-organization, and hydrogel formation*. Colloid & Polymer Science, 2010. **288**(5): p. 499-517.
167. Bohorquez, M., et al., *A Study of the Temperature-Dependent Micellization of Pluronic F127*. J. Colloid Interface Sci., 1999. **216**: p. 34-40.
168. Moore, T., et al., *Experimental investigation and mathematical modeling of Pluronic® F127 gel dissolution: drug release in stirred systems*. Journal of Controlled Release, 2000. **67**(2-3): p. 191-202.
169. Heyd, A., *Polymer-drug interaction: Stability of aqueous gels containing neomycin sulfate*. Journal of Pharmaceutical Sciences, 1971. **60**(9): p. 1343-1345.
170. Jain, N.J., et al., *Micellar Structure of an Ethylene Oxide–Propylene Oxide Block Copolymer: A Small-Angle Neutron Scattering Study*. The Journal of Physical Chemistry B, 1998. **102**(43): p. 8452-8458.
171. Lee, H.-N. and T.P. Lodge, *Lower Critical Solution Temperature (LCST) Phase Behavior of Poly(ethylene oxide) in Ionic Liquids*. J. Phys. Chem. Lett., 2010. **1**: p. 1962-1966.
172. Rungseevijitprapa, W. and R. Bodmeier, *Injectability of biodegradable in situ forming microparticle systems (ISM)*. Eur. J. Pharm. Sci., 2009. **36**: p. 524-531.
173. Cilurzo, F., et al., *Injectability evaluation: an open issue*. AAPS PharmSciTech, 2011. **12**(2): p. 604-9.
174. Gill, H.S. and M.R. Prausnitz, *Does Needle Size Matter?* Journal of diabetes science and technology (Online), 2007. **1**(5): p. 725-729.
175. Matheus, S., et al., *Liquid high concentration IgG1 antibody formulations by precipitation*. J Pharm Sci, 2009. **98**(9): p. 3043-57.

176. Gong, C.Y., et al., *Thermosensitive PEG–PCL–PEG hydrogel controlled drug delivery system: Sol–gel–sol transition and in vitro drug release study*. Journal of Pharmaceutical Sciences, 2009. **98**(10): p. 3707-3717.
177. Yang, Y., et al., *A novel mixed micelle gel with thermo-sensitive property for the local delivery of docetaxel*. Journal of Controlled Release, 2009. **135**(2): p. 175-182.
178. Jiskoot, W., et al., *Protein instability and immunogenicity: Roadblocks to clinical application of injectable protein delivery systems for sustained release*. Journal of Pharmaceutical Sciences, 2012. **101**(3): p. 946-954.
179. Serres, A., M. Baudyš, and S. Kim, *Temperature and pH-sensitive Polymers for Human Calcitonin Delivery*. Pharmaceutical Research, 1996. **13**(2): p. 196-201.
180. Vintiloiu, A., et al., *In situ-forming oleogel implant for rivastigmine delivery*. Pharm Res, 2008. **25**(4): p. 845-52.
181. Leach, J.B. and C.E. Schmidt, *Characterization of protein release from photocrosslinkable hyaluronic acid-polyethylene glycol hydrogel tissue engineering scaffolds*. Biomaterials, 2005. **26**(2): p. 125-35.
182. Kim, Y.J., et al., *Controlled release of insulin from injectable biodegradable triblock copolymer*. Pharm Res, 2001. **18**: p. 548-50.
183. Qiu, B., et al., *A hydrogel prepared by in situ cross-linking of a thiol-containing poly(ethylene glycol)-based copolymer: a new biomaterial for protein drug delivery*. Biomaterials, 2003. **24**(1): p. 11-8.
184. Huang, X. and C.S. Brazel, *On the importance and mechanisms of burst release in matrix-controlled drug delivery systems*. Journal of Controlled Release, 2001. **73**(2–3): p. 121-136.